Extensional Tectonics in Western Anatolia, Turkey: Eastward continuation of the Aegean Extension

E. J. Catlos[1], T. M. Etzel[1,2], and I. Çemen[3]

[1] The University of Texas at Austin, Jackson School of Geosciences, Dept. of Geological Sciences, Austin TX 78712-1722, USA
[2]ExxonMobil, 22777 Springwoods Village, Parkway Spring, TX 77389, USA
[3]University of Alabama, Dept. of Geological Sciences, Tuscaloosa, Alabama, 35487-0338, USA

Corresponding author: Elizabeth Catlos (ejcatlos@jsg.utexas.edu)

Index terms
8110 Continental tectonics: general (0905)
8109 Continental tectonics: extensional (0905)
3618 Magma chamber processes (1036)
3651 Thermobarometry
3652 Pressure-temperature-time paths

Keywords
Aegean, Anatolia, extension, Western Turkey, tectonics

Abstract
Western Anatolia is located at the boundary between the Aegean and Anatolian microplates. It is considered a type-location for marking a significant transition between compressional and extensional tectonics across the Alpine-Himalayan chain. The onset of lateral extrusion in Western Anatolia and the Aegean during the Eocene is only one of its transitional episodes. The region has a geological history marked by diverse tectonic events starting from the Paleoproterozoic through the Cambrian, Devonian, and Late Cretaceous, as recorded by its suture zones, metamorphic history, and intrusions of igneous assemblages. Extension in Western Anatolia initiated in a complex lithospheric tectonic collage of multiple sutured crustal fragments from ancient orogens. This history can be traced to the Aegean microplate, and today both regions are transitioning or have transitioned to a stress regime dominated by strike-slip tectonics. The control for extension in Western Anatolia is widely accepted as the rollback of the African (Nubian) slab along the Hellenic arc, and several outstanding questions remain regarding subduction dynamics. These include the timing and geometry of the Hellenic arc and its connections to other subduction systems along strike. Slab tear is proposed for many regions across the Anatolian and Aegean microplates, either trench-parallel or perpendicular, and varies in scale from regional to local. The role of magma in driving and facilitating extension in Western Anatolia and where and why switches in stress regimes occurred along the Anatolia and Aegean microplates are still under consideration. The correlation between Aegean and Anatolian tectonic events requires a better understanding of the detailed metamorphic history recorded in Western Anatolia rocks, possible now with advances in garnet-based themobarometric approaches. Slab tear and ultimate delamination impact lithospheric dynamics, including generating economic and energy deposits, facilitating lithospheric thinning, and influencing the onset of transfer zones that accommodate deformation and provide conduits for magmatism.

1 Introduction

The Aegean and eastern Mediterranean are considered the most rapidly deforming regions across the Alpine-Himalayan chain (Figure 1) (e.g., Papazachos & Delibasis 1969; Papazachos & Comninakis, 1971; McKenzie, 1972; Şengör et al., 1985; Taymaz et al., 1991; Jackson, 1994; Reilinger et al., 1997; Nyst & Thatcher, 2004; Le Pichon et al., 2019; Meng et al., 2021). The Aegean and Anatolia microplates, sometimes classified as the single Aegean-Anatolian microplate, are a complex amalgamation of a series of terranes that today experience seismicity (e.g., Şengör & Yılmaz, 1981; Okay et al., 1996; Reilinger et al., 1997; Nyst & Thatcher, 2004; Tan, 2013). The Anatolian microplate is a large peninsula that coincides with over two-thirds of the country of Turkey (Figure 1) (Le Pichon et al., 1995; Oral et al., 1995; Reilinger et al., 1997; Papazachos, 1999). It is the westernmost protrusion of the Asian continent, with a pole of rotation located in the northern Sinai Peninsula (e.g., Reilinger et al., 2010). The Black Sea bounds it to the north and the Mediterranean Sea to the south. The Aegean microplate is largely comprised of continental crust and sediments obscured by the Aegean Sea (Le Pichon & Angelier, 1981; Jolivet & Patriat, 1999; Makris et al., 2013). The Sea of Marmara connects the Black and Aegean Seas through the Bosphorus and Dardanelles straits and separates a fragment of Eurasia's microplate (Nyst & Thatcher, 2004).

Deciphering the assembly of the Aegean and Anatolian microplates and their past and present-day deformation drivers impacts our understanding of continental tectonics, subduction zone processes, lithospheric deformation, ore generation process, and hazards (e.g., Jackson, 1994; Meng et al., 2021; Rabayrol & Hart, 2021). The borders of the Aegean and Anatolian microplates coincide with fault systems that played vital roles in triggering changes in their tectonic nature (e.g., McKenzie, 1972; 1978). The microplates share some borders, including the right-lateral strike-slip North Anatolian transform fault and the Western Anatolian Extensional Province (WTEP) (Figure 1) (e.g., Ketin, 1948; Şengör et al., 1985; Barka, 1992; Armijo et al., 1999; Çemen et al., 2006; Barka et al., 2000; McClusky et al., 2000; Chousianitis et al., 2015). The subducting Hellenic and Cyprus arcs and the complex dynamics coinciding with the Florence Rise make up their southern borders (e.g., Le Pichon & Angelier, 1979; Angelier et al., 1982; Anastasakis & Kelling 1991; Papazachos et al., 2000; Ergün et al., 2005; Suckale et al., 2009; Royden & Papanikolaou, 2011). Global Positioning System (GPS) constraints show that the principal northern boundaries of the southwestern Aegean plate are the North Aegean Trough (NAT) and Kephalonia (also Cephalonia and Kefalonia) Transform Zone (KTZ) (McKenzie 1972; Pichon et al. 1995; Kahle et al. 2000; Pearce et al., 2012; Chousianitis et al. 2015; Haddad et al. 2020). The southern boundary is separated from the Anatolia plate by the WTEP., a zone of N-S extension (Figure 1) (McClusky et al., 2000; Chousianitis et al., 2015). Although many of its bounding fault systems are presently active, both the Anatolian and Aegean microplates contain internal structures, including transfer zones (Figure 1 and Figure 2) (e.g., Nyst & Thatcher, 2004; Çemen et al., 2006; Oner et al., 2010; Aktuğ et al., 2013; Özkaymak et al., 2013; Uzel et al., 2013; Seghedi et al., 2015; Barbot & Weiss, 2021).

Several tectonic models applied to the Aegean and Anatolian microplates have transformed our ideas about the lithosphere's response to extensional, strike-slip, and compressional forces (see review in Aktuğ et al., 2013). Advances in tomography and GPS technology have contributed to our understanding of its present-day dynamics (e.g., Barka & Reilinger, 1997; McClusky et al., 2000; Ganas & Parsons, 2009; Komut et al., 2012; Aktuğ et al., 2013; Jolivet et al., 2015; Ventouzi et al., 2018). The deformation, metamorphism, and igneous

activity exposed in the upper portions of the microplate's lithosphere provide constraints on processes that operated in its lower lithosphere over long periods of geological time (e.g., Jackson, 1994; Komut et al., 2012).

This review paper is divided into two primary parts. The first section reviews some of the chronology and tectonic history of the juncture between the Aegean and Anatolian microplates from data available in Western Anatolia (Figure 1 and Figure 2). The goal is to outline how the boundary results from an accumulation of a series of tectonic processes that record stress transitions in the geological past. The second part of the paper aims to present outstanding questions that remain in unraveling its complex dynamics. This particular area of the Anatolian microplate has been the focus of attention for almost fifty years (e.g., McKenzie 1972) and has become the type-locality for understanding subduction zone dynamics, a focus of diverse and multi-disciplinary studies.

2 Geological Background

2.1 Assembly of key components (Paleoproterozic-Eocene)

The Anatolian microplate is comprised of multiple continental fragments separated by oceans that collided and ultimately combined by the Late Cretaceous-Eocene, with exposures of ophiolitic and high-pressure/low-temperature rock assemblages that mark the suture zones (Figure 2, Figure 3, Figure 4) (e.g., Şengör & Yılmaz, 1981; Okay, 2008; Moix et al., 2008; Okay & Tuysuz, 1999; Pourteau et al., 2016; Okay et al., 2020). Western Anatolia is explicitly defined by the amalgamation of two terranes: the Pontides to the north and the Anatolides-Taurides to the south (e.g., Şengör & Yılmaz, 1981; Yilmaz et al., 1997; Okay & Tuysuz, 1999; Pourteau et al., 2016). The Pontides extends across northern Turkey and is comprised mainly of Pan-African basement blocks and Phanerozoic sedimentary cover units that may have originated from the southern Eurasia margin before back-arc extension initiated and created the Black Sea (Yilmaz et al., 1997; Moix et al., 2008; Pourteau et al., 2010; Okay et al., 2013).

The Intra-Pontide suture zone (IPS) is mapped within the Pontide zone between the Sakarya continental zones and Istanbul-Zonguldak Unit (also Istanbul–Zonguldak Zone, Istanbul Nappe, or Istanbul Zone, see Yiğitbaş et al., 2004) (Figure 2, Figure 3, Figure 4). The Istanbul portion of the unit exists in the west (Istanbul, Gebze, south Camdağ regions) and the Zonguldak to the east (north Camdağ, Zonguldak, Safranbolu regions), both being Gondwanan fragments (e.g., Okay et al., 2006; Bozkaya et al., 2012). The IPS has varying interpretations, including an accretionary complex, a suprasubduction zone, and a remnant of a former ocean basin that may have extended into eastern Europe (e.g., Okay et al., 1996; Robertson & Ustaömer, 2004; Göncüoğlu et al., 2012; 2014; Marroni et al., 2014; Akbayram et al., 2016; Sayit et al., 2016; Frassi et al., 2018). Geological units within the IPS may also be from components from the Istanbul-Zonguldak or Sakarya zones, which has led to a debate about its presence and utility of the IPS in paleogeographic reconstructions (Moix et al., 2008).

Magmatic assemblages help us understand the tectonic processes involved in Western Anatolia, so we present a summary of some available time constraints for several key granite bodies dispersed throughout this region in Tables 1-8 and Figure 4. Zircon ages extracted from metagranites and quartzite units indicate that the Istanbul-Zonguldak Unit has a Precambrian basement with Gondwanan units (Chen et al., 2002; Yiğitbaş et al., 2004; Ustaömer et al., 2005; 2011) and stratigraphic similarities with Paleozoic rocks from the southern margin of Laurasia (Görür et al., 1997; Kaldova et al., 2003). Some of the oldest Neoproterozoic granites in Western

Anatolia are found in the Istanbul Zone (Table 1, Karadere or Karabuk metagranite, Figure 4; Chen et al., 2002; Ustaömer et al., 2016; Di Rosa et al. 2019), although zircons from the Karacabey (Tamsali) and Karaburun plutons in the Western Sakarya Zone and the Çine Massif in the southern portion of the Menderes Massif also yield Paleoproterozoic and Neoproterozoic ages (Tables 5 and 8; Loos & Reischmann 1999; Aysal et al., 2012; Ustaömer et al., 2012). The Triassic ages from granites that intrude the Istanbul-Zonguldak Unit are thought to time partial closure of the Paleotethyan Ocean (Table 1, e.g., Ustaömer et al., 2016). Some of the youngest mineral ages from Istanbul-Zonguldak granites are Late Cretaceous ($^{40}Ar/^{39}Ar$ ages, 93.3±2.0 Ma, 86.1±2.0 Ma, Delaloye & Bingöl, 2000), which are similar to estimates for the activity within the subduction-accretion complex associated with the Izmir-Ankara-Erzincan Suture Zone (IAESZ) (Figure 2, Figure 3, Figure 4) (Okay et al., 2020).

The IAESZ separates the Pontide's Sakarya Composite Terrane in the north from the Anatolide-Tauride block to the south (Figure 2 and Figure 4) (Şengör & Yılmaz, 1981; Okay & Tüysüz, 1999; Tekin et al., 2002; Göncüoğlu, 2010). Both the IPS and IAESZ mark late Cretaceous–earliest Tertiary closure of Neo-Tethyan ocean basins (e.g., Pourteau et al., 2010; Akbayram et al., 2016). In the Aegean microplate, the IAESZ is thought to record the closure of the Vardar ocean and link with the Vardar ophiolite (or Axios-Vardar suture zone) (Channell & Kozur, 1997; Okay & Tuysuz, 1999; Tekin et al., 2002; Moix et al., 2008), but its exposure beneath the Aegean Sea is masked (e.g., Burtman, 1994; Stampfli, 2000; Yılmaz et al., 2001; Burchfiel et al., 2008). The Vardar suture may also connect to the IPS that separates the Sakarya Zone from the Istanbul Zone (Şengör & Yılmaz, 1981; Okay & Satir, 2000; Okay et al., 2001; Beccaletto & Jenny, 2004; Okay et al., 2010; d'Atri et al., 2012; Di Rosa et al. 2019), and may connect to the Meliata-Balkan suture of Greece (Stampfli, 2000). The IPS and Vardar connection may be evidenced in the Biga Peninsula by an isolated ophiolite-bearing accretionary complex that was active until the Late Cretaceous (Figure 2 and Figure 4) (e.g., Okay et al., 1991). Some disagree and do not map any major suture within the Biga Peninsula (Altunkaynak & Genc, 2008; Burchfiel et al., 2008; Sengun et al., 2011). Because of the uncertain link between the sutures, the relationship of the basement of the Biga Peninsula to that in the Rhodope-Thrace Massif is debated (Bonev & Beccaletto, 2007; Elmas, 2012). In Western Anatolia, the Pamphylian Suture (Figure 2) may connect to the Alanya and Bitlis suture zones further to the east (Centikaplan et al., 2016) and beneath the Lycian nappes to the Cycladic domain to the west (Stampfli & Kozur, 2006).

In Western Anatolia, blueschist assemblages exposed along the IAESZ are intruded by Suture Zone Granitoids (SZGs) [Topuk, Orhaneli, Tepeldag (Gürgenyayla and Gürgenyayla), Table 2; Figure 4]. These granitoids have Paleocene (63.5±2.8 Ma) to Oligocene (31.4±0.6 Ma) ages but are largely thought to have crystallized in the early Eocene (~45-47 Ma, Okay & Satir, 2006; Altunkaynak, 2007). The SGZs intrude the western portion of the Tavşanlı Zone, a blueschist sequence overlain by a Cretaceous accretionary complex and ophiolitic sheet. The zone formed as a result of northward-dipping subduction and represents the Mesozoic to Eocene closing of the northern branch of the Neo-Tethyan Ocean (Okay, 1986; 2008; Okay & Kelley, 1994; Sherlock et al., 1999; Moix et al., 2008, Shin et al., 2013; Plunder et al., 2013; Fornash & Whitney, 2020). The Tavşanlı Zone is narrow (~50 km) and trends E-W for approximately 250-350 km (Okay & Whitney, 2010; Plunder et al., 2013). The western and central portions contain blueschist facies metavolcanic and metasedimentary rocks with rare metabasalts (Okay, 1980a, 1980b, 1982; Okay & Kelley, 1994, see Seaton et al., 2009).

The Sivrihisar Massif further to the east is the only portion of the Tavşanlı Zone to contain eclogite and blueschist and Barrovian sequences (Figure 4 and Figure 5) (Gautier, 1984; Seaton et al., 2009). Rb-Sr and $^{40}Ar/^{39}Ar$ phengite ages from the Sivrihisar Massif constrain high-pressure/low-temperature (HP/LT) metamorphism to ~88–80 Ma (Sherlock et al., 1999; Seaton et al., 2009; Whitney et al., 2011; Pourteau et al., 2013; Shin et al., 2013). Older ages from the HP/LT assemblages reported from the western portion of the Tavşanlı Zone may suffer from excess argon (see review in Shin et al., 2013). Barrovian-metamorphosed marble from the Sivrihisar massif contains ~59 Ma muscovite ($^{40}Ar/^{39}Ar$), timing their exhumation (Seaton et al., 2009). Late Cretaceous and early Paleocene ages are also reported from eastern Tavşanlı Zone granitoids, which are medium to high K., calc-alkaline, metaluminous, I-type, and post-collisional [Kaymaz, Sivrihisar, Sarıkavak (Topkaya), Günyüzü (Karacaören, Tekoren, Dinek, Kadinicik bodies) Figure 4 and Figure 5, Table 2] (e.g., Shin et al., 2013; Demirbilek et al., 2018). However, these results are interpreted as inheritance (Shin et al., 2013; Demirbilek et al., 2018). The Sivrihisar granite's age is often cited to be 53±3 Ma, based on a hornblende $^{40}Ar/^{39}Ar$ age clearly affected by excess argon (Sherlock et al., 1999) (Figure 5B and C). However, the Sivrihisar granite contains zircon that is 78.4±8.5 Ma (likely inherited) to 41.9±2.3 Ma (U-Pb, ±1σ, Shin et al., 2013). Figure 5B and C show the K-feldspar $^{40}Ar/^{39}Ar$ age from the same sample, which yields a plateau age of 46.02±0.21 Ma (MSWD 4.21), similar to those reported for the Sivrihisar and nearby Kaymaz granite and SZGs (Table 2). The flat $^{40}Ar/^{39}Ar$ age spectrum is consistent with rapid cooling during exhumation (Figure 5D). Paleocene-Eocene ages from the Tavşanlı Zone granites mark the timing of the closure of the IAESZ (e.g., Okay et al., 2020).

The Tavşanlı zone is one component of the larger Anatolide-Tauride block, a microcontinent that rifted away from the northern margin of Gondwana beginning in the early Permian (Figure 2, Figure 3, and Figure 4) (Stampfli & Kozur, 2006) or Triassic (e.g., Şengör & Yılmaz, 1981; Şengör et al., 1984; Okay & Tuysuz, 1999; Robertson & Ustaömer, 2009a, 2009b). The Taurides comprise the southern portion of the Anatolide-Tauride block and is Neoproterozoic-Early Cambrian (Infracambrian) basement overlain by Cambrian to Eocene marine sediments (e.g., Gutnic et al., 1979; Özgül, 1997; Candan et al., 2016). The Anatolide terrane is the metamorphic equivalent of the Taurides and is subdivided into zones based on lithologies and the type and age of metamorphism (see review in Bozkurt & Oberhansli, 2001; Candan et al., 2016; Moix et al., 2008). These include the Tavşanlı Zone, Afyon Zone, Menderes Massif, and Lycian nappes (Figure 2, Figure 3, and Figure 4). The Tavşanlı and Afyon zones are sometimes considered as part of a single Kütahya–Bolkardağ Belt (Özcan et al., 1988; Göncüoğlu et al., 1997; 2012).

Note that a series of granite bodies intrude the IPS between the Sakarya and Istanbul Zones also ages that resemble the SZGs and eastern portions of the Tavşanlı Zone. These Middle Eocene Magmatic Rocks (MEMR), also known as the South Marmara Granitoids [Şevketiye, İlyasdağ tonalite (Marmara Island), Karabiga (Lapeski), Fistikli (Armutlu–Yalova), Kapidağ, and Avsa Island; Figure 4, Table 3] are located in close association with the IPS and range in age from the Late Cretaceous (71.9±1.8 Ma) to Late Eocene (34.3±0.9 Ma). The MEMR are unique in these ages, as further east, along strike of the IPS and into the central portion of the Sakarya Zone, some of the oldest plutons in Western Anatolia are exposed (Pamukova, Gemlik, Inhisar, Gevyke, Bilecik, Söğüt, Figure 4, Table 4). Some of these intrusions are associated with economically important kaolinite deposits (e.g., Kadir & Kart, 2009). The Cambrian Gemlik granite body is located in the vicinity of the MEMR granites (Figure 4). Its age is more

consistent with Cadomian Orogeny (650–550 Ma) granites further north in the Istanbul-Zonguldak and Strandja zones (e.g., Şahin et al., 2014) and similar-age rocks from the basement or core of the Afyon Zone and Menderes Massif (e.g., Dannat, 1997; Loos & Reichmann, 1999; Şahin et al., 2014; Hetzel & Reischmann, 1996). Western Anatolian granites with Cambrian ages are termed the Late Pan-African Granitoids or Cadomian Granitoids and are associated with tectonic events along the northern margin of Gondwana (Gürsu & Göncüoğlu, 2006; Şahin et al., 2014). We identify some of these granites in their particular zones in Figure 4 and distinct sections of Tables 1, 4, and 8. Note that the entire core of the Menderes Massif is considered Pan-African (primarily late Neoproterozoic to Cambrian) basement (see review in Oberhänsli et al., 2010).

Proterozoic zircon ages are found in the Pontides zone, but some of its central and western granite assemblages also record Silurian-Devonian ages [Saricakaya, Table 4; Karaburun, Güveylerobası (Çamlik-related), Karacabey (Tamsali), Eybek (Çamlik), Güveylerobası, Table 5; Figure 4]. These ages are linked to the amalgamation of a fragment of Avalonia terrane in a subduction-zone type setting (Aysal et al., 2012; Sunal, 2012; Topuz et al., 2020). Variscan-age (Carboniferous) granites are also reported for granites in the Central and Western Sakarya Zone and Afyon Zone (Tables 4 and 6; Figure 4). Some of these results could represent inherited cores or xenocrystic grains from the surrounding metamorphic assemblages. For example, the Miocene-age Alaçam granite in the Afyon Zone has reported Carboniferous ages, but the older ages were likely entrained from its basement units (Hasözbek et al. 2010; Candan et al. 2016).

The Afyon zone is considered the southward palaeogeographic extension of the Tavşanlı zone (Candan et al., 2005; Pourteau et al., 2010; Akal, 2013; Özdamar et al., 2013). Although it is often mapped as closely and narrowly paralleling the Tavşanlı Zone, the southern extent of the Afyon Zone is unclear, and a portion may also be exposed between the southern Menderes Massif and Lycian Nappes (Okay, 1986; Candan et al., 2005; Pourteau et al., 2013; Ustaömer et al., 2020). The zone has also been termed the Afyon–Bolkardag Zone (Okay, 1986; Özdamar et al., 2013) and Ören–Afyon Zone (Pourteau et al., 2013). The zone consists of Pan-African-related basement underlying shelf-type Palaeozoic-Mesozoic sequence of the Taurides and metasedimentary and metavolcanic rocks, portions of which have undergone regional greenschist to blueschist facies (Fe–Mg carpholite and glaucophane) metamorphism (Figure 3) (Okay, 1984; Candan et al., 2005, Pourteau et al., 2010; Özdamar et al., 2013). In this sense, its stratigraphy resembles that of the Tavşanlı Zone (Candan et al., 2005). Rhyolitic volcanic assemblages contain zircon that crystallized in the Late Triassic time extension along the northern margin of Gondwana as the Neo-Tethyan Ocean developed (230±2 Ma and 229±2 Ma; Özdamar et al., 2013). Triassic ages reported for granitic assemblages found within the Istanbul-Zonguldak zone, central and western Sarkarya, and Menderes Massif are also attributed to this event (Figure 4; Okay et al., 2020). LT/HP metamorphism in the Afyon Zone is thought to have occurred at 70-65 Ma coincident with the closure of the Neo-Tethyan Ocean (Pourteau et al., 2010, 2013; Özdamar et al., 2013; Plunder et al., 2013). Based on zircon ages from granites intruding Tavşanlı Zone blueschist and altered ophiolitic assemblages, portions of the Afyon Zone may have subducted beneath the Tavşanlı Zone during the Late Cretaceous (Speciale et al., 2012; Shin et al., 2013). Upper Palaeocene-Lower Eocene sedimentary rocks overly the metamorphic rocks of the Afyon Zone (Candan et al., 2005).

The Menderes Massif is considered the metamorphic basement on which the rocks of the Afyon Zone were deposited before regional metamorphism (Okay, 1984). The Menderes Massif exposes ~40,000 km2 of metamorphic and igneous rocks, and its stratigraphy was originally described as a gneiss 'core' and Paleozoic schist envelope with overlying Mesozoic-Cenozoic marble 'cover' (e.g., Schuiling, 1962; Durr, 1975; Şengör et al., 1984). The massif has also been mapped as a large-scale recumbent fold (Okay, 2001; Gessner et al., 2002), a series of nappes stacked during south-directed thrusting (Ring et al., 1999; 2001; Gessner et al., 2001), or north-directed thrusting (Hetzel et al., 1995a,b) (see Gessner et al., 2013). In the nappe model, the core is represented by the Çine and Bozdağ nappes, whereas the cover would be the Bayındır and Selimiye nappes (Ring et al., 2001), although all nappes may be part of the Menderes Massif core series stacked during Eocene out-of-sequence thrusting (Régnier et al., 2007). Timeframes recorded by the massif begin in the Archean and Neoproterozoic based on zircons extracted from metagranites and orthogneisses with geochemical signatures dominated by reworking of old crust (Oberhansli et al., 2010; Zlatkin et al., 2013). During this time, the Menderes Massif was part of a collage of terranes associated with NE Africa and Arabia (Şengör et al., 1984; von Raumer et al., 2015). Some Neoproterozoic zircons (ca. 570 Ma) have an older crust signature, but others suggest a proximal juvenile source resembling the Arabian-Nubian shield (Zlatkin et al., 2013).

Cambrian metagranites, orthogneisses, granulites, and ecologites, mica schists are exposed throughout the massif (Hetzel & Reischmann, 1996; Dannat, 1997; Loos & Reichmann, 1999; Neubauer, 2002; Oberhansli et al., 2010; Zlatkin et al., 2013; Koralay, 2015). Cambrian-Ordovician monazite and zircon inclusions are found in Menderes Massif garnets (Catlos & Çemen, 2005; Etzel et al., 2019). During this time, the Menderes Massif was affected by events related to the Cadomian Orogeny, and its core units were intruded by Pan African S- and I-type granites followed by metamorphism (Neubauer, 2002). Note that other terranes within Western Anatolia likewise have a Cadomian signature (Figure 4, e.g., Kozur & Göncüoğlu, 1998). Granulite-facies metamorphism in the Menderes Massif was suggested to have occurred at 580.0±5.7 Ma to 660±61 Ma by (U-Pb monazite ages, Oelsner et al., 1997; U-Pb zircon ages, Korolay et al., 2006). Middle-Triassic zircons in metagranites are found in its central portions (Figure 4; Dannat, 1997; Koralay et al., 2001).

The timing of Menderes Massif nappe stacking is largely thought to have occurred during the Eocene-Oligocene, or sometime after the Late Cretaceous (Main Menderes Metamorphism, MMM., e.g., Satir & Friedrichsen, 1986; Konak et al., 1987; Dora et al., 1995; Bozkurt & Park, 1999; Bozkurt & Satir, 2000; Bozkurt & Oberhansli, 2001; Candan et al., 2001; Lips et al., 2001; Gessner et al., 2011). Gessner et al. (2001) report that the Bayındır nappe deformed once during the Eocene related to MMM., whereas the Bozdağ, Çine, and Selimiye nappes record pre-MMM and MMM events. Figure 6 shows a paleogeographic reconstruction of the possible setting of the fragments comprising Western Anatolia during the closure of the IAESZ during the Eocene. This paleographic timeframe is critical for understanding the complex tectonic scenario that set the scene before the onset of extension.

The Aegean Orogeny (Searle & Lamont, 2020a) is proposed for the tectonic history further to the west of the Menderes Massif, including the Cycladic Metamorphic Core Complexes but may mirror its development. In this scenario, subduction and a continent-continent collision occur between the Eurasian and Adria-Apulia/Cyclades plates as marked by ophiolite obduction at 74 Ma (Lamont et al., 2020a) and HP eclogite and blueschist facies

metamorphism at 57 Ma–46.5 Ma (Tomaschek et al., 2003; Lagos et al., 2007; Bulle et al., 2010; Dragovic et al., 2012). The HP metamorphism (P = 11-12 kbar) is documented by ophiolitic melanges that may record a cycle of Alpine collisional thickening followed by extension and overprinting via extension (Papanikolau, 1987, Okrusch & Bröcker, 1990; Avigad & Garfunkel, 1991; Katzir et al., 2000; Parra et al., 2002; Laurent et al., 2018; Lamont et al., 2020b). HP metamorphism is recognized as part of a NE-trending subduction-exhumation channel (e.g., Xypolias & Alsop, 2014; Laurent et al., 2018; Gerogiannis et al., 2019). Crustal thickening and regional kyanite – sillimanite grade Barrovian-type metamorphism occur from 22–14 Ma, followed by orogenic collapse. The island of Naxos exemplifies the process with structural data that suggest it is the result of the gravitational collapse of the Aegean orogenic wedge (Vanderhaeghe, 2004). This model emphasizes the role of compression in forming Aegean metamorphic core complexes (e.g., Coney and Harms, 1984; Searle and Lamont, 2020a,b), which is an alternative to the perspective of solely extensionally-driven core complexes discussed in the next section.

2.2 Extensional history (Oligocene-Miocene)

Following the final amalgamation of the various terranes as described in the previous section, Western Anatolia experienced a switch from the dynamics of collision to extension and extrusion (e.g., Berckhemer, 1977; Le Pichon & Angelier, 1979; 1981; Şengör & Yılmaz, 1981; Şengör et al., 1985; Meulenkamp et al., 1988; Buick, 1991; Jolivet et al., 1994; Seyitoğlu & Scott, 1996; Okay & Satir, 2000; Bozkurt, 2001; Çemen et al., 2006). A sequence of partial melting, Barrovian metamorphism, and granitoid emplacement has been cited for providing evidence of a change from crustal shortening to extensional tectonism (e.g., Keay et al., 2001; Altunkaynak, 2007; Dilek & Altunkaynak, 2007; Altunkaynak et al., 2012; Rossetti et al., 2017). The process may be recorded by numerous Oligocene to Miocene-age granites (Figure 4, Tables 5-8) and linked to the development of metamorphic core complexes located from northeastern Greece and southern Bulgaria through the Aegean Sea and western Turkey.

In continental orogenic domains, metamorphic core complexes are deep crustal domes exhumed and deformed during extension and are commonly surrounded by sedimentary and volcanic rocks, which may be partly deposited during their exhumation (Tirel et al., 2008). Core complexes in western Turkey and the Aegean region include the Rhodope, Kazdağ, Uludağ, Cyclades, Menderes, and Crete massifs (Figure 1, Figure 2, and Figure 4) (Sokoutis et al., 1993; Hetzel et al., 1995a,b; Burg et al., 1996; Lips et al., 1999; Bozkurt & Oberhänsli, 2001; Candan et al., 2001; Lips et al., 2001; Ring et al., 2003; Bozkurt & Sözbilir, 2004; Duru et al., 2004; Vanderhaeghe, 2004; Catlos & Çemen, 2005; Brun & Sokoutis, 2007; Okay et al., 2008; Cavazza et al., 2009; Kruckenberg et al., 2011; Gessner et al., 2013; Baran et al., 2017).

In Western Anatolia specifically, the Menderes, Kazdağ, and Uludağ massifs are central locations for studying post-collision extensional tectonics (Figures 1, Figure 2, and Figure 4) (e.g., Şengör et al., 1984, Bozkurt & Park, 1994; Hetzel et al., 1995a,b; Yılmaz et al., 2001; Işik & Tekeli, 2001; Çemen et al., 2006; Topuz & Okay, 2017). The Menderes Massif has global importance due to its role as the largest zone of active continental extension (e.g., Jolivet & Faccenna, 2000; Çemen et al., 2006). The region has long attracted the attention of those seeking to understand the driving forces of extension from a variety of perspectives (e.g., Lister et al., 1984, Thomson & Ring, 2006; Régnier et al., 2007; Gessner et al., 2013; Uzel et al., 2015). Both low-angle detachment faults and high-angle normal faults bound sedimentary basins and separate the Menderes Massif into northern (Gördes), central (Ödemis), and southern (Çine) submassifs

(Figure 2). In the central Menderes Massif, Miocene-age granites are cut by the low-angle Alasehir detachment, helping to constrain the timing of extension (Alasehir, Salihli, Turgutlu, Table 8). The Kazdağ Massif is smaller in scale compared to the Menderes Massif and is a NE-SW oriented structural dome or tectonic window flanked by detachment structures (Figure 2 and Figure 4) (Okay et al., 1991; Okay & Satir, 2000; Duru et al., 2004; Bonev et al., 2009; Cavazza et al., 2009). This massif's Evciler (Kazdağ) pluton routinely yields Oligo-Miocene crystallization ages from a range of chronometers (Table 5). The Uludağ Massif is NW-SE trending and has high-grade metamorphic and intrusive Eocene-Miocene age granitic rocks (Figure 4, Table 5, Okay et al., 2008). Large Neogene basins bind the northern and southern sections of the Uludağ Massif, and late-stage exhumation is largely thought to have occurred during the Early Miocene (e.g., Topuz & Okay, 2017).

Besides these localities, Miocene ages have been reported for granites in the eastern Tavşanlı zone (Table 2) [Kaymaz and Tekoren granodiorite (Günyüzü); Shin et al., 2013; Demirbilek et al., 2018]. These ages likely represent metamorphism and subsequent alteration associated with the large-scale extension/exhumation affecting Western Anatolia during this time. Early Miocene ages also characterize granites closely associated with the Menderes, Kazdağ, and Uludağ metamorphic core complexes. For example, Miocene ages are reported for a group of granites near the Kazdağ Massif, extensively exposed in the Biga Peninsula and western Pontides [Kozak, Eybek, Katrandag, Cataldag (Bozenkoy, Cataltepe, Turfaldag, Balicikhisar), Kuscayir, and Kestanbol (Ezine), Figure 4, Table 5] and from a series of plutons grouped as the Younger South Marmara Granitoids (Yenice, Ilica, Kizildam, Danisment, Sarioluk, Davutlar, and Yeniköy; Figure 4, Table 5; Karacık et al. 2008). North of the Menderes Massif, Miocene-age plutons also intrude the Afyon Zone, in close association with the Simav fault system, which includes the lower angle Simav Detachment Fault (SDF) and higher-angle Simav Fault further south (Koyunoba, Alaçam, and Egrigöz, Figure 2, Figure 4 and Figure 7, Table 7; Isik et al., 2003).

The Simav structures are at the boundary between two dynamically distinct regions in western Turkey: a northern component dominated by the NAFZ that accommodates the lateral extrusion of the Anatolian block and a southern zone of large-scale crustal extension (Seyitoğlu, 1997; Ersoy et al., 2010). The Simav Fault is a distinct, a high-angle (~45-60º) system that extends ~150 km between the towns of Banaz in the east and Sındırgı in the west (Figure 7) (Ambraseys & Tchalenko, 1972; Seyitoğlu, 1997; Ersoy et al., 2010; Hetzel et al., 2013). The structure near the town of Simav has >200 m of relief between the top of the hanging-wall and footwall, and dips steeply to the north, roughly perpendicular to the current extension direction (Tekeli et al., 2001; Işık et al., 2003). This fault is thought to have formed during the Pliocene and is currently active (Seyitoğlu, 1997; Ring & Collins, 2005). Deciphering the sense of motion of the Simav Fault has implications for the understanding of the neotectonic regime of Turkey and is discussed further in the section regarding outstanding questions in Aegean tectonics.

Estimates of timing core complex exhumation and extension in Western Anatolia have relied on calc-alkaline magmatism, widespread continental sedimentation, and mineral chronometers (Sokoutis et al., 1993; Gautier et al., 1999; Catlos & Çemen, 2005; Altunkaynak & Genç, 2008; Brun & Sokoutis 2010; Brun et al., 2016). In some locations, the complexes record progression of magmatism from earlier Eocene-age mantle melts and input from asthenosphere upwelling to later Oligocene to Late Miocene crustal contamination and subduction signatures, with emplacement ages that young to the south (e.g., Delaloye & Bingöl, 2000; Altunkaynak &

Dilek, 2006; Dilek & Altunkaynak, 2007; Altunkaynak, 2007; Altunkaynak & Genç, 2008; Dilek & Altunkaynak, 2009; Altunkaynak et al., 2012; Karaoğlu & Helvacı, 2014). However, this simple scenario of melt origin and emplacement can be complicated, as the melts are influenced by varied protoliths of varying sources, ages, and degrees of crustal anatexis (Pe-piper, 2000; Stouraiti et al., 2010; 2018).

Late Cenozoic (since ~32 Ma) plutonic rocks are also widespread in the Aegean (e.g., Altherr et al., 1982; Henjes-Kunst et al. 1988; Pe-piper, 2000; Keay et al., 2001; Brichau et al., 2007; 2008). The origin of the granites is linked to subduction migration along the Hellenic arc (e.g., Fytikas et al., 1984; Schaarschmidt et al., 2021) or regional, widespread extensional deformation (e.g., Boztuğ et al., 2009). Barrovian metamorphism on Naxos is thought to have influenced the development of fluid-fluxed melts at ca. 8–10 kbar between 18.5 Ma and 17 Ma (Lamont et al., 2019; Searle and Lamont, 2020b). Peak metamorphism is thought to have occurred at 20.7-16.7 Ma (Keay et al., 2001). In some locations, coeval mafic and felsic melts were emplaced (Seyitoğlu & Scott, 1996; Aldanmaz et al., 2000; Okay & Satir, 2000; Pe-Piper & Piper 2001; Ozgenç & Ilbeyli, 2008). Magma compositions were influenced by a range of factors, including inflowing mantle at the site of melting, the nature of the subduction component and the degree of interaction between mantle and subduction components, as well as the melting of fluid-rich mantle and the assimilation/crystallization history of the resulting hydrous magma (e.g., Pearce & Stern, 2006). Extensive geochemical and isotopic studies of Miocene I-type granitoid plutons of the central Aegean Sea show little evidence for a significant contribution of mantle-derived magmas (Altherr & Siebel, 2002).

Cenozoic magmatism in the Anatolian microplate consists of three distinct, continuous geochemical phases (Innocenti et al., 2005; Dilek & Altunkaynak, 2007; Altunkaynak & Genc, 2008; Akay, 2009; Altunkaynak et al., 2012). Magmatic rocks represent a Late Eocene-Middle Miocene phase with orogenic character and a petrological affinity ranging from calc-alkaline to dominant high-K calc-alkaline to shoshonites. During the Late Miocene–Early Pliocene, alkaline volcanic rocks appear. The third phase is characterized by Pliocene–Quaternary Na-enriched alkali basalts with an oceanic island basalt (OIB) signature (Aldanmaz, 2012). The first volcanic activity in the South Aegean Active Volcanic Arc occurred between 5 and 2 Ma (e.g., Müller et al., 1979; Fytikas et al., 1984; Matsuda et al., 1999; Elburg & Smet, 2020). The driver of extension is widely thought to be the rollback of a subducting African slab (Figure 8, Figure 9, and Figure 10) (e.g., Jolivet & Faccenna, 2000; Çemen et al., 2006; van Hinsbergen, 2010; Royden 1993; Faccenna et al. 2003, 2014; Brun & Faccenna 2008). We discuss the slab and arc dynamics, geometry, and age in the section regarding outstanding questions in Aegean tectonics.

2.3 Strike-slip History (Late Miocene, Pliocene-present)

The Aegean and Anatolian microplates have emerged to be type-localities for the model of tectonic escape based on GPS vectors (Reilinger et al., 2006). In this scenario, the Anatolian plate moves westward in response to the collision of Arabia and Eurasia (e.g., Şengör & Yılmaz, 1981; Şengör et al., 1985; Bozkurt, 2001). The North and East Anatolian transform fault systems accommodate extrusion, and rollback along the Hellenic arc is suggested to provide space to accommodate the escaping plate (McKenzie, 1972; Dewey & Şengör, 1979; Le Pichon & Angelier, 1979; Jackson & McKenzie, 1984; Barka & Kadinsky-Cade, 1988; Taymaz et al., 1991; Reilinger et al., 1997; McClusky et al., 2000; Tatar et al., 2013). Philippon et al. (2014) suggest a two-stage evolution of the arc. At 30 Ma, extension was only driven by the southward retreat of the Hellenic trench at a rate lower than 1 cm/yr, but since the last 13 Ma, the

interaction of trench retreat with Anatolia escape accelerated the rate of trench retreat in the southwest direction at a rate of up to 3 cm/yr.

In western Turkey, extrusion tectonics is dominated by the active right-lateral North Anatolian strike-slip fault (NAF) and North Anatolian Shear Zone (NASZ), which extends for ~1200 from the Karlıova triple junction through the Sea of Marmara and Biga Peninsula (Figure 1) (Ketin, 1948; Barka, 1992; Armijo et al., 1999; Şengör & Zabcı, 2019). The NASZ contains the NAF and is speculated to have accommodated from 25 to 110 km of displacement, depending on location since the late Miocene (Westaway 1994; Yoshioka 1996; Armijo et al., 1999; Hubert-Ferrari et al. 2002; Şengör & Zabcı, 2019). The structure accommodates ~24 mm/year of slip along northern Turkey (McClusky et al., 2000; Bulut et al., 2018). The geometries of its western and eastern terminations are poorly defined (Barbot & Weiss, 2021).

The NAF splits into three strands as it trends westward into Western Anatolia and the Aegean Sea (Figure 1) (e.g., Emre et al., 1998; Kürçer et al., 2008; Beniest et al., 2016; Şengör & Zabcı, 2019). Each segment is comprised of several en échelon fragments (Emre et al., 1998; Kürçer et al., 2008). The northernmost E-W striking segments within the Sea of Marmara change strike in the Northern Aegean Sea towards a NE-SW orientation in the North Aegean Trough, maintaining its right-lateral strike-slip character but splits across three basins and two transpressional ridges (Bulut et al., 2018). A branch between the northern and central segments originates southeast of Sapanca Lake (Kürçer et al., 2008) and terminates at the western end of the North Aegean Trough (Ferentinos et al., 2018). This structure enters the Aegean Sea and trends into the Northern Skyros Basin. Strands of the NAF have also been linked to the KTZ through the transtensional Central Hellenic Shear Zone (Royden & Papanikolaou, 2011; Evangelidis, 2017). In the Western Anatolia -Marmara region, the NAF may have been active since the Pliocene (e.g., Ünay et al., 2001).

Sakellariou et al. (2013) suggest that the southwestward expansion and stretching of the Aegean microplate during Plio-Quaternary is accommodated by a northern right lateral tectonic boundary marked by the KTZ and NASZ, and a southern left-lateral tectonic boundary, marked by the Pliny and Strabo trenches (Figure 9). Papanikolaou and Royden (2007) note that regional extension has a much-reduced role in the dynamics of the Aegean microplate and that, in fact, no active extensional strain is present, except for a small southeastern domain (Figure 1) (Corinth rift, south Viotia, south of Evia, and across the Sperchios-Kammena Vourla rift; Brooks & Ferentinos 1980; Chousianitis et al., 2013, 2015). Maggini & Caputo (2020) report that seismogenic faults in the internal Aegean domain associated with the Hellenic subduction arc are characterized by pure normal and strike-slip kinematics or by a combination and that active thrusting is limited to the central and western sectors of the Hellenic subduction zone and the offshore regions external to it.

Figure 11 shows the focal mechanisms for some recent earthquakes (2010-2020) that appear along the Aegean-Anatolian microplate boundary. Recent earthquakes with focal mechanisms consistent with reverse faulting have occurred south of Crete, including those associated with an Mw 6.4 earthquake on 5/2/2020. These earthquakes occurred at relatively shallow depths (6.5-9.6 km, Table 10) and may be associated with a plate interface zone defined by the upper plate and splay-thrust faults (Saltogianni et al., 2020). Observations and modeling of historical and recent earthquakes have shown that uplift along the Hellenic arc margin offshore of Crete is controlled by reverse fault motion with little contribution from plate-interface slip (e.g., Mouslopoulou et al., 2015).

Extrusion and deformation in Western Anatolia are also accommodated by transfer zones, where strain is transferred from one structural element to another and displacement changes between individual fault and basin segments (e.g., Gawthorpe & Hurst, 1993; Barbot & Weiss, 2021). Some examples of these zones include the NE-SW trending strike-slip dominated Izmir–Balıkesir transfer zone (İBTZ), Uşak-Mugla Transfer Zone (UMTZ), and Southwestern Anatolian Shear Zone (SWASZ) (Figure 1 and Figure 2) (Çemen et al., 2006; Oner et al., 2010; Sözbilir et al., 2011; Gessner et al., 2013; Özkaymak et al., 2013; Uzel et al., 2013; Karaoğlu & Helvacı, 2014; Seghedi et al., 2015). These transfer zones have been considered as significant portions of the larger Western Anatolian Shear Zone (WASZ) or Western Anatolian Extensional Province (Figure 1) and may have developed due to mantle processes related to the subduction of the Aegean slab (e.g., Gessner et al., 2013; Uzel et al. 2020). Some transfer zones trend into other fault systems. For example, the İBTZ is speculated to connect to the Mid-Cycladic Lineament (MCL) in central Greece and the NASZ in northern Turkey (Figure 1, Figure 11) (Uzel et al., 2013; Seghedi et al., 2015; Westerweel et al., 2020). The MCL is a strike-slip structure that may be the result of the reactivation of the Vardar suture zone, evidenced by the North Cycladic Detachment (Figure 11), to accommodate westward extrusion of Anatolia in the Late Miocene (e.g., Philippon et al., 2014). These transfer zones have been used to illustrate that the Aegean and Anatolian microplates experienced or are currently transitioning from a stress regime dominated by extension to transform tectonics (Papanikolaou & Royden, 2007; Cavazza et al., 2009).

Presently, normal fault motion exists within the İBTZ as illustrated by focal mechanisms from a 2020 Mw 6.6 earthquake and 2018 Mw 4.5 earthquake within the zone. An Mw 4.4 earthquake with normal motion occurred off the coast of Amorgos near the 1956 Mw 7.7 (or 7.8) earthquake, one of the strongest earthquakes of the 20th century in the area of the South Aegean (Okal et al., 2009; Alatza et al., 2020). The 1956 event has debated focal mechanisms, as either strike-slip or normal faulting geometries (see Okal et al., 2009). A normal sense of motion also is found with some recent earthquakes near the NASZ, including 2017 Mw 6.2 and 2017 Mw 5.3 earthquakes (Figure 11, Table 10). These events are likely associated with transtensional motion.

3. Outstanding Questions in Aegean Tectonics

As outlined in the previous section, significant contributions have been made regarding the fundamental tectonics and geological history recorded by rocks throughout the Western Anatolian microplate. However, outstanding questions remain to be addressed regarding the boundary between the Aegean and Anatolian microplates that affect our understanding of the mechanisms that drive extension in the Earth's lithosphere. Most of these questions center on how upper lithospheric and crustal deformation are linked and are related to lower lithosphere and mantle processes.

3.1. Slab dynamics

3.1.1 African slab geometry and connections to other subduction systems

Based on several geophysical, tectonic, and geochemical developments, the subducting African (Nubian or Aegean) slab has emerged as the primary driver for extension in the Aegean and Anatolian microplates and the development of their metamorphic core complexes (Figure 1, Figure 2, Figure 8, Figure 9, and Figure 10) (e.g., Jolivet et al. 2013; Jolivet & Faccenna, 2000; Çemen et al., 2006; Dilek & Sandvol, 2009; van Hinsbergen et al., 2010; van Hinsbergen & Schmid 2012; Salaün et al., 2012; Faccenna et al., 2014; El-Sharkawy et al., 2020; Barbot &

Weiss, 2021). The Hellenic and Cyprus arcs are the surface expression of the subducting African plate and eastern Mediterranean lithosphere beneath the Anatolian and Aegean microplates (e.g., Le Pichon & Angelier, 1979; Angelier et al., 1982; Anastasakis & Kelling, 1991; Papazachos et al., 2000; Ergün et al., 2005; Ganas & Parsons, 2009; Hall et al., 2009; Royden & Papanikolaou, 2011; Hall et al., 2014; Symeou et al., 2018; Ventouzi et al. 2018).

Although it has a well-developed Wadati-Benioff zone dipping ~30º from 20-100 km depth and ~45º from 100-150 km depths (Figure 10B) (e.g., Papazachos & Comninakis, 1971; Papazachos et al., 2000; Sukale et al., 2009; Hayes, 2018), it has a debated slab geometry at intermediate depths (150-250 km, Suckale et al., 2009; Agostini et al., 2010; see review in Hansen et al., 2019; El-Sharkawy et al., 2020). Seismic body wave tomography shows it extends into the upper and lower mantle to 1400±100 km depth (Figure 10A) (e.g., Spakman et al., 1988; Bijwaard et al., 1998; van der Meer et al., 2018; see review in Bocchini et al., 2018). However, the slab may be a single folded body that overturned in the lower mantle (Faccenna et al., 2003), or two slabs, located between 2000-1500 km and from 1500 km to the surface (van Hinsbergen et al., 2005; van der Meer et al., 2018). Mantle tomography has shown multiple subducted slabs beneath the Aegean and Anatolian microplates (e.g., Spakman et al., 1988; Spakman, 1990; 1991; Wortel & Spakman, 2000; Govers & Fichtner, 2016; van der Meer et al., 2018; Wei et al., 2019). Blom et al. (2019) show the Hellenic slab, visible in both S and P velocity, extending from the surface to the transition zone in a bent, arcuate shape. A high-velocity structure exists beneath the Hellenic arc and the Aegean Sea that flattens from the 410 km discontinuity and is not seen at deeper levels. Wei et al. (2020) show a gap in the subducting slab at depths of 60-100 km just west of the south Hellenides. In the South Hellenides, slab tear may be visible at the 660 km discontinuity, whereas four slabs are imaged beneath the North Hellenides.

Interpretations of these tomographic images have indicated that more slab is imaged than is reflected by seismicity (e.g., Spakman et al., 1988; Papadopoulos, 1997; Bijwaard et al., 1998), and that a variation of slab exists thickness across the Aegean Sea (e.g., Karagianni et al., 2002). Mantle tomography has also shown that not all slabs in the Mediterranean region are connected to the lithosphere at the surface, consistent with past delamination (e.g., Spakman et al., 1988; Dilek & Sandvol, 2009; Wortel & Spakman, 2000). Challenges in imaging the subduction zone include its small size, its spatially highly variable nature, and the uneven distribution of its seismic stations (El-Sharkawy et al., 2020).

The Hellenic subduction system is comprised of three regions: an outer compressional non-volcanic arc, a volcanic arc, and an extensional back-arc region that makes up the broader Aegean Sea region (Figure 8) (McKenzie 1972; Papazachos, 2019). Although the Western Hellenic Arc (also termed the North and Southern Hellenic arc, Royden & Papanikolaou, 2011) has a well-defined topography, trench, sedimentation, and strain pattern (Stanley et al., 1978; Papadopoulos et al., 1988; Hatzfeld et al., 1990; Cocard et al., 1999), the central and eastern portions of the Hellenic arc are more difficult to characterize as the boundary becomes diffuse (Beißer et al., 1990; Shaw & Jackson, 2010; Özbakır et al., 2013). The Hellenic arc's connection with the Cyprus arc and even the nature of plate motion along strike of the Cyprus arc has been debated (Anastasakis & Kelling, 1991; Woodside et al., 2002; Ergün et al., 2005; Hall et al., 2009; Harrison et al., 2012; Kinnaird & Robertson, 2012; Symeou et al., 2018). The surface morphology of the southern and eastern portions of the Hellenic arc and its connection to the Cyprus arc is obstructed by up to 300-km wide, 6-10 km-thick section of sediments that comprise the Mediterranean Ridge (Figure 8 and Figure 9; Heezen & Ewing, 1963; Emery et al.,

1966; Le Pichon et al., 1982; Kenyon et al. 1982; Kastens et al., 1992; Foucher et al., 1993; Westbrook & Reston, 2002; Kopf et al., 2003). The ridge is a giant accretionary complex, extending ~2000 km from the Calabrian Rise east of Greece to the Florence Rise, and is the largest structural unit of the Eastern Mediterranean Sea (Liminov et al., 1996; Cita et al., 1996). The front of subduction of the Hellenic arc is located south of the Mediterranean Ridge (e.g., Jost et al., 2002; Westbrook & Reston, 2002; Jolivet et al., 2013). The majority of the subducting African plate beneath the ridge is oceanic, except along the central sector of its southern margin, where the accretionary complex collides with the African continental margin (Chaumillon & Mascle, 1997; Westbrook & Reston, 2002). The ridge may be the fastest outward growing wedge in most recent Earth history, with a rate of up to 10 km/Myr (Kastens, 1991; Kopf et al., 2003). It has been speculated to grow by off scraping against a backstop formed by the Alpine nappes of the Hellenic Arc (Kastens, 1991).

The intensively folded and faulted rocks of the Mediterranean Ridge vary in geometry along strike (Cita et al., 1996; Chaumillon & Mascle, 1997; Westbrook & Reston, 2002; Kopf et al., 2003). In its western and eastern portions, the wedge accumulates sediments, but in its central portion between Libya and Crete, the ridge behaves unlike a typical accretionary complex. In this area, a trench system (the Hellenic trenches; Ptolemy, Pliny, and Strabo; Figure 9) developed in between the accretionary complex and volcanic arc, likely as a result of back-thrusting beneath the northern edge of the complex (Galindo-Zaldivar et al., 1996; Westbrook & Reston, 2002). The accretionary complex is unusual compared to others worldwide, not only because of these back thrusts but also because it appears to have formed in a continent-continent collisional setting and contains shallow, Messinian-age evaporites (e.g., Cita et al., 1996; Chaumillon & Mascle, 1997). These evaporites influence its deformation and fast growth rate due to their mechanical properties and effect upon fluid flow and pressure (Kastens, 1991; Westbrook & Reston, 2002; Kopf et al., 2003). Understanding the development of the Mediterranean Ridge is critical to determining the initiation age of the Hellenic arc, as described in the next section.

3.1.2 The age of subduction of the African slab

The Subduction Zone Initiation (SZI) age is defined as the onset of downward plate motion forming a new slab, which later evolves into a self-sustaining subduction zone (Crameri et al., 2020). Constraints regarding SZI age of the present-day expression of the Hellenic arc developed from several independent approaches, including timing sedimentation within the Mediterranean Ridge (Kastens, 1991; Kopf et al., 2003), analysis of topography combined with estimates of slab age and depth (McKenzie, 1978; Le Pichon et al., 2019), reconstructions of subducted slabs using tomography (e.g., Spakman et al., 1988), paleomagnetism (Savostin et al., 1986; Marsellos et al., 2010), and the timing of metamorphism and volcanic activity (e.g., Fytikas et al., 1984). Early estimates for the initiation of Hellenic arc subduction are 13±3-5 Ma (Le Pichon & Angelier, 1979) to 5-10 Ma (McKenzie, 1978; Mercier, 1981) based on interpretations of seismic activity coupled with assumptions regarding the age of subducted lithosphere and subduction depths. These ages are similar to the onset of the KTZ based on geodynamic modeling and GPS data (Figure 1) (6-8 Ma, Royden & Papanikolaou, 2011) and the timing of the earliest volcanic activity in the South Aegean arc (Pliocene, Pe-Piper & Piper, 2005). Reconstructions of fault systems in the northern margin of the eastern Mediterranean Sea are consistent with estimates of 15 Ma (Le Pichon et al., 2019).

However, interpretations of the Aegean seismic velocity structure, tomography, and seismicity data in the Aegean area suggest older estimates (26-40 Ma; Meulenkamp et al., 1988;

Spakman et al., 1988; Papadopoulos, 1997; Brun & Sokoutis, 2010). These ages are more consistent with the ages of granitic intrusions found throughout Western Anatolia (Figure 4, Tables 5-8) and the timing of the onset of sedimentation associated with the Mediterranean Ridge at 23.6-33 Ma (Fytikas et al., 1984; Kastens, 1991). Younger estimates from the ridge are also reported (~19 Ma, Kopf et al., 2003). Plate reconstructions suggest that the Northern Hellenic trench experienced the onset of subduction from 27-34 Ma, whereas the southern Hellenic segment was active at 34 Ma (Royden & Papanikolaou, 2011).

If the incoming lithosphere is heterogeneous in terms of thickness and compositions, subduction zones may behave chaotically, in that they may, over time, retreat, advance, or remain stationary at different stages (e.g., Royden & Husson 2009; Husson et al., 2009). The progressive deceleration in motion of Africa with respect to Europe in the Mediterranean region is observed to have occurred since 35 Ma, and in the eastern Mediterranean from 35 Ma to 10 Ma to a convergence rate of a few mm/yr (Savostin et al., 1986; Marsellos et al., 2010). The rate of trench retreat is estimated to have accelerated from ~0.6 cm/y during the first 30 M.y. of subduction to 3.2 cm/yr during the past 15 m.y., perhaps due to Middle Miocene-Pliocene slab tear (Brun et al., 2017). Differences in the timing of initiation and rate of subduction exist between segments along the Western Hellenic Arc and should also be expected to occur along other portions of the Hellenic and Cyprus arcs (Royden & Papanikolaou, 2011; Pearce et al., 2012). The timing of interpreted ductile 'extensional' shear fabrics in metamorphic rocks can also be complicated as these may record extrusion instead of processes associated with slab rollback (see Searle and Lamont, 2020b).

These Late Cenozoic estimates are difficult to reconcile with the model in which the Hellenic arc is a single, evolving subduction zone system that initiated in the Mesozoic (Jurassic) (Faccenna et al., 2003; van Hinsbergen, 2005; Royden & Papanikolaou, 2011; Jolivet et al., 2013; Malandri et al., 2017). In this scenario, the Vardar suture in Greece, equivalent to the IAESZ (Channell & Kozur, 1997; Okay & Tuysuz, 1999; Moix et al., 2008), and Pindos suture zone, equivalent to units within the Antalya domain and Dilek peninsula (Stampfli & Kozur, 2006) had buoyant microcontinents that entered and locked subduction, triggering southward slab rollback and migration of the volcanic arc (van Hinsbergen et al. 2005; Brun & Faccenna 2008; Jolivet & Brun 2010; Jolivet et al., 2013; Cornée et al., 2018). The model eliminates the need for multiple sutures and subducted slabs to be present beneath western Turkey and the Aegean and simplifies the evolution of the Aegean microplate to a single evolving, long-lived subduction system. The present-day curvature of the Hellenic forearc thus represents oblique subduction and a plate-boundary expression that grew systematically over long periods of geological time (Huchon et al., 1982; Le Pichon et al., 1995; ten Veen & Kleinspehn, 2003; Gautier et al. 1999; Le Pichon et al., 2002; Wallace et al., 2005, 2008; van Hinsbergen & Schmid, 2012; Philippon et al., 2014; Cornée et al., 2018).

The single subduction system requires all the lower plate continental crust to be accreted into the upper plate while subducting continental lithosphere and requires the entire Aegean Crust from the Vardar suture to the Mediterranean ridge was derived from the lower plate (e.g., Figure 2 in van Hinsbergen et al. 2005). Oceans between the accreted domains were of significant size (500 km in some cases), and the process would lead to significant elevation changes, crustal thicknesses, and critical changes in the zone of subduction transitions occurred from oceanic to continental shear zones (see discussion in Le Pichon et al., 2019). Not all units

record blueschist facies conditions, and some experienced Barrovian prograde (burial) P-T paths, such as on the island of Naxos (e.g., Lamont et al., 2019).

Currently, the Hellenic arc is migrating SW faster than the counterclockwise rotation of Anatolia (ten Veen & Kleinspehn, 2003), and the rate of convergence between Africa and Eurasia is 4 cm/yr (Reilinger et al., 1997; Kahle et al., 2000; McClusky et al., 2000; Hollenstein et al., 2008). Timing constraints on Aegean forearc curvature, due to opposite rotations, clockwise in the west and counterclockwise in the east, are Eocene and Middle Miocene (Morris & Robertson 1993; Cornée et al., 2018). Trench bending and rollback increased subduction obliquity over time, which has been accommodated by strain partitioning within the upper Eurasian plate (Philippon et al. 2014; Brun et al. 2016; Cornée et al., 2018). Subduction zones with limited trench-parallel lengths on the order of the Hellenic arc (600-800 km) and narrow slabs (<1,500 km) typically have rapid retreat rates (Schellart et al., 2007; Bolhar et al., 2010).

3.1.3 The number, location, and impacts of slab detachments and tears

An additional key focus of study has been identifying the location, depth, and relationship of ancient and present-day active subducting slabs and their detachment mechanisms beneath the Aegean and Anatolian microplates (see review in Hansen et al., 2019; El-Sharkawy et al., 2020). Several locations across the Aegean and Anatolian microplates have been suggested to be affected by slab tear, either trench parallel or perpendicular (Figure 1). The tearing process in the near term can lead to intermediate-depth seismicity (e.g., Meighan et al., 2013) and explain earthquakes that appear inconsistent with a coherent subducting slab (e.g., Clark et al., 2008). Tears can lead to large volume magmatism (e.g., Cocchi et al., 2017), changes in igneous geochemistry, and facilitate the ore-forming process and mineral deposits (e.g., de Boorder et al., 1998; Rabayrol et al., 2019; Rabayrol and Hart, 2021). The process leads to asthenosphere upwelling and changes in thermal and fluid regimes (e.g., Roche et al., 2018; Gessner et al., 2018). Slab tear has been related to present and past geothermal activity in Western Anatolia and the generation of a late Eocene-Miocene metallogenic period (Pb-Zn- followed by Au-rich) (Menant et al., 2018; Gessner et al., 2018; Rabayrol & Hart, 2021). Their presence significantly affects plate dynamics, including subduction rates, plate motion, and mantle dynamics (e.g., Gianni et al., 2019).

These sites vary in scale from regional to local and include the boundary between the Hellenic and Cyprus arcs (Wortel & Spakman, 1992; Biryol et al., 2011), at the Anaximander Mountains (Woodside et al., 1992), south of Crete at the Pliny–Strabo Shear Zone (Özbakır et al., 2013), the İBTZ transfer zone (e.g., Kaya, 1981; Gessner et al., 2013), and beneath the Menderes Massif itself (Biryol et al., 2011; Rabayrol & Hart, 2021). A tear is speculated to generate a ~200 km-depth low-velocity anomaly below western Turkey (Roche et al., 2019). Slab tear has been used to interpret the deep Rhodes Basin (Faccenna et al., 2014; Woodside et al., 2000) and tectonic activity within southwest Anatolia (Biryol et al., 2011; Roche et al., 2019).

Trench-parallel tear affects the subducting African lithosphere between northern Greece and the Gulf of Corinth along the Western Hellenic Arc (Hansen et al., 2019). Trench-perpendicular tear may accommodate the region between the Hellenic and Cyprian arcs, which differ in subduction steepness and material subducted (Dilek & Sandvol, 2009). The Cyprian arc involves shallower subduction dynamics with the Eratosthenes seamount and Anixamander Mountains (mud volcanoes; Lykousis et al., 2009) impinging on the trench (Figure 9) (Kempler

& Ben-Avraham 1987; Zitter et al. 2003). The back thrusts and tectonic geometry of the Mediterranean Ridge has led to speculation that the African slab detached in the region between Libya and Crete (Kopf et al., 2003). Alternatively, a Subduction Transform Edge Propagator (STEP., a tear fault or a hinge fault, Govers & Wortel, 2005) may exist in this region (Özbakır et al., 2013). Nine of these structures have been proposed to exist beneath southern Greece, segmenting the subducting African slab and contributing to seismicity and deformation (Sachpazi et al., 2016). A STEP is also proposed for the transition between the Cyprus and Hellenic arcs (e.g., Salaün et al., 2012; Elitez et al., 2016; Portner et al., 2018).

The KTZ (Figure 1 and Figure 9) has been a particular subject of the debate regarding slab tear (see Bocchini et al., 2018; Hansen et al., 2019). The structure is part of the Western Hellenic Subduction Zone, considered one of the most seismically active areas in Europe (Pearce et al., 2012; Halpaap et al., 2018). The KTZ may represent a vertical tear along oceanic and continental lithosphere (Suckale et al., 2009), forming the KTZ as a STEP-fault (Govers & Wortel, 2005). The STEP fault may be in its initial stages of forming (Evangelidis, 2017; Özbakır et al., 2020), or the slab may have entirely detached (Wortel & Spakman, 2000). A smooth transition has also been proposed between two segments, without the presence of a tear between, at least at depths shallower than 100 km (Pearce et al., 2012; Halpaap et al., 2018).

Despite the fragmentation of the subducting African lithosphere, the thickness of the Aegean and Anatolian crust is remarkably similar (Zhu et al., 2005; Sodoudi et al., 2006; Karabulut et al., 2019). Estimates from the central Menderes Massif are 28–30 km (Zhu et al., 2005), whereas the thickness beneath the Aegean Sea averages ~25 km (Zhu et al., 2005; Tirel et al., 2004; Kind et al., 2015). The crustal thickness in the southern and central parts of the Aegean is reported to be thinner (20–22 km), whereas the northern Aegean Sea shows a relatively thicker crust (25–28 km) (Karagianni et al., 2005; Sodoudi et al., 2006). Depending on the model used, the crustal thickness beneath western Crete could be 32.5-35 km or up to 45 km (Snopek et al., 2007). Karabulut et al. (2019) demonstrates large crustal thickness variations (20–47 km) from western Greece to eastern Anatolia but shows that these are fairly uniform within specific regions. In Western Anatolia, the crustal thicknesses are 25–30 km, increasing slightly to the north, whereas in southern Anatolia, crustal thicknesses decrease from 35 to 25 km in the Mediterranean Sea, except north of Antalya Bay, where the thickness locally reaches 40 km. A thickness of 40 km is in line with estimates of Eastern Anatolia (Kind et al., 2015), western Greece (Karagianni et al., 2005), and the Anatolian plateau (Saunders et al., 1998).

These thickness estimates seem at odds with large-scale back-arc thinning typically seen in subduction zone settings (e.g., Saunders & Tarney 1984). The Aegean is not a typical back-arc basin (Agostini et al., 2010; Doglioni et al., 2002) because it is underlain by a thick layer of continental crust and lacks an ocean floor (e.g., Makris, 1978), is disrupted by the active North Anatolian Shear Zone (NASZ) in its northern portion (e.g., Brooks & Ferentinos, 1980; Gürer et al., 2006; Kokkalas et al., 2006; Kreemer et al., 2004; Lyberis, 1984). The region displays a complex tensional regime where crustal stretching is inconsistent with the geometry and direction of the subducting Hellenic slab (e.g., Mantovani et al., 1997; Agostini et al., 2010). The premise of extrusion tectonics driven by convergence in the west requires a free lateral boundary in the east. However, the Aegean plate is constructed mainly of continental lithosphere and has a similar thickness as the Anatolian plate, as seen in both bathymetry (Figure 9) and seismic reflection (e.g., Zhu et al., 2005; Sodoudi et al., 2006). However, slab ruptures associated with the differential retreat, inherited lower plate lithospheric heterogeneities, and mantle upwelling

would provide accommodation for the microplates to extrude (Agostini et al., 2010; Govers & Fichtner et al., 2016; Karabulut et al., 2019). The onset of the NASZ may be the result of slab deformation and detachment beneath the Bitlis–Hellenic subduction zone, which accelerated slab retreat in the west and indentation of the continent along the Bitlis–Zagros suture zone (Figure 1) (Faccenna et al., 2006; Schildgen et al., 2014)

3.2 Timing, number, and geometry of transfer zones

Transfer zones play a significant role in accommodating tectonic escape (Barbot & Weiss, 2021), and despite their importance in accommodating the present-day subduction dynamics, when, how, and why specific transfer zones occur across Western Anatolia is debated. For example, the İBTZ is a deep crustal transform fault zone consisting of NE-trending active strike-slip dominated faults and accommodates differential deformation between the Cycladic and Menderes core complexes (Uzel et al., 2013; 2020). The İBTZ is also mapped as the Western Anatolian Transfer Zone (WATZ, Gessner et al., 2013; 2017). The zone may be the surface expression of a tear in the subducting African slab (Gessner et al., 2013; Uzel et al., 2015; Sümer et al., 2018) or a transition between extensional and strike-slip dynamics due to the southward rotation rollback of the subduction zone (Ersoy & Palmer, 2013; Özkaymak et al., 2013; Ersoy et al., 2014; Ersoy et al., 2017; Uzel et al., 2020). Based on a compilation of data from igneous rocks throughout Western Anatolia, Uzel et al. (2020) suggest that volcanic activity in the region is always associated with the İBTZ as recorded by the positions of the eruption centers that follow the trend of the transfer zone. A lack of $^{40}Ar/^{39}Ar$ ages from igneous assemblages between 15.97 and 13.82 Ma is attributed to a pulse of core complex exhumation and a change in partitioning extension between the Cyclades and Menderes Massif. Geochemical compositions of Miocene-age (17.48–14.94 Ma) volcanoes within the transfer zone indicate their origins are decompression melting of the upper mantle/lower crust, consistent with the outcome of regional transtensional movements in a post-collisional setting (Seghedi et al., 2015). Slab-tear typically results in asthenosphere-derived (Ocean-Island Basalt, OIB-like) Na-alkaline basalts, which are only exposed in the region within the northern Menderes Massif (Kula volcanics) (Holness & Bunbry, 2006; Ersoy et al., 2017).

The İBTZ may trend further south into the MCL, an extensional fault exposed near or on the island of Paros that records orogen-parallel extension or transform fault motion (Figure 11) (Morris & Anderson, 1996; Avigad et al., 1998; Walcott & White, 1998; Pe-Piper et al., 2002; Tirel et al., 2009; Gessner et al., 2013; Philippon et al., 2014; Beniest et al., 2016; Malandri et al., 2017). Besides the İBTZ, the SWASZ and UMTZ are located near each other on the border of the Menderes Massif, but their influence on each other is presently unclear (Figure 2).

3.3 Magmatic influence in driving extension

Throughout Western Anatolia, magmatic pulses are exposed as geochemically variable extrusive and intrusive igneous rocks (Tables 1-9; Figure 4; e.g., Rossetti et al., 2017). Metamorphic core complexes with their associated post-collisional magmatic suites offer insights into the tectonic processes controlling crustal extension (e.g., Perkins et al., 2018). Extensional systems cut igneous intrusions in Western Anatolia metamorphic core complexes, and their ages are critical for timing events that facilitated their emplacement. Geochemical data regarding the depths of granite formation lends additional insight into how the mantle processes operated in the past. The picture, however, is complicated by the influence of the collisional dynamics that characterized the earlier assembly of the microplate (see Assembly section).

Granite crystallization ages provide information regarding how extension during the Eocene to Miocene migrated through Western Anatolia and the Aegean region in the past (e.g., Delaloye & Bingöl, 2000; Pe-Piper, 2000; Altunkaynak & Dilek, 2006; Altunkaynak et al., 2012).

Magma bodies can drive extension through the conductive transfer of heat from upwelling of hot, asthenospheric mantle beneath significantly extended crust, and small volume partial melts can exploit crustal pathways developed during extensional deformation (e.g., McKenzie & Bickle 1988; von Blanckenburg & Davies 1995; Perkins et al., 2018). Volatiles facilitate additional crustal deformation and metamorphism, resulting in feedbacks between decompression and mantle upwelling and driving additional lithospheric melting (Teyssier & Whitney, 2002; Kendall et al., 2005; Whitney et al., 2013; Platt et al., 2015; Perkins et al., 2018). The Menderes Massif of western Turkey is suggested to be a key area to study feedback relationships between magma generation/emplacement, rheological weakening, activation of extensional detachment tectonics (Rossetti et al., 2017). The island of Naxos likewise illustrates the interplays between lower crustal flow and upper crustal extension and between buoyancy- and isostasy-driven controls in developing migmatite domes (Kruckenberg et al., 2011). The connections between detachment faulting and magma emplacement have also been explored in the Cyclades (e.g., Rabillard et al., 2018).

To determine the role between magma generation and extension requires understanding intrusive rock relationships to fault structures. In Western Anatolia, maps of the same pluton are commonly inconsistent in terms of the locations of structures that may have affected or result from exhumation. For example, the northern boundary of the Kozak pluton (Figure 4) is shown by some as an intrusive contact (Akal & Helvacı, 1999) but by others as fault-bounded (Altunkaynak & Yilmaz, 1998; 1999; Yilmaz et al., 2001). The Eğrigöz, Koyunoba, and Alaçam plutons (Figure 4) have been the focus of many field-based, geochemical and geochronological studies, but conflicting ideas exist regarding their relationship to the SDF (Figure 7) (see Catlos et al., 2012). For example, Işık and Tekeli (2001) map the SDF only along the northern portion of the Eğrigöz pluton, whereas Ring and Collins (2005) and Işık et al. (2004) indicate the SDF is exposed along the western edge of both the northern Eğrigöz and Koyonba plutons. Seyitoğlu et al. (2004) place the SDF within the central portion of the Eğrigöz pluton, whereas Ersoy et al. (2010) mark the structure as following the outer boundaries of the Eğrigöz and Koyunoba bodies. Thomson and Ring (2006) place the detachment prominently along the northern edge and central portion of the Eğrigöz granite and along the eastern edge of the Koyunoba body. Recent gravity measurements suggest an igneous intrusion at depth near the Simav Fault (Toker et al., 2018, 2019). The 12-15 km-thick intrusion is located in the NE margin of the Simav graben at 2.5-3 km below the surface and has been suggested to be a primary driver of recent-day seismicity. Developing links between magmatism and extensional dynamics requires a critical structural understanding of the granite petrology, structures, and clear delineation between how it appears affected by fault systems (e.g., Kruckenberg et al., 2011; Rabillard et al., 2018).

In Western Anatolia, many published maps also do not distinguish different granite types or textural orientations (Karacik & Yılmaz, 1998; Akal & Helvacı, 1999; Şahin et al., 2010). Mineral lineations and solid-state or magmatic fabrics associated with faulting or shearing are rarely reported. Besides the standard structural and petrographic analyses, cathodoluminescence (CL) images of extensional-related Western Anatolia granites (Salihli and Turgutlu, Catlos et al., 2010; Eğrigöz, Koyunoba, and Alaçam, Catlos et al., 2012; Figure 4) help document mineral zoning, deformation, and fluid alteration (e.g., Ramseyer et al., 1992; Catlos et al., 2016).

Western Anatolia granites share many similar microtextural characteristics in CL., including evidence for fluid interactions and multiple generations of microcracks. The samples show secondary alteration textures, mineral growth generations, and evidence for fluid migration. The generations of microfractures, microcracks, and microfaults seen in CL document that these granites experienced brittle deformation multiple times, both at depth and at lower temperatures near the surface (Catlos et al., 2010; 2012). CL imagery is a powerful tool for identifying mineral textural relationships, growth histories, and deformation structures of Western Anatolia granite assemblages.

3.4 Timing the switches in the stress regimes in Western Anatolia

The Simav Fault system illustrates another outstanding question regarding deciphering stress regimes within Western Anatolia (Figure 7). On 19 May 2011, a magnitude 5.7 (Mww, USGS and Turkish Ministry of the Interior, Disaster and Emergency Management Presidency, Earthquake Department, AFAD) earthquake occurred near the town of Simav. The epicenter was located ~53 km NNW of Uşak and ~82 km WSW from Kütahya in western Turkey at 20:15:23.4 GMT. The estimated depth of the earthquake varies (Doğangün et al., 2013). Table 9 reports the 24.46 km result from AFAD, although the USGS Earthquake Catalog suggests a shallower 7.0 km depth. Görgün (2014) estimated a best-fit hypocenter depth of 10 km and 6.0 magnitude (Mw). Karasözen et al. (2016) indicate that the centroid depth was 7–9 km, but the hypocenters of the mainshock and largest aftershocks were located systematically deeper at depths of 10–22 km. In approximately the same location, an Mw ~5.1 event preceded the mainshock on 17 February 2009, and an Mw 4.4 foreshock occurred 15 min before the mainshock (e.g., Karasözen et al., 2016).

The Simav region is considered to be one of the most seismically active portions of Western Anatolia (Inel et al., 2013; Görgün, 2014), and the 19 May 2011 Simav (Kütahya) earthquake was the largest felt in the region since the destructive 1969 Demirci and 1970 Gediz earthquake sequences (e.g., Ilhan, 1971; Ambraseys & Tchalenko, 1972; Eyidoğan & Jackson, 1985). All of these earthquakes involved dominant normal faulting with nucleation zones from 6-10 km depth and dips of 30-50° (Eyidoğan & Jackson, 1985; Emre & Duman, 2011; Görgün, 2014; Karasözen et al., 2016). However, a strike-slip component is recorded by some of the aftershocks of the 1969 and 1970 earthquakes and the 2011 Simav event (Figure 7B) (Ambraseys & Tchalenko, 1972; Eyidoğan & Jackson, 1985; Emre & Duman, 2011). In addition, Figure 7B shows that some earthquakes in the Simav region after the 2011 event also yield fault plane solutions that include some or a significant strike-slip component.

The epicenters of these earthquakes occurred near the Simav Fault (Figure 7) (Seyitoğlu, 1997; Ersoy et al., 2010). The fault extends ~150 km between the towns of Banaz in the east and Sındırgı in the west (Ambraseys & Tchalenko, 1972; Seyitoğlu, 1997; Ersoy et al., 2010). It may be part of a larger extensional Akşehir-Simav Fault System (Koçyiğit & Deveci, 2007), which extends >250 km from the town of Akşehir in south-central Turkey and includes the Sultandağ Fault in the east (Aksarı et al., 2010). Or, it may be part of the Sındırgı-Sincanlı Fault Zone (SSFZ) between the towns of Soma and Afyon (Doğan & Emre, 2006). The Simav Fault may also connect to the Muratdağ Fault near the town of Gediz in an en echelon pattern, which lends support for a right-lateral system (Ambraseys & Tchalenko, 1972). Where the Akşehir-Simav Fault System is located between the cities of Uşak and Afyon is unclear (e.g., Karasözen et al. 2016).

The Simav Fault is assigned as an active right-lateral strike-slip fault in active tectonic maps of Turkey (Şaroğlu et al., 1992; Emre et al., 2011). This sense of motion is based on offsets of metamorphic zones east of Simav (Konak, 1982; Seyitoğlu, 1997) and its relationship to the formation of the NAFZ (Konak, 1982; Doğan & Emre, 2006; Emre & Duman, 2011). The strike-slip motion is also consistent with uniform (magnitude and orientation) GPS plate velocity vectors that show the region is extruding through an SW motion from 30–40 mm/yr (McClusky et al., 2000; Reilinger et al., 2006, 2010). However, the detailed analysis of the Simav fault mechanisms consistently indicates a normal mechanism (Görgün, 2014; Yolsal-Çevikbilen et al., 2014; Demirci et al., 2015; Karasözen et al., 2016; Bello et al., 2017; Mutlu, 2020). This origin is linked to subduction-related extension along the Hellenic and Cyprus arcs (e.g., Seyitoğlu, 1997; Işik et al., 2003; Ersoy et al., 2010; Görgün, 2014; Yolsal-Çevikbilen et al., 2014; Demirci et al., 2015; Karasözen et al. 2016; Bello et al., 2017).

If the Simav Fault was initiated as a strike-slip system but switched to extension sometime after the Late Miocene is possible (Oygür & Erler, 2000). Strike-slip motion has also been speculated to predate subsidence currently experienced by Western Anatolia and may be related to Eocene to Oligocene compression (Oygür & Erler, 2000). Based on an analysis of the available data from the 19 May 2011 event, Görgün (2014) indicate that the hypocenter distribution is consistent with the activation of two nearly parallel faults: one northern one with a fault plane trending mainly E–W and dipping towards SE and a southern fault plane trending NW–SE and dipping towards SE. The strike-slip mechanisms are delegated to smaller fault segments that experience a stress change after the mainshock and more minor secondary faults in the region with different mechanisms. Karasözen et al. (2016) suggest the potential involvement of structures inherited from earlier deformation phases of shortening and extension in evaluating the nature of motion along the structure.

The Simav E-W trending-graben hosts one of Turkey's most important geothermal systems (Bello et al., 2017). Based on a study of geothermal activity, soil radon gas release, and regional seismicity patterns, İnan et al. (2012) suggests that the epicentral area of the 19 May 2011 Simav earthquake is located within a block that is tectonically separated from Aegean Extensional Province and the Marmara Region. The observation is also supported by geodetic data that show a region surrounding the event behaves distinctly from the Aegean Extensional Province (Tiryakioğlu, 2011). Yolsal-Çevikbilen et al. (2014) suggest the magnitude of the stress drop associated with the 19 May 2011 event (62 bars) is more consistent with an intraplate earthquake compared to those associated with Aegean plate boundaries (3-11 bars).

3.5 Relating geological units and events across boundaries

As noted in the Geological Background section, several units and structures can be correlated from Western Anatolia to the Aegean region. For example, the Cyclades Blueschist Unit (CBU) from the southern portion of the Menderes Massif (Figure 12A) is often matched to outcrops exposed in the Cyclades (Ring et al., 1999; Roche et al., 2018; Çetinkaplan et al., 2020; Barbot and Weiss, 2021), but distinguishing structures developed during subduction-related burial and prograde metamorphism from those that formed due to decompression and retrogression is problematic (e.g., Rosenbaum et al., 2002; Xypolias et al., 2012; Çetinkaplan et al., 2020). The CBU experienced multiple phases of deformation and mineralogical transformations (e.g., Seman et al., 2017; Gerogiannis et al., 2019). Identifying local internal structures from those that would correlate as significant deformation zone poses a challenge.

Çetinkaplan et al. (2020) suggest that the contact between the Menderes Massif and the CBU, now defined by a ductile thrust fault, was originally a lithosphere-scale transform fault zone.

The timing of detachment systems in the Menderes Massif are similar to those estimated in the Cyclades. Three major Aegean microplate detachment systems include the North Cycladic Detachment on Andros, Tinos, and Mykonos (Figure 11) (e.g., Jolivet et al., 2010), the Naxos-Paros Detachment on Naxos and Paros (Buick, 1991; John & Howard, 1995; Cao et al., 2013), and the West Cycladic Detachment on Serifos (Grasemann et al., 2012). The North Cycladic Detachment may have initiated activity in the Oligocene until the Late Miocene (e.g., Jolivet et al., 2010). The Naxos-Paros Detachment records retrogression associated with its latest activity in the Late Miocene (e.g., Cao et al., 2017). These time frames are similar to constraints estimated for the activity of detachment faulting in the central Menderes Massif (Hetzel et al., 1995a, Hetzel et al., 1995b, Işık et al., 2003, Glodny & Hetzel, 2007; Catlos et al., 2010). The Cyclades Detachments cross-cut blueschist-amphibolite facies fabrics and post-date HP metamorphism and peak Barrovian metamorphism (Searle and Lamont, 2020a).

Another correlation links the lithologies, conditions, and metamorphic history of Menderes Massif nappes to those in the Cyclades (e.g., Robertson et al., 1991; Ring et al., 1999; Stampfli, 2000; Çetinkaplan et al., 2020). Menderes Massif nappes have zoned garnets useful for generating P-T conditions and paths (e.g., Figure 12B and Figure 13). These paths are often developed by connecting peak metamorphic conditions of individual rocks, inferences from mineral assemblages, pseudosections, or Gibbs method thermodynamic modeling (e.g., Ashworth & Evirgen, 1984; 1985a,b; Ring et al., 2001; Whitney & Bozkurt, 2002; Cenki-Tok et al., 2016; Etzel et al., 2019; 2020). Despite these studies, the number and timing of garnet-growth events recorded in the rocks remain unclear. Some Çine nappe rocks experienced two stages of garnet growth (Ring et al., 2001), whereas other samples are consistent with one episode (Régnier et al., 2007). Pan-African garnet growth is recorded in the Menderes Massif, and conditions could reflect events unrelated to MMM (Ring et al., 2004; Catlos & Çemen, 2005). Gessner et al. (2001) report that the Bayındır nappe deformed once during the Eocene related to MMM., whereas the Bozdağ, Çine, and Selimiye nappes record pre-MMM and MMM events. This contradicts Oberhaensli et al. (1997), who suggest the cover sequence records deformation during the Eocene, but structurally lower units record pre-MMM events. Studies of Bozdağ nappe rocks show prograde burial, but conditions decrease downward by ~40°C/kbar per km of structural section (inverted metamorphism, Ring et al., 2001). Selimiye nappe rocks record exhumation and retrogression (Régnier et al., 2007). Paths in Figure 12B were generated by connecting peak metamorphic conditions of individual rocks, inferring from mineral assemblages, pseudosections, or Gibbs method thermodynamic modeling. P-T paths that decrease in pressure or temperature suggest the potential for tectonic switching as unloading and refrigeration occur when the thrust reverses and experiences extension.

Challenges for generating P-T conditions and paths include a prior garnet-producing history and retrograde fluid-inducted alteration and overprinting as the core complex formed (e.g., Satir & Taubald, 2001; Régnier et al., 2003; Catlos & Çemen, 2005; Baker et al., 2008; Candan et al., 2011). Menderes Massif rocks are known to yield problematic P-T estimates based on evidence of disequilibrium among phases and the application of barometers to inappropriate (uncalibrated) mineral compositions (Ashworth & Evirgen, 1984; 1985a,b). In some cases, calculated conditions appear at odds with observed mineral assemblages and structural data (Ring et al., 2001; Whitney & Bozkurt, 2002). Pressure estimates using conventional approaches

are challenging to obtain due to the lack of appropriate mineral assemblages (Iredale et al., 2013). Problems may arise if the chosen mineral compositions for thermobarometric calculations are associated with retrogression instead of the desired prograde conditions. P-T paths that only rely on core and rim measurements are also limited in their ability to test models developed regarding lithospheric response to perturbations, including motion within fault zones.

One promising avenue to address this issue is the application of isochemical phase equilibria modeling. Figure 13 shows this approach applied to garnets from the Menderes Massif's Çine, Selimiye, and Bayindir nappe from Etzel et al. (2019) and Etzel et al. (2020) and a sample from the Northern Menderes Massif from Cenki-Tok et al. (2016). The researchers report petrological details, X-ray element maps, and geochemical data from the rocks. They compositionally analyzed micaschists with a mineral assemblage of garnet + biotite + plagioclase + muscovite + quartz + rutile ± ilmenite ± apatite ± pyrite ± zircon ± monazite. The sample from the Northern Menderes Massif contains kyanite and small porphyroblasts of staurolite. Using data reported in the papers, isochemical phase diagrams were created using rock bulk compositions, the software package Theriak-Domino (de Capitani & Brown, 1987; de Capitani & Petrakakis, 2010) with the Holland and Powell (1998; 2010) thermodynamic data set, and appropriate mixing models in the system MnO–Na2O–CaO–K2O–FeO–MgO–Al2O3–SiO2–H2O–TiO2. Isopleths of ±0.01 mole fraction spessartine, almandine, pyrope, and grossular corresponding with the garnet core composition, are plotted on the phase diagram. This portion of the diagram with intersecting isopleths approximates the chemical system at the time garnet began growth. This diagram also tests if the thermodynamic data set and mixing models used in the modeling are appropriate for these particular samples, as expected mineral assemblages appeared in the phase diagrams with intersecting isopleths.

After the garnet core conditions are estimated, a Matlab script was applied to each step along a garnet compositional traverse from core to rim to yield both an estimate of the P-T conditions of incremental growth and a new effective bulk rock composition, ultimately culminating in a high-resolution P-T path. High-resolution P-T paths are defined as those derived from fractionated equilibrium phase diagram modeling and the resolution is an outcome of the number of garnet fractionated steps. Garnets with complex zoning profiles, modified by diffusion, or rocks that experienced major changes in bulk composition over their growth history are not candidates (e.g., Catlos et al., 2018). However, even these types of samples may provide clues by exploring the reason for their failure (e.g., Catlos et al., 2018; Etzel et al., 2020). Ideal samples are those with garnets that preserve prograde, gradational core-to-rim zoning profiles. Garnets from the Selimiye and Bayindir nappes of the Southern and Central Menderes Massif, respectively, show similar trajectories. However, the Çine nappe garnet yields an N-shape path and a significantly different metamorphic history.

Either tectonically-driven extension may have created the N-shaped P-T path during orogenesis or the result of erosional exhumation during pulses of thrust motion (Etzel et al., 2019). Etzel et al. (2019) developed two thermal models: erosional denudation followed by fault reactivation (Figure 14A) and tectonic switching (Figure 14B), which are briefly summarized here. Figure 14A and Figure 14B show an upper equilibrium thermal grid (depth vs. horizontal distance) before faulting with the position of fault (grey line) arbitrarily selected at 30°. Fault displacement varies linearly across shear zones. The grid includes reflecting side boundaries and top and bottom maintained at 25°C and 700°C and an initial geothermal gradient at 25°C/km indicated by shaded zones. A hatched area shows the position of the Selimiye samples, and the

grey bar represents the approximate initial location of the Çine nappe garnet with the N-shaped P-T path. This position is also represented by point 1 in the P-T path insets. In Figure 14C and Figure 14D, the fault is active. A finite-difference solution to the diffusion-advection equation is used to examine the P-T variations in the hanging wall and footwall due to its motion. The rock sample experiences the point 1 to 2 in the P-T path insets. Fault motion stops and denudation occurs in Figure 14E and, whereas extension occurs in Figure 14F. This process is based on the mid-rim lower pressure portion of the garnet P-T path and is represented by points 2 to 3 on the P-T path insets. Although the end, the surface geometry in the denudation phase (Figure 13E) and extensional phase (Figure 14F) are similar, the shape of the isotherms is different and leads to the development of a decrease in temperature in the P-T loop observed in the tectonic switching model. Finally, the fault is reactivated, represented by Figure 14G to Figure 14H. The decrease in pressure with increasing temperature is related to an episode of denudation (model 1) rather than a tectonic switch from compression to extension (Etzel et al., 2019).

The P-T paths reported in Figure 13 approximate how a garnet with specific compositional zoning would behave in a closed system of a known bulk composition as it evolves during increasing T. A critical assumption is that the minerals in a sample experienced equilibrium, which can never be proven for any rock system (e.g., Spear & Peacock, 1989; Lanari & Duesterhoeft, 2019). Closed system behavior also requires the original compositions of the mineral phases, and the bulk rock has not changed significantly since metamorphism (e.g., Lanari and Engi, 2017). Multiple sources of error are inherent, including uncertainty in the accuracy of end-member reactions, electron microprobe analyses, calibration errors, variations in activity models, compositional heterogeneity, and uncertainty associated with the thermodynamic properties inherent in the choice of internally consistent database (e.g., Kohn & Spear, 1991; White et al., 2014; Palin et al., 2016; Lanari & Duesterhoeft, 2019). Garnets with significant changes in composition over short distances from core to the rim and those affected by diffusion cannot be modeled. Garnets in samples that experienced significant changes in bulk composition or multiple deformation episodes resulting in modification of composition are also unsuitable.

A significant value of the high-resolution P-T path and isopleth approaches is that a user can detect when systems stray from the equilibrium and closed system assumptions. Confidence in paths and conditions increases when minerals assemblages agree with rock observations and if the P-T paths reproduce trends in garnet zoning. Samples collected from the same outcrop or nearby should yield similar P-T conditions and paths. In addition, a user can gauge the extent of overlapping mineral isopleths in P-T space, including if matrix mineral compositions overlap the garnet rim conditions. These paths are the first steps in developing critical insights into the metamorphic history of the assembly of the Menderes Massif and, combined with age information from the garnet itself or matrix or mineral inclusions, can be used to test models for the development of Western Anatolia.

4. Conclusions

This paper is divided into two major sections. The first outlines, as much as is possible, our present-day understanding of the geological history of Western Anatolia from its assembly through its extensional and strike-slip history. We aim to illustrate the complex tectonic scenario before the onset of large-scale extension and emphasize the present-day change in stress regime towards strike-slip tectonics. The transitions are also comparable in duration and timing to those experienced by the Aegean microplate.

The second part highlights some outstanding questions that remain to be addressed. These include issues regarding the dynamics of the African slab along the Hellenic arc, the arc's geometry and connections to other subduction systems, and reconciling the Jurassic initiation age of subduction with Late Cenozoic sedimentation, magmatic, and paleogeographic data that are consistent with younger initiation. In addition, a large number of regions of slab tear are proposed throughout the African slab, and their influence on accommodating extrusion, creating economic resources, and driving lithospheric thinning and magmatism should be explored. Other questions include investigating the influence of transfer zones in accommodating deformation and the role of magma in driving extension in Western Anatolia.

The interface between Western Anatolia and the Aegean region exemplifies tectonic transitions and how the interplay between large-scale tectonics influences smaller-scale processes. The Aegean and western Turkey contain helpful assemblages that can be exploited to time these processes that shape the lithosphere and are critical in understanding the region's hazards and mineralizations. Extracting high-resolution P-T paths from Western Anatolia garnet-bearing rocks is a promising approach to evaluate tectonic models and correlate and compare metamorphic histories of nearby assemblages and from those across long distances.

Data Availability Statement

Data supporting the conclusions of this paper and color figures are publically available from Texas Data Repository Dataverse (https://doi.org/10.18738/T8/ER3WQV).

Acknowledgements

We appreciate constructive reviews of the original manuscript from Spyros Pavlides (Aristotle University of Thessaloniki, Greece), Thomas Lamont (University of Bristol) and three anonymous reviewers. We appreciate analytical assistance with the $^{40}Ar/^{39}Ar$ analysis from the Australia National University Argon Facility.

References

Agostini, S., Doglioni, C., Innocenti, F., Manetti, P., & Tonarini, S. (2010). On the geodynamics of the Aegean Rift. In I. Çemen (Ed.), Extensional tectonics in the Basin and Range, the Aegean, and western Anatolia. Tectonophysics, 488, 7-21. https://doi.org/10.1016/j.tecto.2009.07.025

Akal, C. (2013). Coeval shoshonitic–ultrapotassic dyke emplacements within the Kestanbol Pluton, Ezine-Biga Peninsula (NW Anatolia). Turkish Journal of Earth Sciences, 21, 1–20.

Akal, C., & Helvacı, C. (1999). Mafic microgranular enclaves in the Kozak granodiorite, western Anatolia. Turkish Journal of Earth Sciences, 8, 1–17.

Akay, E. (2009). Geology and petrology of the Simav Magmatic Complex (NW Anatolia) and its comparison with the Oligo-Miocene granitoids in NW Anatolia: implications on Tertiary tectonic evolution of the region. International Journal of Earth Sciences, 98, 1655–1675.

Akbayram, K., Şengör, A. M. C., & Ozcan, E. (2016). The evolution of the intra-Pontide suture; implications of the discovery of late Cretaceous-early Tertiary melanges. In R. Sorkhabi (Ed.), Tectonic evolution, collision, and seismicity of southwest Asia; in honor of Manuel Berberian's forty-five years of research contributions. Special Paper - Geological Society of America (Vol. 525). https://doi.org/10.1130/2016.2525(18)

Aksari, D., Karabulut, H., Ozalaybey, S. (2010). Stress interactions of three moderate size earthquakes in Afyon, southwestern Turkey. Tectonophysics, 485, 141-153. https//doi.org/10.1016/j.tecto.2009.12.010

Aktuğ, B., Parmaksız, E., Kurt, M., Lenk, O., Kılıçoğlu, A., Ali, M., & Soner Özdemir, G. (2013). Deformation of Central Anatolia: GPS implications. Journal of Geodynamics, 67, 78-96. https://doi.org/10.1016/j.jog.2012.05.008

Aldanmaz, E. (2012). Osmium isotope and highly siderophile element geochemistry of mantle xenoliths from NW Turkey: implications for melt depletion and metasomatic history of the sub-continental lithospheric mantle. International Geology Review, 54(7), 799-815. https://doi.org/10.1080/00206814.2011.581799

Aldanmaz, E., Pearce, J. A., Thirlwall, M. F., & Mitchell, J. G. (2000). Petrogenetic evolution of Late Cenozoic, post-collision volcanism in Western Anatolia, Turkey. Journal of Volcanology and Geothermal Research, 102, 67–95.

Alatza, S., Papoutsis, I., Paradissis, D., Kontoes, C., & Papadopoulos, G.A. (2020). Multi-Temporal InSAR Analysis for Monitoring Ground Deformation in Amorgos Island, Greece. Sensors, 20(2), 338. https://doi.org/10.3390/s20020338

Altherr R., Henjeskunst, F., Matthews, A., Friedrichsen, H., Hansen, & B.T. (1988). O-Sr isotopic variations in Miocene granitoids from the Aegean—evidence for an origin by combined assimilation and fractional crystallization. Contributions to Mineralogy and Petrology, 100(4), 528–541

Altherr, R., & Siebel, W. (2002). I-type plutonism in a continental back-arc setting: Miocene granitoids and monzonites from the central Aegean Sea, Greece. Contribution to Mineralogy and Petrology, 143, 397–415. https://doi.org/10.1007/s00410-002-0352-y

Altunkaynak, Ş. (2007). Collision-driven slab breakoff magmatism in northwestern Anatolia, Turkey. Journal of Geology, 115, 63–82

Altunkaynak, Ş., & Dilek, Y. (2006). Timing and nature of postcollisional volcanism in western Anatolia and geodynamic implications. In Y. Dilek, S. Pavlides (Eds.), Postcollisional tectonics and magmatism in the Mediterranean region and Asia. Special Paper - Geological Society of America, 409, 321-351.

Altunkaynak, Ş., & Genc, S. (2008). Petrogenesis and time-progressive evolution of the Cenozoic continental volcanism in the Biga Peninsula, NW Anatolia (Turkey). In: Xu, Y., Farmer, L., Menzies, M., Rudnick, R., Zhou Meifu, Z. Continental volcanism and chemistry of the Earth's interior. Lithos, 102, 316-340.

Altunkaynak, Ş., & Yılmaz, Y. (1998). The mount Kozak magmatic complex, western Anatolia. Journal of Volcanology and Geothermal Research, 85, 211–231.

Altunkaynak, Ş., Dilek, Y., Genç, C. Ş., Sunal, G., Gertisser, R., Furnes, H., Foland, K.A., & Yang, J. (2012). Spatial, temporal and geochemical evolution of Oligo–Miocene granitoid magmatism in western Anatolia, Turkey. Gondwana Research, 21(4), 961-986. https://doi.org/10.1016/j.gr.2011.10.010

Amaru, M.L. (2007). Global travel time tomography with 3-D reference models. PhD Thesis Utrecht University. http://dspace.library.uu.nl/bitstream/handle/1874/19338/index.htm;jsessionid=88B6AA4941C5E76FD65034D89D4065E0?sequence=17

Ambraseys, N.N., & Tchalenko, J.S. (1972). Seismotectonic aspects of the Gediz, Turkey, Earthquake of March 1970. Geophysical Journal of the Royal Astronomical Society, 30(3), 229-52,

Anastasakis, G., & Keling, G. (1991). Tectonic connection of the Hellenic & Cyprus arcs & related geotectonic elements. Marine Geology, 97(3-4), 261-277. https://doi.org/10.1016/0025-3227(91).90120-S

1165 Angelier, J., Lybéris, N., Le Pichon, X., Barrier, E., & Huchon, P. (1982). The tectonic
1166 development of the hellenic arc & the sea of crete: A synthesis. Tectonophysics, 86(1-3),
1167 159-196. https://doi.org/10.1016/0040-1951(82).90066-X
1168 Armijo, R., Meyer, B., Hubert, A., & Barka, A. (1999). Westward propagation of the North
1169 Anatolian fault into the northern Aegean: Timing and kinematics. Geology, 27, 267-270. ,
1170 https//doi.org/10.1130/0091-7613(1999)027<0267:WPOTNA>2.3.CO;2
1171 Ashworth, J. R., & Evirgen, M. M. (1984). Garnet and associated minerals in the southern
1172 margin of the Menderes Massif, Southwest Turkey. Geological Magazine, 121(4), 323-337.
1173 Ashworth, J. R., & Evirgen, M. M. (1985a). Plagioclase relations in pelites, central Menderes,
1174 Massif, Turkey; II., Perturbation of garnet-plagioclase geobarometers. Journal of
1175 Metamorphic Geology, 3(3), 219-229.
1176 Ashworth, J. R., & Evirgen, M. M. (1985b). Plagioclase relations in pelites, central Menderes
1177 Massif, Turkey; I., The peristerite gap with coexisting kyanite. Journal of Metamorphic
1178 Geology, 3(3), 207-218.
1179 Avigad, D., Baer, G., & Heimann, A. (1998). Block rotations and continental extension in the
1180 central Aegean Sea: Palaeomagnetic and structural evidence from Tinos and Mykonos
1181 (Cyclades, Greece). Earth and Planetary Science Letters, 157, 23–40.
1182 https//doi.org/10.1016/S0012-821X(98)00024-7
1183 Avigad, D. & Garfunkel, Z. (1991). Uplift and exhumation of high-pressure metamorphic
1184 terrains: the example of the Cycladic blueschist belt (Aegean Sea). Tectonophysics, 188,
1185 357–372.
1186 Aydoğan, M.S., Coban, H., Bozcu, M., & Akinci, O. (2008). Geochemical and mantle-like
1187 isotopic (Nd, Sr). composition of the Baklan Granite from the Muratdagi region (Banaz,
1188 Usak), western Turkey; implications for input of juvenile magmas in the source domains of
1189 western Anatolia Eocene-Miocene granites. Journal of Asian Earth Sciences, 33, 155-176.
1190 https://doi.org/10.1016/j.jseaes.2006.10.007
1191 Aysal, N., Ongen, S., Peytcheva, I., & Keskin, M. (2012). Origin and evolution of the Havran
1192 Unit, western Sakarya basement (NW Turkey); new LA-ICP- MS U-Pb dating of the
1193 metasedimentary-metagranitic rocks and possible affiliation to Avalonian microcontinent. In
1194 E. Bozkurt (Ed.), Tectonics of the Eastern Mediterranean-Black Sea region; Part A.,
1195 Dedicated in honor of Aral Okay's 60th birthday. Geodinamica Acta (Vol. 25, pp. 226-247).
1196 https//doi.org/10.1080/09853111.2014.882536
1197 Aysal, N., Şahin, S.Y., Güngör, Y., Peytcheva, I., & Öngen, S. (2018). Middle Permian-early
1198 Triassic magmatism in the Western Pontides, NW Turkey: Geodynamic significance for the
1199 evolution of the Paleo-Tethys. Journal of Asian Earth Sciences, 164, 83-103.
1200 https://doi.org/10.1016/j.jseaes.2018.06.026
1201 Bağcı, M., Ilbeyli, N., Yildiz, A., Kibici, Y., & Demirbilek, M. (2012). Geochemical and
1202 geochronological (Rb/Sr) properties of the Günyüzü granitoids (Sivrihisar, Eskişehir). 12th
1203 International Multidisciplinary Scientific GeoConference, www.sgem.org, SGEM2012
1204 Conference Proceedings, 1, 47-56. https://doi.org/10.5593/SGEM2012/S01.V1007
1205 Baker, C.B., Catlos, E.J., Sorensen, S.S., Çemen, I., & Hancer, M. (2008). Evidence for
1206 polymetamorphic garnet growth in the Cine (southern Menderes). Massif, Western Turkey.
1207 IOP Conference Series, Earth & Environmental Sciences, 2, 012020.
1208 https://doi.org/10.1088/1755- 1307/2/1/012020

1209 Baran, Z.O., Dilek, Y., & Stockli, D. (2017). Diachronous uplift & cooling history of the
1210 Menderes core complex, western Anatolia (Turkey), based on new zircon (U-Th)./He ages.
1211 Tectonophysics, 694, 181-196. https://doi.org/10.1016/j.tecto.2016.12.005
1212 Barbot, S., & Weiss, J.R. (2021). Connecting subduction, extension and shear localization across
1213 the Aegean Sea and Anatolia. Geophysical Journal International, 226(1), 422–445.
1214 https://doi.org/10.1093/gji/ggab078
1215 Barka, A.A. (1992). The north Anatolian fault zone. Annales Tectonicae, 6, 64-195.
1216 Barka, A.A., & Kadinsky-Cade, K. (1988). Strike-slip fault geometry in Turkey and its influence
1217 on earthquake activity, Tectonics, 7(3), 663– 684. https://doi.org/10.1029/TC007i003p00663
1218 Barka, A.A., & Reilinger, R. (1997). Active tectonics of the Eastern Mediterranean Region:
1219 deduced from GPS., neotectonic and seismicity data. Annelis de Geofisica, 40(3), 587–610.
1220 Beccaletto, L., Bonev, N., Bosch, D., Bruguier, O. (2007). Record of a Palaeogene syn-
1221 collisional extension in the north Aegean region: evidence from the Kemer micaschists (NW
1222 Turkey). Geological Magazine, 144(2), 393–400.
1223 https://doi.org/10.1017/S001675680700310X
1224 Beccaletto, L., & Jenny, C. (2004). Geology and Correlation of the Ezine Zone: A Rhodope
1225 Fragment in NW Turkey? Turkish Journal of Earth Sciences, 13, 45-176.
1226 Beißer, M., Wyss, M., & R. Kind, R. (1990). Inversion of source parameters for subcrustal
1227 earthquakes in the Hellenic Arc. Geophysics Journal International, 103, 439-450.
1228 Bello, O.A., Özgür, N., & Çalışkan, T.A. (2017). Hydrogeological, Hydrogeochemical and
1229 Isotope Geochemical Features of Geothermal Waters in Simav and Environs, Western
1230 Anatolia, Turkey. Procedia Earth and Planetary Science, 17, 29-32.
1231 https://doi.org/10.1016/j.proeps.2016.12.014.
1232 Beniest, A., Brun, J.P., Gorini, C., Crombez, V., Deschamps, R., Hamon, Y., & Smit, J. (2016).
1233 Interaction between trench retreat and Anatolian escape as recorded by neogene basins in the
1234 northern Aegean Sea. Marine and Petroleum Geology, 77, 30-42.
1235 https://doi.org/10.1016/j.marpetgeo.2016.05.011
1236 Berckhemer H (1977). Some aspects of the evolution of marginal seas deduced from
1237 observations in the Aegean region. In B. Biju-Duval, L. Montadert (Eds.), Structural History
1238 of the Mediterranean Basins. Ed. Technip: Paris France, p. 303-314.
1239 Bijwaard, H., W. Spakman, & E. R. Engdahl (1998). Closing the gap between regional and
1240 global travel time tomography, Journal of Geophysical Research, 103, 30,055 – 30,078.
1241 Birkle, P. (1992). Petrologie-Geochemie und Geochronologic des miozănen Magmatismus auf
1242 der Biga-Halbinsel (Ezine, NW-Türkie). Diplomarbiet an der Geowissenscahftlichen Fakultät
1243 der Eberhard-Karls-Universität Tübingen, 1992.
1244 Biryol, C.B., Beck, S.L., Zandt, G., & Ozacar, A.A. (2011). Segmented African lithosphere
1245 beneath the Anatolian region inferred from teleseismic P-wave tomography. Geophysics
1246 Journal International, 184, 1037–1057. https://doi.org/0.1111/j.1365-246X.2010.04910.x
1247 Black, K.N., Catlos, E.J., & Oyman, T. (2013). Timing Aegean extension: Evidence from in situ
1248 U–Pb geochronology and cathodoluminescence imaging of granitoids from NW Turkey
1249 (Special Issue: Geodynamics and Magmatism). Lithos, 180-181, 92-108.
1250 https://doi.org/10.1016/j.lithos.2013.09.001
1251 Blom, N., Gokhberg, A., Fichtner, A. (2019). Seismic waveform tomography of the central and
1252 eastern Mediterranean upper mantle. Solid Earth, 11, 669-690. https://doi.org/10.5194/se-11-
1253 669-2020.

Bocchini, G.M., Brüstle, A., Becker, D., Meier, T., van Keken, P.E., Ruscic, M., Papadopoulos, G.A., Rische, M., & Friederich, W. (2018). Tearing, segmentation, and backstepping of subduction in the Aegean: New insights from seismicity. Tectonophysics, 734–735, 96-118. https://doi.org/10.1016/j.tecto.2018.04.002.

Bolhar, R., Ring, U., & Allen, C.M. (2010). An integrated zircon geochronological and geochemical investigation into the Miocene plutonic evolution of the Cyclades, Aegean Sea, Greece: Part 1: Geochronology. Contributions to Mineralogy and Petrology,160, 719–742. https://doi.org/10.1007/s00410-010-0504-4

Bonev, N., & Beccaletto, L. (2007). From syn- to post-orogenic Tertiary extension in the north Aegean region: constraints on the kinematics in the eastern Rhodope–Thrace, Bulgaria–Greece and the Biga Peninsula, NW Turkey. Geological Society, London, Special Publications, 291, 113-142. https://doi.org/10.1144/SP291.6

Bonev, N., Beccaletto, L., Robyr, M., & Monié, P. (2009). Metamorphic and age constraints on the Alakeçi shear zone: Implications for the extensional exhumation history of the northern Kazdağ Massif, NW Turkey, Lithos, 113(1-2), 331-345. https://doi.org/10.1016/j.lithos.2009.02.010

Bozkaya, Ö, Yalçın, H., & Göncüoğlu, M.C. (2012). Diagenetic and very low-grade metamorphic characteristics of the Paleozoic series of the Istanbul Terrane (NW Turkey). Swiss Journal of Geoscience, 105, 183–201. https://doi.org/10.1007/s00015-012-0108-2

Bozkurt, E. (2001). Neotectonics of Turkey - a synthesis. Geodinamica Acta, 14, 3-30.

Bozkurt, E., & Oberhänsli, R. (2001). Menderes Massif (western Turkey).; structural, metamorphic and magmatic evolution; a synthesis. Geologische Rundschau = International Journal of Earth Science [1999], 89(4), 679-708.

Bozkurt, E., & Park, R. G. (1994). Southern Menderes Massif; an incipient metamorphic core complex in western Anatolia, Turkey. Journal of the Geological Society of London, 151(22), 213-216.

Bozkurt, E., & Park, R.G. (1999). The structure of the Palaeozoic schists in the Southern Menderes Massif, western Turkey: A new approach to the origin of the Main menderes metamorphism and its relation to the Lycian Nappes. Geologische Rundschau = International Journal of Earth Sciences, 12(1), 25-42. https://doi.org/10.1016/S0985-3111(99).80021-7

Bozkurt, E., & Satir, M. (2000). The southern Menderes Massif (western Turkey).; geochronology and exhumation history. Geological Journal, 35(3-4), 285-296.

Bozkurt, E., & Sözbilir, H. (2004). Tectonic evolution of the Gediz Graben: Field evidence for an episodic, two-stage extension in western Turkey. Geological Magazine, 141(1), 63-79. https://doi.org/10.1017/S0016756803008379

Boztuğ, D., Harlavan, Y., Jonckheere, R., Can, İ, & Sari, R. (2009). Geochemistry and K-Ar cooling ages of the Ilıca, Çataldağ (Balıkesir) and Kozak (İzmir) granitoids, west Anatolia, Turkey. Geological Journal, 44, 79-103. https://doi.org/10.1002/gj.1132

Brichau, S., Ring, U., Carter, A., Monié, P., Bolhar, R., Stockli, D., & Brunel, M. (2007). Extensional faulting on Tinos Isl&, Aegean Sea, Greece: How many detachments? Tectonics, 26, TC4009. https://doi.org/10.1029/2006TC001969

Brichau, S., Ring, U., Carter, A., Bolhar, R., Monie, P., Stockli, D., & Brunel, M. (2008). Timing, slip rate, displacement and cooling history of the Mykonos detachment footwall, Cyclades, Greece, and implications for the opening of the Aegean Sea basin. Journal of the Geological Society, 165, 263–277.

Brooks, M., & Ferentinos, G. (1984). Tectonics and sedimentation in the Gulf of Corinth and the Zakynthos and Kefallinia channels, Western Greece. Tectonophysics, 101(1-2). 25-54. https://doi.org/10.1016/0040-1951(84)90040-4

Brun, J.-P., & Faccenna, C. (2008). Exhumation of high-pressure rocks driven by slab rollback, Earth and Planetary Science Letters, 272, 1-7. https://doi.org/10.1016/j.epsl.2008.02.038

Brun, J-P., Faccenna, C., Gueydan, F., Sokoutis, D., Philippon, M., Kydonakis, K., Gorini, C. (2016). The two-stage aegean extension, from localized to distributed, a result of slab rollback acceleration. Canadian Journal of Earth Sciences, National Research Council Canada, 53(11), 1142-1157. https://doi.org/10.1139/cjes-2015-0203ff. ffinsu-01271296f

Brun, J-P., Faccenna, C., Gueydan, F., Sokoutis, D., Philippon, M., Kydonakis, K., & Gorini, C. (2017). Effects of slab rollback acceleration on Aegean extension. Bulletin of the Geological Society of Greece, 50(1), 5-23. https://doi.org/10.12681/bgsg.11697

Brun, J-P., Sokoutis, D. (2007). Kinematics of the Southern Rhodope Core Complex (North Greece). International Journal of Earth Sciences, 96(6), 1079-1099. https://doi.org/10.1007/s00531-007-0174-2

Brun, J-P., & Sokoutis, D. (2010).45 m.y. of Aegean crust and mantle flow driven by trench retreat. Geology, 38(9), 815–818. https://doi.org/10.1130/G30950.1

Buick I.S. (1991). The late Alpine evolution of an extensional shear zone, Naxos, Greece. Journal of the Geological Society of London, 148, 93-103.

Bulle, F., Bröcker, M., Gärtner, C., & Keasling, A. (2010). Geochemistry and geochronology of HP mélanges from Tinos and Andros, cycladic blueschist belt, Greece. Lithos, 117(1–4), 61-81. https://doi.org/10.1016/j.lithos.2010.02.004

Bulut, F., Özener, H., Doğru, A., Aktuğ, B., & Yaltırak, C. (2018). Structural setting along the Western North Anatolian Fault and its influence on the 2014 North Aegean Earthquake (Mw 6.9). Tectonophysics, 745, 382-394. https://doi.org/10.1016/j.tecto.2018.07.006

Burchfiel, B.C., Nakov, R., Dumurdzanov, N., Papanikolaou, D., Tzankov, T., Serafimovski, T., King, R.W., Kotzev, V., Todosov, A., & Nurce, B. (2008). Evolution and dynamics of the Cenozoic tectonics of the South Balkan extensional system. Geosphere, 4, 918–938.

Burg, J.-P., Ricou, L.-E., Ivano, Z., Godfriaux, I., Dimov, D., & Klain, L. (1996). Syn-metamorphic nappe complex in the Rhodope Massif. Structure and kinematics. Terra Nova, 8, 6-15. https://doi.org/10.1111/j.1365-3121.1996.tb00720.x

Burtman, V.S. (1994). Meso-Tethyan oceanic sutures and their deformation. Tectonophysics, 234, 305–327.

Candan, O., Akal, C., Koralay, O.E., Okay, A.I., Oberhäsli, R., Prelević, D., & Mertz-Kraus, R. (2016). Carboniferous granites on the northern margin of Gondwana, Anatolide-Tauride Block, Turkey - Evidence for southward subduction of Paleotethys. Tectonophysics, 683, 349-366.

Candan, O., Çetinkaplan, M., Oberhänsli, R., Rimmelé, G., & Akal, C. (2005). Alpine high-P/low-T metamorphism of the Afyon zone and implications for the metamorphic evolution of Western Anatolia, Turkey. Lithos, 84, 102–124.

Candan, O., Dora, O.O., Oberhansli, R., Cetinkaplan, M., Partzsch, J.H., Warkus, F.C., & Durr, S. (2001). Pan-African high-pressure metamorphism in the Precambrian basement of the Menderes Massif, western Anatolia, Turkey. International Journal of Earth Science, 89, 793-811.

Candan, O., Oberhansli, R., Dora, O. O., Cetinkaplan, M., Koralay, E., Rimmele, G., & ... Akal, C. (2011). Polymetamorphic evolution of the Pan-African basement and Palaeozoic-early

Tertiary cover series of the Menderes Massif. Bulletin of Mineral Resources and Exploration Turkey, 142, 121163.

Cao, S., Neubauer, F., Bernroider, M., Genser, J., Liu, J., & Friedl, G. (2017). Low-grade retrogression of a high-temperature metamorphic core complex: Naxos, Cyclades, Greece. Geological Society of America Bulletin, 129 (1-2), 93–117. https://doi.org/10.1130/B31502.1

Cao, S., Neubauer, F., Bernroider, M., & Liu, J. (2013). The lateral boundary of a metamorphic core complex: The Moutsounas shear zone on Naxos, Cyclades, Greece. Journal of Structural Geology, 54, 103–128. https://doi.org/10.1016/j.jsg.2013.07.002

Catlos, E.J., & Çemen, I. (2005). Monazite ages and the evolution of the Menderes Massif, western Turkey, Geologische Rundschau = International Journal of Earth Science [1999], 94, 204 -217.

Catlos, E.J., Baker, C., Sorensen, S.S., Çemen, I., & Hancer, M. (2010). Geochemistry, geochronology, and cathodoluminescence imagery of the Salihli and Turgutlu granites (central Menderes Massif, western Turkey): Implications for Aegean tectonics. Tectonophysics, 488, 110-130. https://doi.org/10.1016/j.tecto.2009.06.001

Catlos, E.J., Jacob, Lg, Oyman, T., & Sorensen S.S. (2012). Long-term exhumation of an Aegean metamorphic core complex granitoids in the northern Menderes Massif, western Turkey. American Journal of Science, 312, 534-571. https://doi.org/10.2475/05.2012.03

Catlos, E.J., Lovera, O.M., Kelly, E.D., Ashley, K.T., Harrison, T.M., & Etzel, T. (2018). Modeling High-resolution Pressure-Temperature Paths across the Himalayan Main Central Thrust (central Nepal): Implications for the Dynamics of Collision. Tectonics, 37, 2363-2388. https://doi.org/10.1029/2018TC005144

Catlos, E.J., Reyes, E., Brookfield, M., &Stockli, D.F. (2016). Age and Emplacement of the Permian- Jurassic Menghai Batholith, Western Yunnan, China. International Geology Review, 59(8), 919-945. https://doi.org/10.1080/00206814.2016.1237312

Cavazza, W., Okay, A.I., & Zattin, M. (2009). Rapid early-middle Miocene exhumation of the Kazdağ Massif (western Anatolia). Geologische Rundschau = International Journal of Earth Science [1999], 98, 1935–1947. https://doi.org/10.1007/s00531-008-0353-9

Çemen, I., Catlos, E. J., Gogus, O., & Ozerdem, C. (2006). Postcollisional extensional tectonics and exhumation of the Menderes Massif in the western Anatolia extended terrane, Turkey. Special Paper - Geological Society of America, 409, 353-379.

Cenki-Tok, B., Expert, M., Işık, V., Candan, O., Monié, P., & Bruguier, O. (2016). Complete Alpine reworking of the northern Menderes Massif, western Turkey. Geologische Rundschau = International Journal of Earth Science [1999], 105, 1507. http://dx.doi.org/10.1007/s00531-015-1271-2.

Çetinkaplan, M., Pourteau, A., Candan, O., Koralay, O., Oberhänsli, R., Okay, A., Chen, F., Kozlu, H., & Sengün, F. (2016). P–T–t evolution of eclogite/blueschist facies metamorphism in Alanya Massif: time and space relations with HP event in Bitlis Massif, Turkey. Geologische Rundschau = International Journal of Earth Science [1999], 105(1), 247-281. https://doi.org/10.1007/s00531-014-1092-8

Çetinkaplan, M., Candan, O., Oberhänsli, R., Sudo, M., & Cenki-Tok, B. (2020). P–T–t evolution of the Cycladic Blueschist Unit in Western Anatolia/Turkey: Geodynamic implications for the Aegean region. Journal of Metamorphic Geology, 38, 379– 419. https://doi.org/10.1111/jmg.12526

1389 Channell, J.E.T., & Kozur H.W. (1997). How many oceans? Meliata, Vardar and Pindos oceans
1390 in Mesozoic Alpine paleogeography. Geology 25(2), 183–186. https://doi.org/10.1130/0091-
1391 7613(1997)025<0183:HMOMVA>2.3.CO;2
1392 Chaumillon, E., & Mascle, J. (1997). From foreland to forearc domains: New multichannel
1393 seismic reflection survey of the Mediterranean ridge accretionary complex (Eastern
1394 Mediterranean). Marine Geology, 138, 237-259. https://doi.org/10.1016/S0025-
1395 3227(97)00002-9
1396 Chen, F., Siebel, W., Satir, M. et al. (2002). Geochronology of the Karadere basement (NW
1397 Turkey) and implications for the geological evolution of the Istanbul zone Geologische
1398 Rundschau = International Journal of Earth Science [1999], 91, 469–481.
1399 https://doi.org/10.1007/s00531-001-0239-6
1400 Chousianitis, K., Ganas, A., & Evangelidis, C. P. (2015). Strain and rotation rate patterns of
1401 mainland Greece from continuous GPS data and comparison between seismic and geodetic
1402 moment release. Journal of Geophysical Research Solid Earth, 120, 3909– 3931.
1403 https://doi.org/10.1002/2014JB011762
1404 Chousianitis, K., Ganas, A., & Gianniou, M. (2013). Kinematic interpretation of present-day
1405 crustal deformation in central Greece from continuous GPS measurements. Journal of
1406 Geodynamics, 71, 1-13. https://doi.org/10.1016/j.jog.2013.06.004
1407 Cita, M.B., Erba, E., Lucchi, R., Pott, M., van der Meer, R., & Nieto, L. (1996). Stratigraphy and
1408 sedimentation in the Mediterranean Ridge diapiric belt, Marine Geology, 132(1–4), 131-150.
1409 https://doi.org/10.1016/0025-3227(96)00157-0
1410 Clark, S. A., Sobiesiak, M., Zelt, C. A., Magnani, M. B., Miller, M. S., Bezada, M. J., &
1411 Levander, A. (2008). Identification and tectonic implications of a tear in the South American
1412 plate at the southern end of the Lesser Antilles, Geochemistry, Geophysics, Geosystems, 9,
1413 Q11004, https://doi.org/10.1029/2008GC002084
1414 Cocard, M., Kahle, H.-G., Peter, Y., Geiger, A., Veis, G., Felekis, S., Paradissis, D., & Billiris,
1415 H. (1999). New constraints on the rapid crustal motion of the Aegean region: recent results
1416 inferred from GPS measurements (1993-1998). across the West Hellenic Arc, Greece. Earth
1417 and Planetary Science Letters, 172(1-2), 39-47.
1418 Cocchi, L., Passaro, S., Tontini, F.C., & Ventura, G. (2017). Volcanism in slab tear faults is
1419 larger than in island-arcs and back-arcs. Nature Communications, 8, 1451.
1420 https://doi.org/10.1038/s41467-017-01626-w
1421 Coney, P.J., & Harms, T.A. (1984). Cordilleran metamorphic core complexes: Cenozoic
1422 extensional relics of Mesozoic compression. Geology, 12(9), 550–554.
1423 https://doi.org/10.1130/0091-7613(1984)12<550:CMCCCE>2.0.CO;2
1424 Cornée, J-J., Quillévéré, F., Moissette, P., Fietzke, J., López-Otálvaro, G.E., Melinte-
1425 Dobrinescu, M., Philippon, M., van Hinsbergen, D.J.J., Agiadi, K., Koskeridou, E., &
1426 Münch, P. (2018). Tectonic motion in oblique subduction forearcs: insights from the
1427 revisited Middle and Upper Pleistocene deposits of Rhodes, Greece. Journal of the
1428 Geological Society, 176 (1), 78–96. https://doi.org/10.1144/jgs2018-090
1429 Crameri, F., Magni, V., Domeier, M. et al. (2020). A transdisciplinary and community-driven
1430 database to unravel subduction zone initiation. Nature Communications, 11, 3750.
1431 https://doi.org/10.1038/s41467-020-17522-9
1432 Dannat, C. (1997). Geochemie, Geochronologie und Nd- und Sr-Isotopie der granitoiden
1433 Kerngneise des Menderes Massivs, SW-Türkei: Ph.D. thesis, Universität Mainz, 120 p.

d'Atri, A., Zuffa, G.G., Cavazza, W., Okay, A.I., & Di Vincenzo, G. (2012). Detrital supply from subduction/accretion complexes to the Eocene–Oligocene post-collisional southern Thrace Basin (NW Turkey and NE Greece). Sedimentary Geology, 243–244, 117-129. https://doi.org/10.1016/j.sedgeo.2011.10.008

de Boorder, H., Spakman, W., White, S.H., & Wortel, M.J.R. (1998). Late Cenozoic mineralization, orogenic collapse and slab detachment in the European Alpine Belt. Earth and Planetary Science Letters, 164(3–4), 569-575. https://doi.org/10.1016/S0012-821X(98)00247-7

de Capitani, C., & Brown, T. H. (1987). The computation of chemical equilibrium in complex systems containing non-ideal solutions. Geochimica et Cosmochimica Acta, 51(10). 2639-2652.

de Capitani, C., & Petrakakis, K. (2010). The computation of equilibrium assemblage diagrams with Theriak/Domino software. American Mineralogist, 95(7), 1006-1016.

Delaloye, M., & Bingöl, E. (2000). Granitoids from western and northwestern Anatolia: geochemistry and modeling of geodynamic evolution. International Geology Review, 42, 241–268.

Demirbilek, M., Mutlu, H., Fallick, A.E., Sarıiz, K., & Kibici, Y. (2018). Petrogenetic evolution of the Eocene granitoids in eastern part of the Tavşanlı Zone in northwestern Anatolia, Turkey, Lithos, 314–315, 236-259. https://doi.org/10.1016/j.lithos.2018.06.003

Dewey, J.F., & Şengör, A.M.C. (1979). Aegean and surrounding regions: Complex multiplate and continuum tectonics in a convergent zone. Geological Society of America Bulletin, 90(1). 84–92. https://doi.org/10.1130/0016-7606(1979)90<84:AASRCM>2.0.CO;2

Di Rosa, M., Farina, F., Marroni, M., Pandolfi, L., Göncüoğlu, M.C., Ellero, A., & Ottria, G. (2019). U-Pb zircon geochronology of intrusive rocks from an exotic block in the Late Cretaceous – Paleocene Taraklı Flysch (northern Turkey): Constraints on the tectonics of the Intrapontide suture zone, Journal of Asian Earth Sciences, 171, 277-288. https://doi.org/10.1016/j.jseaes.2018.11.017

Dilek, Y., & Altunkaynak, Ş. (2007). Cenozoic Crustal Evolution and Mantle Dynamics of Post-Collisional Magmatism in Western Anatolia. International Geology Review, 49(5), 431-453. https://doi.org/10.2747/0020-6814.49.5.431

Dilek, Y., & Sandvol, E. (2009). Seismic structure, crustal architecture and tectonic evolution of the Anatolian-African Plate Boundary and the Cenozoic Orogenic Belts in the Eastern Mediterranean Region. Geological Society, London, Special Publications, 327, 127-160. https://doi.org/10.1144/SP327.8

Doğan, A., & Emre, O. (2006). Ege Graben Sisteminin Kuzey Sınırı: Sındırgı-Sincanlı Fay Zonu (Northern Boundary of Aegean Graben System: Sındırgı-Sincanlı Fault Zone). 59. Türkiye Jeoloji Kurultayı, Bildiriler Kitabı.

Doğangün, A., Ural, A., Sezen, H., Güney, Y., & Fırat, F.K. (2013). The 2011 Earthquake in Simav, Turkey and Seismic Damage to Reinforced Concrete Buildings. Buildings 3(1), 173-190. https://doi.org/10.3390/buildings3010173

Doglioni, C., Agostini, S., Crespi, M., Innocenti, F., Manetti, P., Riguzzi, F., & Savasçin, Y. (2002). On the extension in western Anatolia and the Aegean sea. In G. Rosenbaum, G.S. Lister (Eds.), Reconstruction of the evolution of the Alpine-Himalayan Orogen. Journal of the Virtual Explorer, 8, 161-176.

Dora, O.O., Candan, O., Durr, S., & Oberhansli, R. (1995) New evidence on the geotectonic evolution of the Menderes Massif. In O. Piskin, M. Ergun, M.Y. Svascin, G. Tarcan (Eds.),

Proceedings of the International Earth Science Colloquium on the Aegean Region. Izmir, Turkey (Vol. 1, pp. 53-72).

Dora, O.Ö, Candan, O., Kaya, O., Koralay, E., & Akal, C. (2005). Menderes Masifi Çine Asmasifi' ndeki Koçarlý - Bafa - Yataðan - Karacasu arasýnda uzanan gnays / þist dokanaðýnýn niteliði: Jeolojik, tektonik, petrografik ve jeokronolojik bir yaklaþým. YDABÇAG - 101 Y 132 nolu Türkiye Bilimsel ve Teknolojik Araþtýrma Kurumu (TÜBÝTAK) projesi, 197p. (unpublished).

Dragovic, B., Samanta, L.M., Baxter, E.F., & Selverstone, J. (2012). Using garnet to constrain the duration and rate of water-releasing metamorphic reactions during subduction: An example from Sifnos, Greece. Chemical Geology, 314–317, 9-22. https://doi.org/10.1016/j.chemgeo.2012.04.016

Dürr, S. (1975). Über Alter und geotektonische Stellung des Menderes Kristallins/SW Anatolien und seine Äquivalente in der Mittleren Aegean. Habilitation Thesis, University of Marburg.

Duru, M., Pehlivan, S., Şenturk, Y., Yavaş, F., & Kar, H. (2004). New Results on the Lithostratigraphy of the Kazdağ Massif in Northwest Turkey. Turkish Journal of Earth Sciences, 13, 177-186.

Elburg, M.A., & Smet, I. (2020). Geochemistry of lavas from Aegina and Poros (Aegean Arc, Greece): Distinguishing upper crustal contamination and source contamination in the Saronic Gulf area, Lithos, 358–359, 105416. https://doi.org/10.1016/j.lithos.2020.105416.

Elitez, İ, Cenk Yaltırak, C., & Aktuğ, B. (2016). Extensional and compressional regime driven left-lateral shear in southwestern Anatolia (eastern Mediterranean): The Burdur-Fethiye Shear Zone. Tectonophysics, 688, 26-35. https://doi.org/10.1016/j.tecto.2016.09.024

Elmas, A. (2012). Basement types of the Thrace Basin and a new approach to the pre-Eocene tectonic evolution of the northeastern Aegean and northwestern Anatolia: a review of data and concepts. Geologische Rundschau = International Journal of Earth Sciences, 101, 1895–1911 (2012). https://doi.org/10.1007/s00531-012-0756-5

El-Sharkawy, A., Meier, T., Lebedev, S., Behrmann, J. H., Hamada, M., Cristiano, L., et al. (2020). The slab puzzle of the Alpine-Mediterranean region: Insights from a new, high-resolution, shear wave velocity model of the upper mantle. Geochemistry, Geophysics, Geosystems, 21, e2020GC008993. https://doi.org/10.1029/2020GC008993

Emery, K.O., Heezen, B., & Allan, T.D. (1966). Bathymetry of the Eastern Mediterranean sea. Deep Sea Research, 13, 173-192.

Emre, Ö, & Duman, T. (2011). 19 May 2011 Simav-Kutahya earthquake (Mw:5.8) in Turkey pre-assessment, earthquake report. General Directorate of Mineral Research and Exploration (MTA). Ankara, Turkey: Earth Dynamics Research Center. Turkish.

Emre, Ö., Duman, T.Y., & Özalp, S. (2011). 1:250000 scale Active Fault Map Series of Turkey, Kutahya (NJ 35-4) Quadrangle, Serial Number 10, General Directorate of Mineral Research and Exploration, Ankara, Turkey.

Emre, Ö, Erkal, T., Tchepalyga, A., Kazancı, N., Keçer, M., & Ünay, E. (1998). Neogene quaternary evolution of the Eastern Marmara Region, Northwest Turkey. Bulletin of the Mineral Research Exploration Institute of Turkey, 120, 119-145.

Erdoğan, B., Akay, E., Hasözbek, A., Satır, M., & Siebel, W. (2013). Stratigraphy and tectonic evolution of the Kazdag Massif (NW Anatolia) based on field studies and radiometric ages. International Geology Review, 55(16), 2060- 2082.

Ergün, M., Okay, S., Sari, C., Oral, E.Z., Ash, M., Hall, J., & Miller, H. (2005). Gravity anomalies of the Cyprus Arc and their tectonic implications. Marine Geology, 221(1–4), 349-358. https://doi.org/10.1016/j.margeo.2005.03.004

Ersoy, E.Y., & Palmer, M.R. (2013). Eocene-Quaternary magmatic activity in the Aegean: Implications for mantle metasomatism and magma genesis in an evolving orogeny, Lithos, 180–181, 5-24. https://doi.org/10.1016/j.lithos.2013.06.007

Ersoy, E.Y., Çemen, I., Helvacı, C., & Billor, Z., 2014. Tectono-stratigraphy of the Neogene basins in western Turkey: implications for tectonic evolution of the aegean extended region. Tectonophysics, 635, 33e58. http://dx.doi.org/10.1016/j.tecto.2014.09.002

Ersoy, E.Y., Helvacı, C., & Sozbilir, H. (2010). Tectono-stratigraphic evolution of the NE-SW-trending superimposed Selendi basin: implications for late Cenozoic crustal extension in Western Anatolia, Turkey. Tectonophysics, 488, 210–232.

Ersoy, E.Y., Palmer, M.R., Genç Ş, C., Prelević, D., Akal, C., & Uysal, I. (2017). Chemo-probe into the mantle origin of the NW Anatolia Eocene to Miocene volcanic rocks: Implications for the role of, crustal accretion, subduction, slab roll-back and slab break-off processes in genesis of post-collisional magmatism, Lithos, 288–289, 55-71. https://doi.org/10.1016/j.lithos.2017.07.006

Etzel, T.E., Catlos, E.J., Atakturk, K., Kelly, E.D., Lovera, O.M., Çemen, I., Diniz, E., & Stockli, D. (2019). Implications for thrust-related shortening punctuated by extension from P-T paths and geochronology of garnet-bearing schists. Tectonics 38(6), 1974-1998. https://doi.org/10.1029/2018TC005335

Etzel, T.M., Catlos, E.J., Çemen, I., Ozerdem, C., Oyman, T., & Miggins, D. (2020). Documenting exhumation in the central and northern Menderes Massif (western Turkey): New insights from garnet-based P-T estimates and K-feldspar $^{40}Ar/^{39}Ar$ geochronology. Lithosphere, 1, 8818289. https://doi.org/10.2113/2020/8818289

Evangelidis, C.P. (2017). Seismic anisotropy in the Hellenic subduction zone: Effects of slab segmentation and subslab mantle flow. Earth and Planetary Science Letters, 480, 97-106. https://doi.org/10.1016/j.epsl.2017.10.003

Eyidoğan, H., & Jackson, J. (1985). A seismological study of normal faulting in the Demirci, Alaşehir and Gediz earthquakes of 1969–70 in western Turkey: implications for the nature and geometry of deformation in the continental crust. Geophysical Journal of the Royal Astronomical Society, 81, 569-607. https://doi.org/10.1111/j.1365-246X.1985.tb06423.x

Faccenna, C., Becker, T.W., Auer, L., Billi, A., Boschi, L., Brun, J.-P., Capitanio, F.A., Funiciello, F., Horvàth, F., Jolivet, L., Piromallo, C., Royden, L., Rossetti, F., & Serpelloni, E. (2014). Mantle dynamics in the Mediterranean, Review of Geophysics, 52, 283– 332. https://doi.org/10.1002/2013RG000444

Faccenna, C., Bellier, O., Martinod, J., Piromallo, C., & Regard, V. (2006). Slab detachment beneath eastern Anatolia: A possible cause for the formation of the North Anatolian fault. Earth and Planetary Science Letters, 242(1–2), 85-97. https://doi.org/10.1016/j.epsl.2005.11.046.

Faccenna, C., Jolivet, L., Piromallo, C., & Morelli, A. (2003). Subduction and the depth of convection in the Mediterranean mantle. Journal of Geophysical Research, 108(B2). https://doi.org/10.1029/2001JB001690

Ferentinos, G., Georgiou, N., Christodoulou, D., Geraga, M., & Papatheodorou, G. (2018). Propagation and termination of a strike slip fault in an extensional domain: The westward

growth of the North Anatolian Fault into the Aegean Sea, Tectonophysics, 745, 183-195. https://doi.org/10.1016/j.tecto.2018.08.003

Fornash, K.F., & Whitney, D.L. (2020). Lawsonite-rich layers as records of fluid and element mobility in subducted crust (Sivrihisar Massif, Turkey). Chemical Geology, 533, 119356, ttps://doi.org/10.1016/j.chemgeo.2019.119356

Foucher, J.P., Chamot-Roocke, N., Alexandry, S., Augustin, J.M., Monti, S., Pavlakis, P., & Voisset, M. (1993). Multibeam bathymetry and seabed reflectivity maps of the MEDRIFT corridor across the eastern Mediterranean Ridge. In: UEG VII., Strasbourg, France. Terra Cognita, Abstracts, pp. 278-279.

Frassi, C., Marroni, M., Pandolfi, L., Göncüoğlu, M.C., Ellero, A., Ottria, G., Sayit, K., McDonald, C.S., Balestrieri, M.L., & Malasoma, A. (2018). Burial and exhumation history of the Daday Unit (central Pontides, Turkey); implications for the closure of the Intra-Pontide oceanic basin. In G. Capponi, A. Festa, G. Rebay (Eds.), Birth and death of oceanic basins; geodynamic processes from rifting to continental collision in Mediterranean and circum-Mediterranean orogeny. Geological Magazine, 155, 356-376.

Fytikas, M., Innocenti, F., Manetti, P., Mazzuoli, R., Peccerillo, A., & Villari, L. (1984). Tertiary to quaternary evolution of volcanism in the Aegean region. In JE Dixon, AHF Robertson (Eds.), The Geological Evolution of the Eastern Mediterranean, Geological Society of London, Special Publications (Vol. 17, pp. 687–699).

Galindo-Zaldivar, J., Nieto, L., & Woodside, J. (1996). Structural features of mud volcanoes and the fold system of the Mediterranean Ridge, south of Crete. Marine Geology, 132(1-4), 95-112. https://doi.org/10.1016/0025-3227(96)00155-7

Ganas A., & Parsons T. (2009). Three-dimensional model of Hellenic Arc deformation and origin of the Cretan uplift. Journal of Geophysical Research, 114(B06404), 1–14. https://doi.org/10.1029/2008JB005599

Gautier, P., Brun, J-P., Moriceau, R., Sokoutis, D., Martinod, J., & Jolivet, L. (1999). Timing, kinematics and cause of Aegean extension: a scenario based on a comparison with simple analogue experiments. Tectonophysics, 315(1–4), 31-72. https://doi.org/10.1016/S0040-1951(99)00281-4

Gautier, Y. (1984). Déformations et métamorphismes associés à la fermeture téthysienne en Anatolie centrale (région de Sivrihisar, Turquie). PhD thesis, University Paris-Sud, France. 236.

Gawthorpe, R.L., & Hurst, M. (1993). Transfer Zones in Extensional Basins: Their Structural Style and Influence on Drainage Development and Stratigraphy. Journal of the Geological Society, London, 150, 1137-1152. https://doi.org/10.1144/gsjgs.150.6.1137

Genç, SC. (1998). Evolution of the Bayramic¸ magmatic complex, northwestern Anatolia. Journal of Volcanology and Geothermal Research, 85, 233–249.

Gerogiannis, N., Xypolias, P., Chatzaras, V., Aravadinou,E., & Papapavlou, K. (2019). Deformation within the Cycladic subduction–exhumation channel: new insights from the enigmatic Makrotantalo nappe (Andros, Aegean). International Journal of Earth Sciences, 108, 817–843. https://doi.org/10.1007/s00531-019-01680-3

Gessner, K., Collins, A.S., Ring, U., & Güngör, T. (2004). Structural and thermal history of polyorogenic basement. Journal of the Geological Society of London, 161, 93–101. http://dx.doi.org/10.1144/0016-764902-166

1613 Gessner, K., Gallardo, L. A., Markwitz, V., Ring, U., & Thomson, S. N. (2013). What caused the
1614 denudation of the Menderes Massif; review of crustal evolution, lithosphere structure, and
1615 dynamic topography in southwest Turkey. Gondwana Research, 24(1), 243-274.
1616 Gessner, K., Markwitz, V., & Güngör, T. (2017). Crustal fluid flow in hot continental extension:
1617 tectonic framework of geothermal areas and mineral deposits in western Anatolia. Geological
1618 Society, London, Special Publications, 453, 289-311. https://doi.org/10.1144/SP453.7
1619 Gessner, K., Piazolo, S., Gungor, T., Ring, U., Kroener, A., & Passchier, C. W. (2001). Tectonic
1620 significance of deformation patterns in granitoid rocks of the Menderes nappes, Anatolide
1621 Belt, Southwest Turkey. Geologische Rundschau = International Journal of Earth Sciences,
1622 89(4). 766-780.
1623 Gessner, K., Ring, U., & Gungor, T. (2011). Field guide to Samos and the Menderes Massif;
1624 along-strike variations in the Mediterranean Tethyan Orogen. GSA Field Guide, 23.
1625 Gessner, K., Ring, U., Passchier, C. W., Hetzel, R., & Okay, A. I. (2002). Stratigraphic and
1626 metamorphic inversions in the central Menderes Massif; a new structural model; discussion
1627 and reply. Geologische Rundschau = International Journal of Earth Sciences, 91(1), 168-178.
1628 Gianni, G.M., Navarrete, C. & Spagnotto, S. (2019). Surface and mantle records reveal an
1629 ancient slab tear beneath Gondwana. Scientific Reports, 9, 19774.
1630 https://doi.org/10.1038/s41598-019-56335-9
1631 Glodny, J., & Hetzel, R. (2007). Precise U-Pb ages of syn-extensional Miocene intrusions in the
1632 central Menderes Massif, western Turkey. Geological Magazine, 144, 1–12.
1633 Göncüoğlu, M.C. (2010). Introduction to the Geology of Turkey: Geodynamic Evolution of the
1634 Pre-Alpine and Alpine Terranes. General Directorate of Mineral Research and Exploration
1635 Monography Series, 5, 1-66.
1636 Göncüoğlu, M. C., Dirik, K., & Kozlu, H. (1997). General characteristics of pre-alpine and
1637 Alpine Terranes in Turkey: explanatory notes to the terrane map of Turkey. Annales
1638 Géologique de Pays Hellenique, 37, 515–536.
1639 Göncüoğlu, M.C., Marroni, M., Pandolfi, L., Ellero, A., Ottria, G., Catanzariti, R., Tekin, U.K.,
1640 & Sayit, K. (2014). The Arkot Dag Melange in Arac area, central Turkey; evidence of its
1641 origin within the geodynamic evolution of the Intra-Pontide suture zone. Journal of Asian
1642 Earth Sciences, 85, 117-139.
1643 Göncüoğlu, M.C., Marroni, M., Sayit, K., Tekin, U.K., Ottria, G., Pandolfi, L., & Ellero, A.
1644 (2012). The Ayli Dag ophiolite sequence (central-northern Turkey); a fragment of Middle
1645 Jurassic oceanic lithosphere within the Intra-Pontide suture zone. Ofioliti, 37, 77-92.
1646 Görgün, E. (2014). Source characteristics and Coulomb stress change of the 19 May 2011 Mw
1647 6.0 Simav–Kütahya earthquake, Turkey. Journal of Asian Earth Sciences, 87, 79-88.
1648 https://doi.org/10.1016/j.jseaes.2014.02.016.
1649 Görür, N., Monod, O., Okay, A.I., Sengör, A.M.C., Tüysüz, O., Yigitbas, E., Sakinç, M., &
1650 Akkök, R. (1997). Palaeogeographic and tectonic position of the Carboniferous rocks of the
1651 western Pontides (Turkey). in the frame of the Variscan belt. Bulletin de la Société
1652 Géologique de France, 168, 197–205.
1653 Govers, R., & Wortel, M.J.R. (2005). Lithosphere tearing at STEP faults: response to edges of
1654 subduction zones. Earth and Planetary Science Letters, 236(1–2), 505-523.
1655 https://doi.org/10.1016/j.epsl.2005.03.022.
1656 Grasemann, B., Schneider, D.A., Stöckli, D.F., Iglseder, C. (2012). Miocene bivergent crustal
1657 extension in the Aegean: Evidence from the western Cyclades (Greece). Lithosphere, 4 (1),
1658 23–39. https://doi.org/10.1130/L164.1

1659 Gürer, Ö, Sangu, E., & Özburan, M. (2006). Neotectonics of the SW Marmara region, NW
1660 Anatolia, Turkey. Geological Magazine, 143 (2): 229–241.
1661 https://doi.org/10.1017/S0016756805001469
1662 Gürsu, S., & Göncüoglu, M.C. (2006). Petrogenesis and tectonic setting of Cadomian felsic
1663 igneous rocks, Sandıklı area of the western Taurides, Turkey. Geologische Rundschau =
1664 International Journal of Earth Sciences, 95, 741–757 (2006). https://doi.org/10.1007/s00531-
1665 005-0064-4
1666 Gürsu, S., Göncüoglu, M.C., & Bayhan, H. (2004). Geology and geochemistry of the pre-Early
1667 Cambrian rocks in Sandıklı area: implications for the Pan-African evolution in NW
1668 Gondwanaland. Gondwana Research, 7(4), 923–935.
1669 Gutnic, M., Monod, O., Poisson, A., & Dumont, J.F. (1979). Geologie des Taurides Occidentales
1670 (Turquie). Memoirs of the Geological Society of France, 58(137), 109pp.
1671 Haddad, A., Ganas, A., Kassaras, I., & Lupi, M. (2020). Seismicity and geodynamics of western
1672 Peloponnese and central Ionian Islands: Insights from a local seismic deployment.
1673 Tectonophysics, 778, 228353. https://doi.org/10.1016/j.tecto.2020.228353.
1674 Hall, J., Aksu, A.E., Elitez, I., Yaltırak, C., & Çifçi, G. (2014). The Fethiye–Burdur Fault Zone:
1675 A component of upper plate extension of the subduction transform edge propagator fault
1676 linking Hellenic and Cyprus Arcs, Eastern Mediterranean. Tectonophysics, 635, 80-99.
1677 https://doi.org/10.1016/j.tecto.2014.05.002
1678 Hall, J., Aksu, A.E., Yaltırak, C., & Winsor, J.D. (2009). Structural architecture of the Rhodes
1679 Basin: A deep depocentre that evolved since the Pliocene at the junction of Hellenic and
1680 Cyprus Arcs, eastern Mediterranean. Marine Geology, 258(1-4), 1-23.
1681 https://doi.org/10.1016/j.margeo.2008.02.007
1682 Hall, R., Audley-Charles, M.G., & Carter, D.J. (1984). The significance of Crete for the
1683 evolution of the Eastern Mediterranean. Geological Society, London, Special Publications,
1684 17, 499-516. https://doi.org/10.1144/GSL.SP.1984.017.01.37
1685 Halpaap, F., Rondenay, S., & Ottemöller, L. (2018). Seismicity, deformation, and metamorphism
1686 in the Western Hellenic Subduction Zone: New constraints from tomography. Journal of
1687 Geophysical Research: Solid Earth, 123, 3000– 3026. https://doi.org/10.1002/2017JB015154
1688 Hansen, S.E., Evangelidis, C.P., & Papadopoulos, G.A. (2019). Imaging slab detachment within
1689 the Western Hellenic Subduction Zone. Geochemistry, Geophysics, Geosystems, 20, 895–
1690 912. https://doi.org/10.1029/2018GC007810
1691 Harris, N.B.W., Kelly, S., & Okay, A.I. (1994). Postcollision magmatism and tectonics in
1692 northwest Anatolia. Contributions to Mineralogy and Petrology, 117, 241–252.
1693 Harrison, R.W., Tsiolakis, E., Stone, B.D., Lord, A., McGeehin, J.P., Mahan, S.A., & Chirico, P.
1694 (2012). Late Pleistocene and Holocene uplift history of Cyprus: implications for active
1695 tectonics along the southern margin of the Anatolian microplate. Geological Society,
1696 London, Special Publications, 372, 561-584. https://doi.org/10.1144/SP372.3
1697 Hasözbek, A., Akay, E., Erdoğan, B., Satır, M., & Siebel, W. (2010). Early Miocene granite
1698 formation by detachment tectonics or not? A case study from the northern Menderes Massif
1699 (Western Turkey). Journal of Geodynamics, 50, 67–80.
1700 Hatzfeld, D., Pedotti, G., Hatzidimitriou, P., & Makropoulos, K. (1990). The strain pattern in the
1701 western Hellenic arc deduced from a microearthquake survey. Geophysical Journal
1702 International, 101(1), 181-202.
1703 Hayes, G. (2018). Slab2 - A Comprehensive Subduction Zone Geometry Model: U.S. Geological
1704 Survey data release, https://doi.org/10.5066/F7PV6JNV

Heezen, B.C., & Ewing, M., 1963. The Mid Oceanic Ridge. In M.N. Hill (Ed.), The Seas (Vol. 3, pp. 388-410), Interscience, New York.

Henjes-Kunst F., Altherr, R., Kreuzer. H., Hansen, B.T. (1988). Disturbed U-Th-Pb systematics of young zircons and uranothorites—the case of the Miocene Aegean granitoids (Greece). Chemical Geology, 73(2), 125–145.

Hetzel, R., & Reischmann, T. (1996). Intrusion age of Pan-African augen gneisses in the southern Menderes Massif and the age of cooling after Alpine ductile extensional metamorphism. Geological Magazine, 133(5), 505-572.

Hetzel, R., Passchier, C. W., Ring, U., & Dora, O. O. (1995a). Bivergent extension in orogenic belts; the Menderes Massif (southwestern Turkey). Geology, 23(5), 455-458.

Hetzel, R., Ring, U., Akal, C., & Troesch, M. (1995b). Miocene NNE-directed extensional unroofing in the Menderes Massif, southwestern Turkey. Journal of the Geological Society of London, 152, 4639654.

Holland, T.B., & Powell, R. (1998). An internally consistent thermodynamic data set for phases of petrological interest. Journal of Metamorphic Geology, 16(3), 309-343.

Holland, T.B., & Powell, R. (2011). An improved and extended internally consistent thermodynamic dataset for phases of petrological interest, involving a new equation of state for solids. Journal of Metamorphic Geology, 29(3), 333-383.

Hollenstein, C., Müller, M.D., Geiger, A., & Kahle, H.-G. (2008). Crustal motion and deformation in Greece from a decade of GPS measurements, 1993e2003. Tectonophysics, 449, 17e40. http://dx.doi.org/10.1016/j.tecto.2007.12.006.

Holness, M.B., & Bunbury, J.M. (2006). Insights into continental rift-related magma chambers: Cognate nodules from the Kula Volcanic Province, Western Turkey, Journal of Volcanology and Geothermal Research, 153(3-4), 241-261. https://doi.org/10.1016/j.jvolgeores.2005.12.004

Hosseini, K. , Matthews, K. J., Sigloch, K. , Shephard, G. E., Domeier, M. & Tsekhmistrenko, M. (2018). SubMachine: Web-Based tools for exploring seismic tomography and other models of Earth's deep interior. Geochemistry, Geophysics, Geosystems, 19. https://doi.org/10.1029/2018GC007431

Hubert-Ferrari, A., Armijo, R., King, G., Meyer, B., & Barka, A. (2002). Morphology, displacement, and slip rates along the North Anatolian Fault, Turkey, Journal of Geophysical Research, 107(B10), 2235. https://doi.org/10.1029/2001JB000393

Huchon, P., Lybéris, N., Angelier, J., Le Pichon, X., & Renard, V. (1982). Tectonics of the hellenic trench: A synthesis of sea-beam and submersible observations, Tectonophysics, 86(1-3), 69-112. https://doi.org/10.1016/0040-1951(82)90062-2

Husson, L., Brun, J-P., Yamato, P., & Faccenna, C. (2009). Episodic slab rollback fosters exhumation of HP–UHP rocks. Geophysics Journal International, 179, 1292–1300

Ilhan, E. (1971). Earthquakes in Turkey. In A.S. Campbell (Ed.), Geology and History of Turkey, (pp. 431-442). Petroleum Exploration Society of Libya, Tripoli.

İnan, S., Pabuçcu, A., Kulak, F., Ergintav, S., Tatar, O., Altunel, E., Akyüz, S., Tan, O., Seyis, C., Çakmak, R., Saatçılar, R., & Eyidoğan, H. (2012). Microplate boundaries as obstacles to pre-earthquake strain transfer in Western Turkey: Inferences from continuous geochemical monitoring. Journal of Asian Earth Sciences, 48, 56-71. https://doi.org/10.1016/j.jseaes.2011.12.016.

Inel, M., Ozmen, H.B. & Akyol, E. (2013). Observations on the building damages after 19 May 2011 Simav (Turkey) earthquake. Bulletin of Earthquake Engineering, 11, 255–283. https://doi.org/10.1007/s10518-012-9414-3

Innocenti, F., Agostini, S., Di Vincenzo, G., Doglioni, C., Manetti, P., Savaşçin, M.Y., & Tonarini, S. (2005). Neogene and Quaternary volcanism in Western Anatolia: Magma sources and geodynamic evolution, Marine Geology, 221(1–4), 397-421. https://doi.org/10.1016/j.margeo.2005.03.016

Iredale, L. J., Teyssier, C., & Whitney, D. L. (2013). Cenozoic pure-shear collapse of the southern Menderes Massif, Turkey. Special Publication - Geological Society of London, 372, 323-342. https://doi.org/10.1144/SP372.15

Işık, V., Seyitoğlu, G., & Çemen, I. (2003). Ductile-brittle transition along the Alasehir detachment fault and its structural relationship with the Simav detachment fault, Menderes Massif, western Turkey. Tectonophysics, 374, 1–18. http://dx.doi.org/10.1016/S0040-1951(03)00275-0.

Işık, V., & Tekeli, O. (2001). Late orogenic crustal extension in the northern Menderes Massif (western Turkey); evidence for metamorphic core complex formation. Geologische Rundschau = International Journal of Earth Sciences, 89(4). 757-765.

Işık, V., Tekeli, O., & Seyitoğlu, G. (2004). The $^{40}Ar/^{39}Ar$ age of extensional ductile deformation and granitoid intrusion in the northern Menderes core complex: implications for the initiation of extensional tectonics in western Turkey. Journal of Asian Earth Sciences, 23, 555–566.

Jackson, J. (1994). Active tectonics of the Aegean region. Annual Reviews of Earth and Planetary Science, 22, 239-71.

Jackson, J., & McKenzie, D. (1984). Active tectonicsof the Alpine-Himalayan belt between western Turkey and Pakistan, Geophysical Journal of the Royal Astronomical Society, 77, 185 – 264.

John, B.E., & Howard, K.A. (1995). Rapid extension recorded by cooling-age patterns and brittle deformation, Naxos, Greece. Journal of Geophysical Research, 100, 9969–9979.

Jolivet, L., & Brun, J.-P. (2010). Cenozoic geodynamic evolution of the Aegean, International Journal of Earth Sciences, 99(1), 109-138. https://doi.org/10.1007/s00531-008-0366-4

Jolivet, L., Brun, J.P., Gautier, P., Lallemant, S., & Patriat, M. (1994). 3D- Kinematics of extension in the Aegean region from the early Miocene to the present, Insights from the ductile crust. Bulletin de la Societe Geologique de France, 165, 195-209.

Jolivet, L., & Faccenna, C. (2000). Mediterranean extension and the Africa-Eurasia collision, Tectonics, 19(6), 1095– 106. https://doi.org/10.1029/2000TC900018

Jolivet, L., Faccenna, C., Huet, B., Labrousse, L., Le Pourhiet, L., et al. (2013). Aegean tectonics: Strain localisation, slab tearing and trench retreat. Tectonophysics, 597-598, 1-33.

Jolivet, L., Lecomte, E., Huet, B., Denèle, Y., Lacombe, O., Labrousse, L., Le Pourhiet, L., & Mehl, C. (2010). The North Cycladic Detachment System. Earth and Planetary Science Letters, 289(1–2), 87-104. https://doi.org/10.1016/j.epsl.2009.10.032

Jolivet, L., Menant, A., Sternai, P., Rabillard, A., Arbaret, L., Augier, R., Laurent, V., Beaudoin, A., Grasemann, B., Huet, B., Labrousse, L., & Le Pourhiet, L. (2015). The geological signature of a slab tear below the Aegean, Tectonophysics, 659, 166-182. https://doi.org/10.1016/j.tecto.2015.08.004

Jolivet, L., & Patriat, M. (1999). Ductile extension and the formation of the Aegean Sea. Geological Society, London, Special Publications, 156, 427-456. https://doi.org/10.1144/GSL.SP.1999.156.01.20

1795 Jost, M.L., Knabenbauer, O., Cheng, J., & Harjes, H-P. (2002). Fault plane solutions of
1796 microearthquakes and small events in the Hellenic arc, Tectonophysics, 356 (1–3), 87-114.
1797 https://doi.org/10.1016/S0040-1951(02)00378-5
1798 Kadir, S., & Kart, F. (2009). The occurrence and origin of the söğüt kaolinite deposits in the
1799 Paleozoic Saricakaya granite-granodiorite complexes and overlying Neogene sediments
1800 (Bilecik, northwestern Turkey). Clays and Clay Minerals, 57, 311–329.
1801 https://doi.org/10.1346/CCMN.2009.0570304
1802 Kahle, H.-G., Cocard, M., Peter, Y., Geiger, A., Reilinger, R., Barka, A., & Veis, G. (2000).
1803 GPS-derived strain rate field within the boundary zones of the Eurasian, African, and
1804 Arabian Plates, Journal of Geophysical Research, 105(B10), 23353– 23370.
1805 https://doi.org/10.1029/2000JB900238
1806 Kaldova, J., Leichmann, J., Babek, O., & Melichar, R. (2003). Brunovistulian terrane (Central
1807 Europe) and Istanbul zone (NW Turkey): Late Proterozoic and Paleozoic tectonostratigraphic
1808 development and paleogeography. Geologica Carpathica, 54(3), 139-152.
1809 Karabulut, H., Paul, A., Özbakır, A.D., Ergün, T., & Şentürk, S. (2019). A new crustal model of
1810 the Anatolia–Aegean domain: evidence for the dominant role of isostasy in the support of the
1811 Anatolian plateau. Geophysical Journal International, 218(1), 57–73.
1812 https://doi.org/10.1093/gji/ggz147
1813 Karacık, Z., & Yılmaz, Y. (1998). Geology of the ignimbrites and the associated volcano-
1814 plutonic complex of the Ezine area, northwestern Anatolia. Journal of Volcanology and
1815 Geothermal Research 85(1–4), 251–264.
1816 Karacık, Z., Yılmaz, Y., Pearce, J.A., & Ece, Ö.I. (2008). Petrochemistry of the south Marmara
1817 granitoids, northwest Anatolia, Turkey. Geologische Rundschau = International Journal of
1818 Earth Sciences 97, 1181–1200. https://doi.org/10.1007/s00531-007-0222-y
1819 Karagianni, E.E., Panagiotopoulos, D.G., Panza, G.F., Suhadolc, P., Papazachos, C.B.,
1820 Papazachos, C.B., Kiratzi, A., Hatzfeld, D., Makropoulos, K., Priestley, K., & Vuan, A.
1821 (2002). Rayleigh wave group velocity tomography in the Aegean area. Tectonophysics,
1822 358(1–4), 187-209. https://doi.org/10.1016/S0040-1951(02)00424-9
1823 Karagianni, E.E., Papazachos, C.B., Panagiotopoulos, D.G., Suhadolc, P., Vuan, A., & Panza,
1824 G.F. (2005). Shear velocity structure in the Aegean area obtained by inversion of Rayleigh
1825 waves. Geophysical Journal International, 160(1), 127–143. https://doi.org/10.1111/j.1365-
1826 246X.2005.02354.x
1827 Karaoğlu, Ö, & Helvacı, C. (2014). Isotopic evidence for a transition from subduction to slab-
1828 tear related volcanism in western Anatolia, Turkey. Lithos, 192–195, 226-239.
1829 https://doi.org/10.1016/j.lithos.2014.02.006
1830 Karasözen, E., Nissen, E., Bergman, E. A., Johnson, K. L., & Walters, R. J. (2016). Normal
1831 faulting in the Simav graben of western Turkey reassessed with calibrated earthquake
1832 relocations, Journal of Geophysical Research Solid Earth, 121, 4553– 4574.
1833 https://doi.org/10.1002/2016JB012828
1834 Kastens, K.A. (1991). Rate of outward growth of the Mediterranean Ridge accretionary complex,
1835 Tectonophysics, 199, 25–50.
1836 Kastens, K.A., Nancy, A.B., & Cita, M.B. (1992). Progressive deformation of an evaporites-
1837 bearing accretionary complex: Sea-Marc I., SeaBeam and Piston core observations from the
1838 Mediterrranean Ridge. Marine Geophysical Research, 14, 249-298.
1839 Katzir, Y., Avigad, D., Matthews, A., Garfunkel, Z. & Evans, B.W. (2000). Origin, HP/LT
1840 metamorphism and cooling of ophiolitic mélanges in southern Evia (NW Cyclades), Greece.

Journal of Metamorphic Geology, 18, 699-718. https://doi.org/10.1046/j.1525-1314.2000.00281.x

Kaya, O. (1981). Miocene reference section for the coastal parts of West Anatolia, Newsletters on Stratigraphy, 10, 164-191.

Keay, S., Lister, G., & Buick, I. (2001). The timing of partial melting, Barrovian metamorphism and granite intrusion in the Naxos metamorphic core complex, Cyclades, Aegean Sea, Greece, Tectonophysics, 342, 275-312. https://doi.org/10.1016/S0040-1951(01)00168-8.

Kempler, D., & Ben-Avraham, Z. (1987). The tectonic evolution of the Cyprean Arc, Annales Tectonicae, 1, 58-71.

Kendall, J.M., Stuart, G., Ebinger, C. et al. (2005). Magma-assisted rifting in Ethiopia. Nature, 433, 146–148. https://doi.org/10.1038/nature03161

Kenyon, N.H., Belderson, R.H., & Stride, A.H. (1982). Detailed tectonic trends on the central part of the Hellenic outer ridge and in the Hellenic trench system. Geological Society of London, 10, 335-343.

Ketin, I. (1948). Über die tektonisch-mechanischen Folgerungen aus den großen anatolischen Erdbeben des letzten Dezenniums. Geologische Rundschau = International Journal of Earth Sciences, 36, 77–83. https://doi.org/10.1007/BF01791916

Kind, R., Eken, T., Tilmann, F., Sodoudi, F., Taymaz, T., Bulut, F., Yuan, X., Can, B., & Schneider, F. (2015). Thickness of the lithosphere beneath Turkey and surroundings from S-receiver functions, Solid Earth, 6, 971–984. https://doi.org/10.5194/se-6-971-2015

Kinnaird, T., & Robertson, A. (2012). Tectonic and sedimentary response to subduction and incipient continental collision in southern Cyprus, easternmost Mediterranean region. Geological Society, London, Special Publications, 372, 585-614. https://doi.org/10.1144/SP372.10

Koçyiğit, A., & Deveci, Ş. (2007). A N-S-trending Active Extensional Structure, the Şuhut (Afyon). Graben: Commencement Age of the Extensional Neotectonic Period in the Isparta Angle, SW Turkey. Turkish Journal of Earth Sciences, 16, 391-416.

Kohn, M.J., & Spear, F.S. (1991). Error propagation for barometers: 2. Application to rocks. American Mineralogist, 76(1-2), 138–147

Kokkalas, S., Paraskevas, X., Koukouvelas, I., & Doutsos, T. (2006). Postcollisional contractional and extensional deformation in the Aegean region. Special Paper of the Geological Society of America, 409, 97-123. https://doi.org/10.1130/0-8137-2409-0.97

Komut, T., Gray, R., Pysklywec, R., & Göğüş, O.H. (2012). Mantle flow uplift of western Anatolia and the Aegean: Interpretations from geophysical analyses and geodynamic modeling. Journal of Geophysical Research, 117(B11412). https://doi.org/10.1029/2012JB009306

Konak, N. (1982). Geology of the Simav region. PhD thesis. Istanbul University, Faculty of Earth Sciences, Department of Geological Engineering (in Turkish with English Abstract, unpublished).

Konak N. (2002). The Geological Map of Turkey, 2002. General Directorate of Mineral Research and Exploration Izmir Area Map.

Konak, N., Akdeniz, N., Öztürk, E.M. (1987). Geology of the south of Menderes Massif. Correlation of Variscan and Pre-Variscan Events of the Alpine Mediterranean Mountain Belt. Field Meeting, IGCP Project 5. Publications of the Mineral Research and Exploration Institute of Turkey, 42–53.

Kopf, A., Mascle, J., & Klaeschen, D. (2003). The Mediterranean Ridge: A mass balance across the fastest growing accretionary complex on Earth, Journal of Geophysical Research, 108(B8), 2372. https://doi.org/10.1029/2001JB000473

Koralay, O.E. (2015). Late Neoproterozoic granulite facies metamorphism in the Menderes Massif, Western Anatolia/Turkey: implication for the assembly of Gondwana, Geodinamica Acta, 27(4), 244-266. https://doi.org/10.1080/09853111.2015.1014987

Koralay, O., Chen, F., Oberhansli, R., Wan, Y., & Candan, O. (2006). Age of Granulite Facies Metamorphism in the Menderes Massif, Western Anatolia / Turkey. 59th Geological Congres Turkey, Abstracts book, 28-29.

Koralay, O., Satir, M., & Dora, O. (2001). Geochemical and geochronological evidence for Early Triassic calc-alkaline magmatism in the Menderes Massif, western Turkey. Geologische Rundschau = International Journal of Earth Sciences, 89, 822–835 (2001). https://doi.org/10.1007/s005310000134

Kozur, H. W., & Göncüoğlu, M. C. (2000). Mean features of the pre-Variscan development in Turkey. Acta Universitatis Carolinae-Geologica, 42, 459–464.

Kreemer, C., Chamot-Rooke, N., & Le Pichon, X. (2004). Constraints on the evolution and vertical coherency of deformation in the Northern Aegean from a comparison of geodetic, geologic and seismologic data, Earth and Planetary Science Letters, 225(3–4), 329-346. https://doi.org/10.1016/j.epsl.2004.06.018

Kruckenberg, S. C., Vanderhaeghe, O., Ferré, E. C., Teyssier, C., & Whitney, D. L. (2011). Flow of partially molten crust and the internal dynamics of a migmatite dome, Naxos, Greece. Tectonics, 30, TC3001, https://doi.org/10.1029/2010TC002751

Kürçer, A., Chatzipetros, A., Tutkun, S. Z., Pavlides, A., Ateş, Ö, & Valkaniotis, S. (2008). The Yenice–Gönen active fault (NW Turkey): Active tectonics and palaeoseismology, Tectonophysics, 453(1–4), 263-275. https://doi.org/10.1016/j.tecto.2007.07.010

Lagos, M., Scherer, E.E., Tomaschek, F., Münker, C., Keiter, M., Berndt, J., & Ballhaus, C. (2007). High precision Lu–Hf geochronology of Eocene eclogite-facies rocks from Syros, Cyclades, Greece. Chemical Geology, 243(1–2), 16-35. https://doi.org/10.1016/j.chemgeo.2007.04.008

Lamont, T. N., Searle, M. P., Gopon, P., Roberts, N. M. W., Wade, J., Palin, R. M., & Waters, D. J. (2020b). The Cycladic Blueschist Unit on Tinos, Greece: Cold NE subduction and SW directed extrusion of the Cycladic continental margin under the Tsiknias Ophiolite. Tectonics, 39, e2019TC005890. https://doi.org/10.1029/2019TC005890

Lamont, T.N., Searle, M.P., Waters, D.J., Roberts, N.M.W., Palin, R.M., Smye, A., Dyck, B., Gopon, P., Weller, O.M., St-Onge, M.R. (2020a). Compressional origin of the Naxos metamorphic core complex, Greece: Structure, petrography, and thermobarometry. Geological Society of America Bulletin, 132(1-2), 149–197. https://doi.org/10.1130/B31978.1

Lanari, P. & Duesterhoeft, E. (2019). Modeling metamorphic rocks using equilibrium thermodynamics and internally consistent databases: Past achievements, problems and perspectives. Journal of Petrology, 60, 19–56. https://doi.org/10.1093/petrology/egy105

Lanari, P., & Engi, M. (2017). Local bulk composition effects on metamorphic mineral assemblages. Reviews in Mineralogy and Geochemistry, 83, 55– 102. https://doi.org/10.2138/rmg.2017.83.3

Laurent, V., Lanari, P., Naïr, I., Augier, R., Lahfid, A., & Jolivet, L. (2018). Exhumation of eclogite and blueschist (Cyclades, Greece): Pressure–temperature evolution determined by

thermobarometry and garnet equilibrium modelling. Journal of Metamorphic Geology, 36, 769– 798. https://doi.org/10.1111/jmg.12309

Le Pichon, X., & Angelier, J. (1979). The Hellenic arc and trench system; A key to the neotectonic evolution of the eastern Mediterranean area. Tectonophysics, 60, 1-42.

Le Pichon X., & Angelier J. (1981). The Aegean Sea. Philosophical Transactions of the Royal Society of London. Series A., Mathematical and Physical Sciences, 300, 357-372, http://doi.org/10.1098/rsta.1981.0069

Le Pichon X., Lybéris, N., Angelier, J., & Renard, V. (1982). Strain distribution over the East Mediterrranean Ridge: a synthesis incorporating new Sea-Beam Data. Tectonophysics, 86, 243-274. https://doi.org/10.1016/0040-1951(82)90069-5

Le Pichon, X., Chamot-Rooke, N., Lallemant, S., Noomen, R., & Veis, G. (1995). Geodetic determination of the kinematics of central Greece with respect to Europe: Implications for eastern Mediterranean tectonics. Journal of Geophysical Research, 100(B7), 12675– 12690. https://doi.org/10.1029/95JB00317

Le Pichon, X., Lallemant, S.J., Chamot-Rooke, N., Lemeur, D., & Pascal, G. (2002). The Mediterranean Ridge backstop and the Hellenic nappes, Marine Geology, 186(1-2), 111-125.https://doi.org/10.1016/S0025-3227(02)00175-5

Le Pichon, X., Şengör, A.M.C., & İmren. C. (2019). A new approach to the opening of the eastern Mediterranean Sea and the origin of the Hellenic subduction zone. Part 2: The Hellenic subduction zone. Canadian Journal of Earth Sciences, 56(11), 1144-1162. https://doi.org/10.1139/cjes-2018-0315

Limonov, A.F., Woodside, J.M., Cita, M.B., & Ivanov, M.K. (1996). The Mediterranean Ridge and related mud diapirism: a background. Marine Geology, 132(1-4), 7-19. https://doi.org/10.1016/0025-3227(96)00150-8

Lips, A.W., Cassard, D., Sözbilir, H., Yilmaz, H., & Wijbrans, J. R. (2001). Multistage exhumation of the Menderes Massif, western Anatolia (Turkey). Geologische Rundschau = International Journal of Earth Sciences, 89(4), 781-792.

Lips, A.L.W., Wijbrans, J. R., & White, S.H. (1999). New insights from $^{40}Ar/^{39}Ar$ laserprobe dating of white mica fabrics from the Pelion Massif, Pelagonian Zone, internal Hellenides, Greece; implications for the timing of metamorphic episodes and tectonic events in the Aegean region. In B. Durand, L. Jolivet, F. Horvath, M. Seranne (Eds.), The Mediterranean basins; Tertiary extension within the Alpine Orogen. Geological Society Special Publications, 156, 457-474.

Lister, G., Banga, G., & Feenstra, A. (1984). Metamorphic core complexes of Cordilleran type in the Cyclades. Aegean Sea, Greece. Geology, 12, 221-225.

Loos, S., & Reischmann, T. (1999). The evolution of the southern Menderes Massif in SW Turkey as revealed by zircon datings. Journal of the Geological Society of London156, 1021–1030.

Lyberis, N. (1984). Tectonic evolution of the North Aegean trough, Geological Society, London, Special Publications, 17, 709-725.

Lykousis, V., Alexandri, S., Woodside, J., de Lange, G., Dählmann, A., Perissoratis, C., Heeschen, K., Ioakim, C., Sakellariou, D., Nomikou, P., Rousakis, G., Casas, D., Ballas, D., & Ercilla, G. (2009). Mud volcanoes and gas hydrates in the Anaximander mountains (Eastern Mediterranean Sea). Marine and Petroleum Geology, 26(6), 854-872. https://doi.org/10.1016/j.marpetgeo.2008.05.002

Maggini, M., & Caputo, R. (2020). Sensitivity analysis for crustal rheological profiles: examples from the Aegean Region. Annals of Geophysics, 63(3), GT334. http://dx.doi.org/10.4401/ag-8244

Makris, J. (1978). The crust and upper mantle of the Aegean region from deep seismic soundings, Tectonophysics, 46(3–4), 269-284. https://doi.org/10.1016/0040-1951(78)90207-X

Makris, J., Papoulia, J., & Yegorova T. (2013). A 3-D density model of Greece constrained by gravity and seismic data. Geophysics Journal International, 194, 1–17. https://doi.org/10.1093/gji/ggt059

Malandri, C., Soukis, C., Maffione, M., Özkaptan, M., Vassilakis, E., Lozios, S., & van Hinsbergen, D.J.J. (2017). Vertical-axis rotations accommodated along the Mid-Cycladic lineament on Paros Island in the extensional heart of the Aegean orocline (Greece). Lithosphere, 9(1), 78–99. https://doi.org/10.1130/L575

Mantovani, E., Albarello, D., Tamburelli, C., Babbucci, D., & Viti, M. (1997). Plate convergence, crustal delamination, extrusion tectonics and minimization of shortening work as main controlling factors of the recent Mediterranean deformation pattern. In E. Mantovani (Ed.), Geodynamics of the Mediterranean region and its implications for seismic and volcanic risk. Annali di Geofisica (Vol. 40, pp. 611-643).

Marroni, M., Frassi, C., Göncüoğlu, M.C., Di Vincenzo, G., Pandolfi, L., Rebay, G., Ellero, A., & Ottria, G. (2014). Late Jurassic amphibolite-facies metamorphism in the Intra-Pontide Suture Zone (Turkey): an eastward extension of the Vardar Ocean from the Balkans into Anatolia? Journal of the Geological Society, 171(5), 605–608. https://doi.org/10.1144/jgs2013-104

Marsellos, A.E., Kidd, W.S.F., & Garver, J.I. (2010). Extension and exhumation of the HP/LT rocks in the Hellenic forearc ridge. American Journal of Science 310(1), 1-36. https://doi.org/10.2475/01.2010.01

Matsuda, J., Senoh, K., Maruoka, T., Sato, H., & Mitropoulos P. (1999). K-Ar ages of the Aegean volcanic rocks and their implication for the arc-trench system. Geochemical Journal, 33, 369-377. https://doi.org/10.2343/geochemj.33.369

McClusky S. et al., (2000). Global positioning system constraints on plate kinematics and dynamics in the eastern Mediterranean and Caucasus. Journal of Geophysical Research, 105(B3), 5695–5719. https://doi.org/10.1029/1999JB900351

McKenzie, D. (1972). Active Tectonics of the Mediterranean Region. Geophysical Journal of the Royal Astronomical Society, 30, 109-185. https://doi.org/10.1111/j.1365-246X.1972.tb02351.x

McKenzie, D. (1978). Active tectonics of the Alpine-Himalayan belt: the Aegean Sea and surrounding regions. Geophysics Journal of the Royal Astronomical Society, 55, 217-254.

McKenzie, D., & Bickle, M.J. (1988). The volume and composition of melt generated by extension of the lithosphere, Journal of Petrology, 29(3), 625-679. https://doi.org/10.1093/petrology/29.3.625

Meier, T., Becker, D., Endrun, B., Rische, M., Bohnhoff, M., Stöckhert, B., & Harjes, H.-P. (2007). A model for the Hellenic subduction zone in the area of Crete based on seismological investigations. Geological Society, London, Special Publications, 291, 183-199. https://doi.org/10.1144/SP291.9

Meighan, H. E., ten Brink, U., & Pulliam, J. (2013), Slab tears and intermediate-depth seismicity, Geophysical Research Letters, 40, 4244– 4248. https://doi.org/10.1002/grl.50830

Menant, A., Jolivet, L., Tuduri, J., Loiselet, C., Bertrand, G., & Guillou-Frottier, L. (2018). 3D subduction dynamics: A first-order parameter of the transition from copper- to gold-rich deposits in the eastern Mediterranean region, Ore Geology Reviews, 94, 118-135. https://doi.org/10.1016/j.oregeorev.2018.01.023

Menant, A., Jolivet, L., & Vrielynck, B. (2016). Kinematic reconstructions and magmatic evolution illuminating crustal and mantle dynamics of the eastern Mediterranean region since the late Cretaceous. Tectonophysics, 675, 103-140. https://doi/org/10.1016/j.tecto.2016.03.007

Meng, J., Sinoplu, O., Zhou, Z., Tokay, B., Kusky, T., Bozkurt, E., Wang, L. (2021). Greece and Turkey Shaken by African tectonic retreat. Scientifc Reports, 11, 6486. https://doi.org/10.1038/s41598-021-86063-y

Mercier, J.L. (1981). Extensional-compressional tectonics associated with the Aegean Arc: comparison with the Andean Cordillera of south Peru-north Bolivia. Philosophical Transactions of the Royal Society of London A (Mathematical and Physical Sciences), 300(1454), 337-355.

Meulenkamp, J.E., Wortel, M.J.R., van Wamel, W.A., Spakman, W., & Hoogerduyn, S.E. (1988). On the Hellenic subduction zone and the geodynamic evolution of Crete since the late middle Miocene. Tectonophysics, 146, 203-215.

Moix, P., Beccaletto, L., Kozur, H.W., Hochard, C., Rosselet, F., & Stampfli, G.M. (2008). A new classification of the Turkish terranes and sutures and its implication for the paleotectonic history of the region. Tectonophysics, 451(1–4), 7-39. https://doi.org/10.1016/j.tecto.2007.11.044

Morris, A., & Anderson, M. (1996). First palaeomagnetic results from the Cycladic Massif, Greece, and their implications for Miocene extension directions and tectonic models in the Aegean, Earth and Planetary Science Letters, 142(3–4), 397-408. https://doi.org/10.1016/0012-821X(96)00114-8

Morris, A., & Robertson, A.H.F. (1993). Miocene remagnetisation of carbonate platform and Antalya Complex units within the Isparta angle, SW Turkey, Tectonophysics, 220(1–4), 243-266. https://doi.org/10.1016/0040-1951(93)90234-B

Mouslopoulou, V., Nicol, A., Begg, J., Oncken, O., & Moreno, M. (2015). Clusters of megaearthquakes on upper plate faults control the Eastern Mediterranean hazard. Geophysical Research.Letters, 42, 10,282–10,289. https://doi.org/10.1002/2015GL066371

Moynihan, D.P., & Pattison, D.M. (2013). An automated method for the calculation of P-T paths from garnet zoning, with application to metapelitic schist from the Kootenay Arc, British Columbia, Canada. Journal of Metamorphic Geology, 31(5). 525-548.

Müller, P., Kreuzer, H., Lenz, H., & Harre, W. (1979). Radiometric dating of two extrusives from a Lower Pliocene Marine Section on Aegina Island, Greece. Newsletters on Stratigraphy, 8(1), 70 – 78. https://doi.ogr/10.1127/nos/8/1979/70

Mutlu, A.K., (2020). Seismicity, focal mechanism, and stress tensor analysis of the Simav region, western Turkey. Open Geosciences, 12(1), 479-490. https://doi.org/10.1515/geo-2020-0010

Neubauer, F. (2002). Evolution of late Neoproterozoic to early Paleozoic tectonic elements in Central and Southeast European Alpine mountain belts: review and synthesis, Tectonophysics, 352(1-2), 87-103. https://doi.org/10.1016/S0040-1951(02)00190-7

Nyst, M., & Thatcher, W. (2004). New constraints on the active tectonic deformation of the Aegean. Journal of Geophysical Research, 109(11), 23. https://doi.org/10.1029/2003JB002830

Oberhänsli, R., Candan, O. Dora, O.O., & Dürr, H.S. (1997). Eclogites within the Menderes crystalline complex, western Turkey, Anatolia. Lithos, 41, 135–150.

Oberhänsli, R., Candan, O., & Wilke, F. (2010). Geochronological Evidence of Pan-African Eclogites from the Central Menderes Massif, Turkey. Turkish Journal of Earth Science, 19(4), 431-447.

Oelsner, F., Candan, O., & Oberhänsli, R. (1997). New evidence for the time of the high-grade metamorphism in the Menderes Massif, SW-Turkey. Terra Nostra, 87. Jahrestagung der Geologischen Vereinigung Fundamental geologic processes, 15

Okal, E.A., Synolakis, C.E., Uslu, B., Kalligeris, N., & Voukouvalas, E. (2009). The 1956 earthquake and tsunami in Amorgos, Greece, Geophysical Journal International, 178(3), 1533–1554. https://doi.org/10.1111/j.1365-246X.2009.04237.x

Okay, A.I. (1980a). Mineralogy, petrology and phase relations of glaucophane–lawsonite zone blueschists from the Tavşanlı region, northwest Turkey. Contributions to Mineralogy and Petrology, 72, 243–255.

Okay, A.I. (1980b). Lawsonite zone blueschists and a sodic amphibole producing reaction in the Tavşanlı region, northwest Turkey. Contributions to Mineralogy and Petrology, 75, 179–186.

Okay, A.I. (1982). Incipient blueschist metamorphism and metasomatism in the Tavşanlı region, northwest Turkey. Contributions to Mineralogy and Petrology, 79, 361–367.

Okay, A.I. (1984). Distribution and characteristics of the north-west Turkish blueschists. In J.E. Dixon, A.H.F. Robertson (Eds.), The Geological Evolution of the Eastern Mediterranean. Geological Society of London Special Publications, 17, 455–466.

Okay, A.I. (1986). High-pressure/low-temperature metamorphic rocks of Turkey. In B.W. Evans, E.H. Brown (Eds.), Blueschists and eclogites. Memoir-Geological Society of America, 164, 333–347.

Okay, A.I. (2001). Stratigraphic and metamorphic inversions in the central Menderes Massif; a new structural model. Geologische Rundschau = International Journal of Earth Sciences, 89(4), 709727.

Okay, A.I. (2008). Geology of Turkey: A synopsis. Anschnitt, 21, 19–42.

Okay, A.I., Bozkurt, E., Satır, M., Yiğitbaş, E., Crowley, Q.G., Shang, C.K. (2008). Defining the southern margin of Avalonia in the Pontides: Geochronological data from the Late Proterozoic and Ordovician granitoids from NW Turkey, Tectonophysics, 461(1-4), 252-264. https://doi.org/10.1016/j.tecto.2008.02.004

Okay, A.I., & Kelley, S.P. (1994). Tectonic setting, petrology and geochronology of jadeite+ glaucophane and chloritoid+glaucophane schists from north-west Turkey. Journal of Metamorphic Geology, 12, 455–466.

Okay, A.I., Monod, O., & Monié, P. (2002). Triassic blueschists and eclogites from northwest Turkey: vestiges of the Paleo-Tethyan subduction. Lithos, 64(3), 155-178. https://doi.org/10.1016/S0024-4937(02)00200-1

Okay, A.I., Ozcan, E., Cavazza, M., Okay, N., & Less, G. (2010). Basement types, Lower Eocene Series, Upper Eocene olistostromes and the initiation of the Southern Thrace Basin, NW Turkey. Turkish Journal of Earth Sciences, 19, 1–25. https://doi.org/10.3906/yer-0902-10

2112 Okay A.I., & Satir, M. (2000). Coeval plutonism and metamorphism in a latest Oligocene
2113 metamorphic core complex in northwest Turkey. Geological Magazine, 137, 495-516.
2114 Okay, A.I., & Satır, M. (2006). Geochronology of Eocene plutonism and metamorphism in
2115 northwest Turkey: evidence for a possible magmatic arc. Geodinamica Acta 19, 251–265.
2116 Okay, A.I., Satır, M., Maluski, H., Siyako, M., Monie, P., Metzger, R., & Akyüz, S. (1996).
2117 Paleo- and Neo-Tethyan events in northwestern Turkey: geologic and geochronologic
2118 constraints. In T.M. Harrison (Ed.), The Tectonic Evolution of Asia. Cambridge University
2119 Press, Cambridge, pp. 420–441.
2120 Okay, A.I., Satır, M., & Siebel, W. (2006). Pre-Alpide orogenic events in the Eastern
2121 Mediterranean region. In D.G. Gee, R.A. Stephenson (Eds.), European Lithosphere
2122 Dynamics. Geological Society, London, Memoirs, 32, 389–405.
2123 Okay, A.I., Satir, M., Tuysuz, O., Akyuzm S., & Chen, F. (2001). The tectonics of Strandja
2124 Massif: late-Variscan and mid-Mesozoic deformation and metamorphism in the northern
2125 Aegean. Geologische Rundschau = International Journal of Earth Sciences, 90, 217–233.
2126 Okay, A.I., Siyako, M., & Burkan, K.A. (1991). Geology and tectonic evolution of the Biga
2127 Peninsula, northwest Turkey. Bulletin of Technical University Istanbul, 44, 191–256.
2128 Okay, A.I., Sunal, G., Sherlock, S., Altner, D., Tuysuz, O., Kylander-Clark, A.R.C., & Aygul,
2129 M. (2013). Early Cretaceous sedimentation and orogeny on the active margin of Eurasia;
2130 southern-central Pontides, Turkey. Tectonics, 32, 1247-1271.
2131 Okay, A.I., Sunal, G., Sherlock, S., Kylander-Clark, A. R. C., & Özcan, E. (2020). İzmir-Ankara
2132 suture as a Triassic to Cretaceous plate boundary—Data from central Anatolia. Tectonics, 39,
2133 e2019TC005849. https://doi.org/10.1029/2019TC005849
2134 Okay A.I., & Tüysüz, O. (1999). Tethyan sutures of northern Turkey. In B. Durand, L. Jolivet, F.
2135 Horváth, M. Séranne (Eds.), The Mediterranean Basins: Tertiary Extension with the Alpine
2136 Orogen. Geological Society, London, Special Publications (Vol. 156, pp. 475–515).
2137 https://doi.org/10.1144/GSL.SP.1999.156.01.22
2138 Okay, A.I., & Whitney, D.L. (2010). Blueschists, eclogites, ophiolites and suture zones in
2139 northwest Turkey: A review and a field excursion guide. Ofioliti, 35(2), 131-172.
2140 Okrusch, M., & Bröcker, M. (1990). Eclogites associated with high-grade blueschists in the
2141 Cyclades archipelago, Greece: a review. European Journal of Mineralogy, 2, 451–478.
2142 Oner, Z., Dilek, Y., & Kadioglu, Y.K. (2010). Geology and geochemistry of the synextensional
2143 Salihli granitoid in the Menderes core complex, western Anatolia, Turkey. International
2144 Geology Review, 52(2-3), 336-368. https://doi.org/10.1080/00206810902815871
2145 Oral B., Reilinger R.E., Nafi Toksöz M., King R.W., Aykut Barka A., Kinik I., & Lenk O.
2146 (1995). Global Positioning System offers evidence of plate motions in eastern Mediterranean.
2147 EOS., Transactions American Geophysical Union, 76, 9–11.
2148 Oygür, V., & Erler, A. (2000). Metalogeny of Simav graben [in Turkish]. Geological Bulletin of
2149 Turkey, 43(1), 7-19.
2150 Özbakır, A.D., Govers, R., & Fichtner, A. (2020). The Kefalonia Transform Fault: A STEP fault
2151 in the making. Tectonophysics, 787, 228471. https://doi.org/10.1016/j.tecto.2020.228471.
2152 Özbakır, A.D., Şengör, A.M.C., Wortel, M.J.R., & Govers, R. (2013). The Pliny–Strabo trench
2153 region: A large shear zone resulting from slab tearing. Earth and Planetary Science Letters,
2154 375, 188-195. https://doi.org/10.1016/j.epsl.2013.05.025
2155 Özcan, A., Göncüöğlu, M.C., Turhan, N., Uysal, S., Şentürk, K., & Işık, A. (1988). Late
2156 Paleozoic evolution of the Kütahya–Bolkardağ Belt. METU Journal of Pure and Applied
2157 Science 21 (1/3), 211–220.

Özdamar, S., Billor, M.Z., Sunal, G., Esenli, F., & Roden, N.F. (2013). First U–Pb SHRIMP zircon and $^{40}Ar/^{39}Ar$ ages of metarhyolites from the Afyon–Bolkardag Zone, SW Turkey: Implications for the rifting and closure of the Neo-Tethys, Gondwana Research, 24(1), 377-391. https://doi.org/10.1016/j.gr.2012.10.006

Ozgenc I., & Ilbeyli, N. (2008). Petrogenesis of the Late Cenozoic Egrigöz pluton in western Anatolia, Turkey: Implications for magma genesis and crustal processes, International Geology Review, 50(4), 375-391. https://doi.org/10.2747/0020-6814.50.4.375

Özgül N. (1997). Stratigraphy of the tectono-stratigraphic units in the region Bozkır–Hadim–Taşkent (northern central Taurides). Maden Tetkik ve Arama Dergisi, 119, 113-174.

Özkaymak, C., Sözbilir, H., & Uzel, B. (2013). Neogene-Quaternary evolution of the Manisa Basin: evidence for variation in the stress pattern of the Izmir-Balikesir Transfer Zone, western Anatolia. Journal of Geodynamics, 65, 117-35.

Özsayin, E., & Dirik, K. (2007). Quaternary activity of the Cihanbeyli and Yeniceoba fault zones: Inönü-Eskiflehir fault system, central Anatolia. Turkish Journal of Earth Sciences, 16, 471–492.

Palin, R.M., Weller, O.M., Waters, D.J., & Dyck, B. (2016). Quantifying geological uncertainty in metamorphic phase equilibria modelling; a Monte Carlo assessment and implications for tectonic interpretations. Geoscience Frontiers, 7(4), 591-607. https://doi.org/10.1016/j.gsf.2015.08.005.

Papadopoulos, G.A. (1997). On the interpretation of large-scale seismic tomography images in the Aegean sea area. Annals of Geophysics, 40(1), 37-42. https://doi.org/10.4401/ag-3933

Papadopoulos, T., Wyss, M., & Schmerge, D.L. (1988). Earthquake locations in the western Hellenic arc relative to the plate boundary. Bulletin of the Seismological Society of America, 78(3), 1222-1231.

Papanikolaou, D. (1987). Tectonic evolution of the Cycladic blueschist belt (Aegean Sea, Greece). In: Chemical Transport in Metasomatic Processes, Helgeson, H. C., (Ed.), pp. 429–450. NATO ASI Series, Reidel, Dordrecht

Papanikolaou, D.J., & Royden, L.H. (2007). Disruption of the Hellenic arc: Late Miocene extensional detachment faults and steep Pliocene-Quaternary normal faults—Or what happened at Corinth? Tectonics, 26, TC5003. https://doi.org/10.1029/2006TC002007

Papazachos B.C., & Comninakis P.E. (1971). Geophysical and tectonic features of the Aegean Arc. Journal of Geophysical Research, 76(8517).

Papazachos B.C., & Delibasis N.D. (1969). Tectonic stress field and seismic faulting in the area of Greece. Tectonophysics, 7, 231–255. https://doi.org/10.1016/0040-1951(69)90069-9

Papazachos B.C., Karakostas, V.G., Papazachos, C.B., & Scordilis, E.M. (2000). The geometry of the Wadati–Benioff zone and lithospheric kinematics in the Hellenic arc. Tectonophysics, 319(4), 275-300. https://doi.org/10.1016/S0040-1951(99)00299-1

Papazachos, C.B. (1999). Seismological and GPS evidence for the Aegean-Anatolia interaction. Geophysical Research Letters, 26(17), 2653-2656.

Papazachos, C.B. (2019). Deep Structure and Active Tectonics of the South Aegean Volcanic Arc. Elements, 15(3), 153–158. https://doi.org/10.2138/gselements.15.3.153

Parra, T., Vidal, O., & Jolivet, L. (2002). Relation between the intensity of deformation and retrogression in blueschist metapelites of Tinos Island (Greece) evidenced by chlorite–mica local equilibria. Lithos, 63(1–2), 41-66. https://doi.org/10.1016/S0024-4937(02)00115-9

Pearce, F.D., Rondenay, S., Sachpazi, M., Charalampakis, M., & Royden, L. H. (2012). Seismic investigation of the transition from continental to oceanic subduction along the western

Hellenic Subduction Zone. Journal of Geophysical Research, 117, B07306, https://doi.org/10.1029/2011JB009023

Pe-Piper, G. (2000). Origin of S-type granites coeval with I-type granites in the Hellenic subduction system, Miocene of Naxos, Greece. European Journal of Mineralogy, 12(4), 859–875. https://doi.org/10.1127/0935-1221/2000/0012-0859

Pe-Piper, G., & Piper, D.J.W. (2001). Late Cenozoic, post-collisional Aegean igneous rocks: Nd, Pb and Sr isotopic constraints on petrogenetic and tectonic models. Geological Magazine, 138, 653–668.

Pe-Piper, G., & Piper, D.J.W. (2005). The South Aegean active volcanic arc: relationships between magmatism and tectonics. In: Michael Fytikas, M., & Vougioukalakis, G.E. (Eds). Developments in Volcanology, 7, 113-133. https://doi.org/10.1016/S1871-644X(05)80034-8

Pe-Piper, G., Piper, D.J.W., & Matarangas, S. (2002). Regional implications of geochemistry and style of emplacement of Miocene I-type diorite and granite, Delos, Cyclades, Greece. Lithos, 60(1–2), 47-66. https://doi.org/10.1016/S0024-4937(01)00068-8

Perkins, R.J., Cooper, F.J., Condon, D.J., Tattitch, B., & Naden, J. (2018). Post-collisional Cenozoic extension in the northern Aegean: The high-K to shoshonitic intrusive rocks of the Maronia Magmatic Corridor, northeastern Greece. Lithosphere, 10(5), 582–601. https://doi.org/10.1130/L730.1

Peterek, A., & Schwarze, J. (2004). Architecture and Late Pliocene to recent evolution of outer-arc basins of the Hellenic subduction zone (south-central Crete, Greece). Journal of Geodynamics, 38(1), 19-55. https://doi.org/10.1016/j.jog.2004.03.002

Philippon, M., Brun, J.-P., Gueydan, F., & Sokoutis, D. (2014). The interaction between Aegean back-arc extension and Anatolia escape since Middle Miocene, Tectonophysics, 631, 176-188. https://doi.org/10.1016/j.tecto.2014.04.039

Piper, J.D.A., Gürsoy, H., Tatar, O., Beck, M.E., Rao, A., Koçbulut, F., & Mesci, B.L. (2010). Distributed neotectonic deformation in the Anatolides of Turkey: A paleomagnetic analysis. Tectonophysics, 488(1–4), 31–50. https://doi.org/10.1016/j.tecto.2009.05.026

Platt, J.D., Brantut, N., & Rice, J.R. (2015). Strain localization driven by thermal decomposition during seismic shear. Journal of Geophysical Research Solid Earth, 120, 4405– 4433. https://doi.org/10.1002/2014JB011493

Plunder, A., Agard, P., Chopin, C., & Okay, A.I. (2013). Geodynamics of the Tavşanlı zone, western Turkey: Insights into subduction/obduction processes, Tectonophysics, 608, 884-903. https://doi.org/10.1016/j.tecto.2013.07.028

Portner, D.E., Delph, J.R., Biryol, C.B., Beck, S.L., Zandt, G., Özacar, A.A., Sandvol, E., & Türkelli, N. (2018). Subduction termination through progressive slab deformation across Eastern Mediterranean subduction zones from updated P-wave tomography beneath Anatolia. Geosphere, 14(3), 907–925. https://doi.org/10.1130/GES01617.1

Pourteau, A., Candan, O., & Oberhänsli, R. (2010). High-pressure metasediments in central Turkey: Constraints on the Neotethyan closure history. Tectonics, 29, 1–18.

Pourteau, A., Oberhänsli, R., Candan, O., Barrier, E., & Vrielynck, B. (2016). Neotethyan closure history of western Anatolia: a geodynamic discussion. Geologische Rundschau = International Journal of Earth Sciences, 105, 203–224. https://doi.org/10.1007/s00531-015-1226-7

Pourteau, A., Sudo, M., Candan, O., Lanari, P., Vidal, O., & Oberhaensli, R. (2013). Neotethys closure history of Anatolia; insights from ^{40}Ar-^{39}Ar geochronology and P-T estimation in highpressure metasedimentary rocks. Journal of Metamorphic Geology, 31(6), 585-606.

Rabayrol, F., & Hart, C.J.R. (2021). Petrogenetic and tectonic controls on magma fertility and the formation of post-subduction porphyry and epithermal mineralization along the late Cenozoic Anatolian Metallogenic Trend, Turkey. Mineralium Deposita, 56, 279–306. https://doi.org/10.1007/s00126-020-00967-9

Rabayrol, F., Hart, C.J.R., & Creaser, R.A. (2019). Tectonic Triggers for Postsubduction Magmatic-Hydrothermal Gold Metallogeny in the Late Cenozoic Anatolian Metallogenic Trend, Turkey. Economic Geology, 114 (7), 1339–1363. https://doi.org/10.5382/econgeo.4682

Rabillard, A., Jolivet, L., Arbaret, L., Bessière, E., Laurent, V., Menant, A., et al. (2018). Synextensional granitoids and detachment systems within Cycladic metamorphic core complexes (Aegean Sea, Greece): Toward a regional tectonomagmatic model. Tectonics, 37, 2328– 2362. https://doi.org/10.1029/2017TC004697

Ramseyer, K., Aldahan, A.A., Collini, B., & Landström, O. (1992). Petrological modifications in granitic rocks from the siljan impact structure: evidence from cathodoluminescence, Tectonophysics, 216(1–2), 195-204. https://doi.org/10.1016/0040-1951(92)90166-4

Régnier, J. L., Mezger, J. E., & Passchier, C. W. (2007). Metamorphism of Precambrian-Palaeozoic schists of the Menderes core series and contact relationships with Proterozoic orthogneisses of the western Cine Massif, Anatolide belt, western Turkey. Geological Magazine, 144(1), 67-104.

Régnier, J. L., Ring, U., Passchier, C. W., Gessner, K., & Gungor, T. (2003). Contrasting metamorphic evolution of metasedimentary rocks from the Cine and Selimiye nappes in the Anatolide Belt, western Turkey. Journal of Metamorphic Geology, 21(7). 699-721

Reilinger, R., et al. (2006). GPS constraints on continental deformation in the Africa-Arabia-Eurasia continental collision zone and implications for the dynamics of plate interactions, Journal of Geophysical Research, 111, B05411. https://doi.org/10.1029/2005JB004051

Reilinger, R.E., McClusky, S.C., Oral, M. B., King, R. W., Toksoz, M. N., Barka, A. A., Kinik, I., Lenk, O., & Sanli, I. (1997). Global Positioning System measurements of present-day crustal movements in the Arabia-Africa-Eurasia plate collision zone. Journal of Geophysical Research, 102(B5), 9983– 9999. https://doi.org/10.1029/96JB03736

Reilinger, R., McClusky, S., Paradissis, D., Ergintav, S., & Vernant, P. (2010). Geodetic constraints on the tectonic evolution of the Aegean region and strain accumulation along the Hellenic subduction zone. Tectonophysics, 488(1-4), 22-30. https://doi.org/10.1016/j.tecto.2009.05.027

Rimmelé, G., Parra, T., Goffé, B., Oberhansli, R., Jolivet, L., & Candan, O. (2005). Exhumation paths of high-pressure–low-temperature metamorphic rocks from the Lycian Nappes and the Menderes Massif (SW Turkey): A multi-equilibrium approach. Journal of Petrology, 46, 641– 669.

Ring, U., Buchwaldt, R., & Gessner, K. (2004). Pb/Pb dating of garnet from the Anatolide belt in western Turkey: Regional implications and speculations on the role Anatolia played during the amalgamation of Gondwana. Zeitschrift der Deutschen Geologischen Gesellschaft, 154(4), 537-555. https://doi.org/10.1127/zdgg/154/2004/537

Ring, U., & Collins, A.S. (2005). U-Pb SIMS dating of synkinematic granites: timing of core-complex formation in the northern Anatolide belt of western Turkey. Journal of the Geological Society, London, 162, 289–298.

Ring, U., Gessner, K., Gungor, T., & Passchier, C.W. (1999). The Menderes Massif of western Turkey and the Cycladic Massif in the Aegean; do they really correlate? Journal of the Geological Society of London, 156(1), 3-6.

Ring, U., Johnson, C., Hetzel, R., & Gessner, K. (2003). Tectonic denudation of a Late Cretaceous-Tertiary collisional belt; regionally symmetric cooling patterns and their relation to extensional faults in the Anatolide Belt of western Turkey. Geological Magazine, 140(4), 421-441.

Ring, U., Willner, A.P., & Lackmann, W. (2001). Stacking of nappes with different pressure-temperature paths; an example from the Menderes Nappes of western Turkey. American Journal of Science, 301(10), 912-944.

Robertson, A.H.F., & Dixon, J.E. (1984). Introduction: aspects of the geological evolution of the Eastern Mediterranean. Geological Society, London, Special Publications, 17, 1-74. https://doi.org/10.1144/GSL.SP.1984.017.01.02

Robertson, A.H.F., & Ustaömer, T. (2004). Tectonic evolution of the Intra-Pontide suture zone in the Armutlu Peninsula, NW Turkey. Tectonophysics, 381(1–4), 175-209. https://doi.org/10.1016/j.tecto.2002.06.002

Robertson, A.H.F., & Ustaömer, T. (2009a). Formation of the Late Palaeozoic Konya Complex and comparable units in southern Turkey by subduction–accretion processes: Implications for the tectonic development of Tethys in the Eastern Mediterranean region. Tectonophysics, 473(1–2), 113-148. https://doi.org/10.1016/j.tecto.2008.10.027

Robertson, A.H.F., & Ustaömer, T. (2009b). Upper Palaeozoic subduction/accretion processes in the closure of Palaeotethys: Evidence from the Chios Melange (E Greece), the Karaburun Melange (W Turkey), and the Teke Dere Unit (SW Turkey). Sedimentary Geology, 220(1-2), 29-59. https://doi.org/10.1016/j.sedgeo.2009.06.005

Robertson, A.H.F., Clift, P.D., Degnan, P.J., & Jones, G. (1991). Paleogeographic and paleotectonic evolution of eastern Mediterranean Neotethys. Palaeogeography, Palaeoclimatology, Palaeoecology, 87, 289–343.

Roche, V., Jolivet, L., Papanikolaou, D., Bozkurt, E., Menant, A., & Rimmelé, G. (2019). Slab fragmentation beneath the Aegean/Anatolia transition zone: Insights from the tectonic and metamorphic evolution of the Eastern Aegean region, Tectonophysics, 754, 101-129. https://doi.org/10.1016/j.tecto.2019.01.016

Roche, V., Conand, C., Jolivet, L., & Augier, R. (2018). Tectonic evolution of Leros Island (Dodecanese, Greece) and correlations between the Aegean Domain and the Menderes Massif. Journal of the Geological Society, Geological Society of London, 1, 836-849. ff10.1144/jgs2018-028ff.ffinsu-01795049

Roche, V., Sternai, P., Guillou-Frottier, L., Menant, A., Jolivet, L., Bouchot, V., & Gerya, T. (2018). Emplacement of metamorphic core complexes and associated geothermal systems controlled by slab dynamics. Earth and Planetary Science Letters, 498, 322-333. https://doi.org/10.1016/j.epsl.2018.06.043

Rosenbaum, G., Avigad, D., Sánchez-Gómez, M (2002). Coaxial flattening at deep levels of orogenic belts: evidence from blueschists and eclogites on Syros and Sifnos (Cyclades, Greece). Journal of Structural Geology, 24(9), 1451-1462. https://doi.org/10.1016/S0191-8141(01)00143-2.

Rossetti, F., Riccardo Asti, R., Faccenna, C., Gerdes, A., Lucci, F., & Theyed, T. (2017). Magmatism and crustal extension: Constraining activation of the ductile shearing along the Gediz detachment, Menderes Massif (western Turkey). Lithos, 282–283, 145–162.

Royden, L.H. (1993). The tectonic expression slab pull at continental convergent boundaries, Tectonics, 12(2), 303– 325. https://doi.org/10.1029/92TC02248

Royden L.H., & Husson L. (2009). Subduction with Variations in Slab Buoyancy: Models and Application to the Banda and Apennine Systems. In S. Lallemand, F. Funiciello (Eds.), Subduction Zone Geodynamics. Frontiers in Earth Sciences. Springer, Berlin, Heidelberg. https://doi.org/10.1007/978-3-540-87974-9_2

Royden, L.H., & Papanikolaou, D.J. (2011). Slab segmentation and late Cenozoic disruption of the Hellenic arc. Geochemistry, Geophysics, Geosystems, AGU and the Geochemical Society, 12(3), https://doi.org/10.1029/2010GC003280

Sachpazi, M., Laigle, M., Charalampakis, M., Diaz, J., Kissling, E., Gesret, A., Becel, A., Flueh, E., Miles, P., & Hirn, A. (2016). Segmented Hellenic slab rollback driving Aegean deformation and seismicity, Geophysical Research Letters, 43, 65-658. https://doi.org/10.1002/2015GL066818

Şahin, S.Y., Aysal, N., Güngör, Y., Peytcheva, I., & Neubauer, F. (2014). Geochemistry and U–Pb zircon geochronology of metagranites in Istranca (Strandja). Zone, NW Pontides, Turkey: Implications for the geodynamic evolution of Cadomian orogeny, Gondwana Research, 26(2), 755-771. https://doi.org/10.1016/j.gr.2013.07.011

Şahin, S.Y., Örgün, Y., & Güngör, Y. (2010). Mineral and whole-rock geochemistry of the Kestanbol Granitoid (Ezine-Çanakkale). and its mafic microgranular enclaves in Northwestern Anatolia: Evidence of felsic and mafic magma Interaction. Turkish Journal of Earth Sciences, 19(1), 101-122.

Sakellariou, D., Mascle, J., & Lykousis, V. (2013). Strike slip tectonics and transtensional deformation in the Aegean region and the Hellenic arc: Preliminary results. Bulletin of the Geological Society of Greece, 47(2), 647-656. https://doi.org/10.12681/bgsg.11098

Salaün, G., Pedersen, H.A., Paul, A., Farra, V., Karabulut, H., Hatzfeld, D., Papazachos, C., Childs, D.M., Pequegnat, C., & SIMBAAD Team (2012). High-resolution surface wave tomography beneath the Aegean-Anatolia region: constraints on upper-mantle structure. Geophysical Journal International, 190(1), 406–420. https://doi.org/10.1111/j.1365-246X.2012.05483.x

Saltogianni, V., Mouslopoulou, V., Oncken, O., Nicol, A., Gianniou, M., & Mertikas, S. (2020). Elastic fault interactions and earthquake rupture along the southern Hellenic subduction plate interface zone in Greece. Geophysical Research Letters, 47, e2019GL086604. https://doi.org/10.1029/2019GL086604

Şaroğlu, F., Emre, Ö., & Kuşçu, İ. (1992). Active Fault Map of Turkey, General Directorate of Mineral Research and Exploration, Ankara, Turkey.

Satir, M., & Friedrichsen, H. (1986). The origin and evolution of the Menderes Massif, W-Turkey; a rubidium/strontium and oxygen isotope study. Geologische Rundschau = International Journal of Earth Sciences, 75(3), 703-714.

Satir, M., & Taubald, H. (2001). Hydrogen and oxygen isotope evidence for fluid-rock interactions in the Menderes Massif, western Turkey. Geologische Rundschau = International Journal of Earth Sciences, 89(4), 812-821.

Saunders, A.D., & Tarney, J. (1984). Geochemical characteristics of basaltic volcanism within back-arc basins. Geological Society, London, Special Publications, 16, 59-76. https://doi.org/10.1144/GSL.SP.1984.016.01.05

Saunders, P., Priestley, K., & Taymaz, T. (1998). Variations in the crustal structure beneath western Turkey. Geophysical Journal International, 134(2), 373–389. https://doi.org/10.1046/j.1365-246x.1998.00571.x

Savostin, L.A., Sibuet, J-C., Zonenshain, L.P., Le Pichon, X., & Roulet, M-J. (1986). Kinematic evolution of the Tethys belt from the Atlantic ocean to the pamirs since the Triassic, Tectonophysics, 123(1-4), 1-35. https://doi.org/10.1016/0040-1951(86)90192-7

Sayit, K., Marroni, M., Göncüoğlu, M.C., Pandolfi, L., Ellero, A., Ottria, G., & Frassi, C. (2016). Geological setting and geochemical signatures of the mafic rocks from the Intra-Pontide Suture Zone: implications for the geodynamic reconstruction of the Mesozoic Neotethys. Geologische Rundschau = International Journal of Earth Sciences, 105(1), 39-64.

Schaarschmidt, A., Haase, K. M., Voudouris, P. C., Melfos, V., & Klemd, R. (2021). Migration of arc magmatism above mantle wedge diapirs with variable sediment contribution in the Aegean. Geochemistry, Geophysics, Geosystems, 22, e2020GC009565. https://doi.org/10.1029/2020GC009565

Schellart, W., Freeman, J., Stegman, D. et al. (2007). Evolution and diversity of subduction zones controlled by slab width. Nature, 446, 308–311. https://doi.org/10.1038/nature05615

Schildgen, T.F., Yıldırım, C., Cosentino, D., & Strecker, M.R. (2014). Linking slab break-off, Hellenic trench retreat, and uplift of the Central and Eastern Anatolian plateaus. Earth-Science Reviews, 128, 147-168. https://doi.org/10.1016/j.earscirev.2013.11.006.

Schuiling, R.D. (1962). On petrology, age and structure of the Menderes migmatite complex (SW-Turkey). Bulletin of the Mineral Research Exploration Institute of Turkey, 58, 71-84.

Searle, M., & Lamont, T. (2020a). Compressional origin of the Aegean Orogeny, Greece. Geoscience Frontiers, https://doi.org/10.1016/j.gsf.2020.07.008.

Searle, M., & Lamont, T. (2020b). Compressional metamorphic core complexes, low-angle normal faults and extensional fabrics in compressional tectonic settings. Geological Magazine, 157(1), 101-118. doi:10.1017/S0016756819000207

Seaton, N.C.A., Whitney, D.L., Teyssier, C., Toraman, E., & Heizler, M.T. (2009). Recrystallization of high-pressure marble (Sivrihisar, Turkey). Tectonophysics, 479(3–4), 241–253. https://doi.org/10.1016/j.tecto.2009.08.015

Seghedi I., Helvacı, C., & Pécskay, Z. (2015). Composite volcanoes in the south-eastern part of İzmir–Balıkesir Transfer Zone, Western Anatolia, Turkey. Journal of Volcanology and Geothermal Research, 291, 72-85. https://doi.org/10.1016/j.jvolgeores.2014.12.019

Senel, M., & Aydal, N. (2002). Geological Map of Turkey (Izmir and Istanbul sheets): Maden Tetkik ve Arama Genel Mudurlugu, Eskisehir Yolu, Turkey, scale 1:500,000.

Seman, S., Stockli, D.F., & Soukis, K. (2017), The provenance and internal structure of the Cycladic Blueschist Unit revealed by detrital zircon geochronology, Western Cyclades, Greece. Tectonics, 36, 1407–1429. https://doi.org/10.1002/2016TC004378.

Şengör, A.M.C., Görür, N., & Şaroğlu, F. (1985). Strike-slip faulting and related basin formation in zones of tectonic escape: Turkey as a case study. In K.T. Biddle, N. Christie-Blick (Eds.), Strike-slip Faulting and Basin Formation, Society for Economic Paleontology Mineralogy Special Publications, 37, 227-264.

Şengör, A.M.C., Satır, M., & Akkök, R. (1984). Timing of tectonic events in the Menderes Massif, Western Turkey. Implications for tectonic evolution and evidence for Pan-African basement in Turkey. Tectonics, 3, 693 -707.

Şengör, A.M.C., & Yılmaz, Y. (1981). Tethyan evolution of Turkey: A plate tectonic approach. Tectonophysics, 75, 181–241.

Şengör, A.M.C., & Zabcı, C. (2019). The North Anatolian Fault and the North Anatolian Shear Zone. In: Landscapes and Landforms of Turkey, Kuzucuoğlu, C., Çiner, A., Kazancı, N. (Eds.), Springer International Publishing, World Geomorphological Landscapes. https://doi.org/10.1007/978-3-030-03515-0_27

Şengün, F., Yiğitbaş, E., & Tunç, E. (2011). Geology and tectonic emplacement of eclogite and blueschists, Biga Peninsula, northwest Turkey. Turkish Journal of Earth Sciences, 20(3), 273-285.

Seyitoğlu, G. (1997). Late Cenozoic tectono-sedimentary development of the Selendi and Us¸ak-Gu¨re basins: a contribution to the discussion on the development of east-west and north trending basins in western Turkey. Geological Magazine, 134, 163–175.

Seyitoğlu, G., & Scott, B.C. (1996). The cause of north-south extensional tectonics in western Turkey: Tectonic escape vs. back-arc spreading vs. orogenic collapse. Journal of Geodynamics, 22, 145 -153.

Seyitoğlu, G., Işık, V., & Çemen, I. (2004). Complete Tertiary exhumation history of the Menderes Massif, western Turkey: an alternative working hypothesis. Terra Nova, 16, 358–363.

Shaw, B., & Jackson, J. (2010). Earthquake mechanisms and active tectonics of the Hellenic subduction zone. Geophysical Journal International, 181, 966-984. https://doi.org/10.1111/j.1365-246X.2010.04551.x

Sherlock, S., Kelley, S., Inger, S., Harris, N., & Okay, A. (1999). ^{40}Ar-^{39}Ar and Rb-Sr geochronology of high-pressure metamorphism and exhumation history of the Tavşanlı Zone, NW Turkey. Contributions to Mineralogy and Petrology, 137, 46–58.

Shin, T.A., Catlos, E.J., Jacob, L., & Black, K. (2013). Relationships between very high pressure subduction complex assemblages and intrusive granitoids in the Tavşanlı Zone, Sivrihisar Massif, central Anatolia. Tectonophysics, 595–596, 183–197.

Snopek, K., Meier, T., Endrun, B., Bohnhoff, M., & Casten, U. (2007). Comparison of gravimetric and seismic constraints on the structure of the Aegean lithosphere in the forearc of the Hellenic subduction zone in the area of Crete. Journal of Geodynamics, 44(3–5), 173-185. https://doi.org/10.1016/j.jog.2007.03.005.

Sodoudi, F., Kind, R., Hatzfeld, D., Priestley, K., Hanka, W., Wylegalla, K., Stavrakakis, G., Vafidis, A., Harjes, H.-P., & Bohnhoff, M. (2006). Lithospheric structure of the Aegean obtained from P and S receiver functions, Journal of Geophysical Research, 111, B12307. https//doi.org/10.1029/2005JB003932

Sokoutis, D., Brun, J.P., Van den Driessche, J., & Pavlides, S. (1993). A major Oligo-Miocene detachment in southern Rhodope controlling north Aegean extension. Journal of the Geological Society, 150, 243-246. https://doi.org/10.1144/gsjgs.150.2.0243

Sözbilir, H., Sari, Uzel, B., Ökmen, S., & Akkiraz, S. (2011). Tectonic implications of transtensional supradetachment basin development in an extension-parallel transfer zone: the Kocacay Basin, western Anatolia, Turkey. Basin Research, 23, 423–448. https://doi.org/10.1111/j.1365-2117.2010.00496.x

Spakman, W. (1990). Tomographic images of the upper mantle below central Europe and the Mediterranean. Terra Nova, 2, 542-553. https://doi.org/10.1111/j.1365-3121.1990.tb00119.x

Spakman, W. (1991). Delay-time tomography of the upper mantle below Europe, the Mediterranean, and Asia Minor, Geophysical Journal International, 107(2), 309–332. https://doi.org/10.1111/j.1365-246X.1991.tb00828.x

2475 Spakman, W., Wortel, M.J.R., & Vlaar, N.J. (1988). The Hellenic subduction zone: A
2476 tomographic image and its geodynamic implications. Geophysical Research Letters, 15, 60–
2477 63.
2478 Spear, F. S., & Peacock, S. M. (1989). Metamorphic pressure-temperature-time paths. American
2479 Geophysical Union Short Course in Geology, 7, 102.
2480 Speciale, P.A., Catlos, E.J., Yıldız, G.O., Shin, T.A., & Black, K.N. (2012). Zircon ages from the
2481 Beypazarı granitoid pluton (north central Turkey): tectonic implications. Geodinamica Acta,
2482 25(3-4), 162-182. https://doi.org/10.1080/09853111.2013.858955.
2483 Stampfli, G.M. (2000). Tethyan oceans. In E. Bozkurt, J.A. Winchester, J.D.A. Piper (Eds.),
2484 Tectonics and magmatism in Turkey and surrounding area. Geological Society of London,
2485 Special Publication, London (Vol. 173, pp. 1-23).
2486 Stamfli, G.M., & Kozur, H.W. (2006). Europe from the Variscan to the Alpine cycles.
2487 Geological Society, London, Memoirs, 32, 57-82.
2488 https://doi.org/10.1144/GSL.MEM.2006.032.01.04
2489 Stanley, D., Knight, R., Stuckenrath, R., & Catani, G. (1978). High sedimentation rates and
2490 variable dispersal patterns in the western Hellenic Trench. Nature, 273, 110–113.
2491 https://doi.org/10.1038/273110a0
2492 Stouraiti, C., Baziotis, I., Asimow, P.D., & Downes, H. (2018). Geochemistry of the Serifos
2493 calc-alkaline granodiorite pluton, Greece: constraining the crust and mantle contributions to
2494 I-type granitoids. Geologische Rundschau = International Journal of Earth Science [1999],
2495 107, 1657–1688. https://doi.org/10.1007/s00531-017-1565-7
2496 Stouraiti, C., Mitropoulos, P., Tarney, J., Barreiro, B., McGrath, A.M., & Baltatzis, E. (2010).
2497 Geochemistry and petrogenesis of late Miocene granitoids, Cyclades, southern Aegean:
2498 Nature of source components. Lithos, 114(3–4), 337-352.
2499 https://doi.org/10.1016/j.lithos.2009.09.010.
2500 Suckale, J., Rondenay, S., Sachpazi, M., Charalampakis, M., Hosa, A., Royden, L.H. (2009).
2501 High-resolution seismic imaging of the western Hellenic subduction zone using teleseismic
2502 scattered waves, Geophysical Journal International, 178(2), 775–791.
2503 https://doi.org/10.1111/j.1365-246X.2009.04170.x
2504 Sümer, Ö, Uzel, B., Özkaymak, C., & Sözbilir, H. (2018). Kinematics of the Havran-Balıkesir
2505 Fault Zone and its implication on geodynamic evolution of the Southern Marmara Region,
2506 NW Anatolia, Geodinamica Acta, 30(1), 306-323.
2507 https://doi.org/10.1080/09853111.2018.1540145
2508 Sunal, G. (2012). Devonian magmatism in the western Sakarya Zone, Karacabey region, NW
2509 Turkey, Geodinamica Acta, 25(3-4), 183-201.
2510 https://doi.org/10.1080/09853111.2013.858947
2511 Symeou, V., Homberg, C., Nader, F. H., Darnault, R., Lecomte, J.-C., & Papadimitriou, N.
2512 (2018). Longitudinal and temporal evolution of the tectonic style along the Cyprus Arc
2513 system, assessed through 2-D reflection seismic interpretation. Tectonics, 37, 30– 47.
2514 https://doi.org/10.1002/2017TC004667
2515 Tan, O. (2013). The dense micro-earthquake activity at the boundary between the Anatolian and
2516 South Aegean microplates. Journal of Geodynamics, 65, 199-217.
2517 Tatar, O., Akpınar, Z., Gürsoy, H., Piper, J.D.A., Koçbulut, F., Mesci, B.L., Polat, A., & Roberts,
2518 A.P. (2013). Palaeomagnetic evidence for the neotectonic evolution of the Erzincan Basin,
2519 North Anatolian Fault Zone, Turkey, Journal of Geodynamics, 65, 244-258.
2520 https://doi.org/10.1016/j.jog.2012.03.009

Taymaz, T., Jackson, J., & McKenzie, D. (1991). Active tectonics of the north and central Aegean Sea. Geophysical Journal International, 106(2), 433–490. https://doi.org/10.1111/j.1365-246X.1991.tb03906.x

Tekin, U.K., Göncüoğlu, M.C., & Turhan, N. (2002). First evidence of Late Carnian radiolarians from the Izmir–Ankara suture complex, central Sakarya, Turkey: implications for the opening age of the Izmir–Ankara branch of Neo-Tethys. Geobios, 35(1), 127-135. https://doi.org/10.1016/S0016-6995(02)00015-3

ten Veen, J. H., & Kleinspehn, K. L. (2002). Geodynamics along an increasingly curved convergent plate margin: Late Miocene-Pleistocene Rhodes, Greece, Tectonics, 21(3), https://doi.org/10.1029/2001TC001287

Teyssier, C., & Whitney, D.L. (2002). Gneiss domes and orogeny. Geology, 30(12), 1139–1142. https://doi.org/10.1130/0091-7613(2002)030<1139:GDAO>2.0.CO;2

Thomson, S.N., & Ring, U. (2006). Thermochronologic evaluation of post collision extension in the Anatolide orogen, western Turkey. Tectonics 25: TC3005.

Tirel, C., Brun, J.-P., & Burov, E. (2008). Dynamics and structural development of metamorphic core complexes. Journal of Geophysical Research, 113, B04403. http://dx.doi.org/10.1029/2005JB003694.fayon

Tirel, C., Gueydan, F., Tiberi, C., & Brun, J-P. (2004). Aegean crustal thickness inferred from gravity inversion. Geodynamical implications. Earth and Planetary Science Letters, 228(3–4), 267-280. https://doi.org/10.1016/j.epsl.2004.10.023.

Tiryakioğlu, İ. (2015). Geodetic aspects of the 19 May 2011 Simav earthquake in Turkey. Geomatics, Natural Hazards and Risk, 6(1), 76-89. https://doi.org/10.1080/19475705.2013.831379

Toker, C.E., Ulugergerli, E.U., Kilic, A.R. (2018). The Naşa intrusion (Western Anatolia) and its tectonic implication: A joint analyses of gravity and earthquake catalog data. Bulletin of Mineral and Resourse Exploration, 156, 247-258.

Toker, C.E., Ulugergerli, E.U., Kilic, A.R. (2019). Using non-deriative filters for the tectonic implications: A case study in Simav graben, western Turkey. Symposium on the Application of Geophysics to Engineering and Environmental Problems 2019. May 2019, 304-307.

Tomaschek, F., Kennedy, A.K., Villa, I.M., Lagos, M., & Ballhaus, C. (2003). Zircons from Syros, Cyclades, Greece—Recrystallization and mobilization of zircon during high-pressure metamorphism. Journal of Petrology, 44(11), 1977–2002. https://doi.org/10.1093/petrology/egg067

Topuz, G., Candan, O., Okay, A.I., von Quadt, A., Othman, M., Zack, T., & Wang, J. (2020). Silurian anorogenic basic and acidic magmatism in Northwest Turkey: Implications for the opening of the Paleo-Tethys, Lithos, 356–357, 105302. https://doi.org/10.1016/j.lithos.2019.105302

Topuz, G., & Okay, A.I. (2017). Late Eocene–Early Oligocene two-mica granites in NW Turkey (the Uludağ Massif): Water-fluxed melting products of a mafic metagreywacke, Lithos, 268–271, 334-350. https://doi.org/10.1016/j.lithos.2016.11.010

Ünay, E., Emre, Ö, Erkal, T., & Keçer, M. (2001). The rodent fauna from the Adapazarı pull-apart basin (NW Anatolia): its bearings on the age of the North Anatolian fault, Geodinamica Acta, 14(1-3), 169-175. https://doi.org/10.1080/09853111.2001.11432442

Ustaömer, A.P., Mundil, R., & Renne, P.R. (2005). U/Pb and Pb/Pb zircon ages for arc-related intrusions of the Bolu Massif (W Pontides, NW Turkey): Evidence for Late Precambrian (Cadomian) age. Terra Nova, 17, 215-223. https://doi.org/10.1111/j.1365-3121.2005.00594.x

Ustaömer, P.A., Ustaömer, T., Collins, A.S., & Robertson, A.H.F. (2009). Cadomian (Ediacaran–Cambrian). arc magmatism in the Bitlis Massif, SE Turkey: Magmatism along the developing northern margin of Gondwana, Tectonophysics, 473(1-2), 99-112. https://doi.org/10.1016/j.tecto.2008.06.010

Ustaömer, P.A., Ustaömer, T., Gerdes, A., & Zulauf, G. (2011). Detrital zircon ages from a Lower Ordovician quartzite of the İstanbul exotic terrane (NW Turkey): evidence for Amazonian affinity. Geologische Rundschau = International Journal of Earth Sciences, 100, 23–41 (2011). https://doi.org/10.1007/s00531-009-0498-1

Ustaömer, P.A., Ustaömer, T., & Robertson, A.H.F. (2012). Ion probe U-Pb dating of the central Sakarya basement: A peri-Gondwana terrane intruded by Late Lower Carboniferous subduction/collision-related granitic rocks. Turkish Journal of Earth Sciences, 21, 905–932.

Ustaömer, T., Ustaömer, P.A., Robertson, A.H.F., & Gerdes, A. (2016). Implications of U–Pb and Lu–Hf isotopic analysis of detrital zircons for the depositional age, provenance and tectonic setting of the Permian–Triassic Palaeotethyan Karakaya Complex, NW Turkey. Geologische Rundschau = International Journal of Earth Sciences, 105, 7–38. https://doi.org/10.1007/s00531-015-1225-8

Ustaömer, T., Ustaömer, P.A., Robertson, A.H.F., & Gerdes, A. (2020). U-Pb-Hf isotopic data from detrital zircons in late Carboniferous and Mid-Late Triassic sandstones, and also Carboniferous granites from the Tauride and Anatolide continental units in S Turkey: implications for Tethyan palaeogeography. International Geology Review, 62(9), 1159-1186. https://doi.org/10.1080/00206814.2019.1636415

Uzel, B., Kuiper, K., Sözbilir, H., Kaymakci, N., Langereis, C.G., & Boehm, K. (2020). Miocene geochronology and stratigraphy of western Anatolia: Insights from new Ar/Ar dataset. Lithos, 352–353, 105305. https://doi.org/10.1016/j.lithos.2019.105305

Uzel, B., Sözbilir, H., C¸ Özkaymaka, Ç, Kaymakcı, N., & Langereis, C.G. (2013). Structural evidence for strike-slip deformation in the Izmir–Balıkesir transfer zone and consequences for late Cenozoic evolution of western Anatolia (Turkey). Journal of Geodynamics, 65, 94–116.

Vanderhaeghe, O. (2004). Structural development of the Naxos migmatite dome. In: Whitney, D.L, Teyssier, C., & Siddoway, C.S. (Eds.), Gneiss domes in orogeny. Geological Society of America Special Paper, 380, 211–228.

van der Meer, D.G., van Hinsbergen, D.J.J., & Spakman, W. (2018). Atlas of the underworld: Slab remnants in the mantle, their sinking history, and a new outlook on lower mantle viscosity. Tectonophysics, 723, 309-448. https://doi.org/10.1016/j.tecto.2017.10.004.

van Hinsbergen, D.J.J., & Schmid, S.M. (2012). Map view restoration of Aegean–West Anatolian accretion and extension since the Eocene, Tectonics, 31, TC5005. https://doi.org/10.1029/2012TC003132

van Hinsbergen, D.J.J., Hafkenscheid, E., Spakman, W., Meulenkamp, J.E., & Wortel, R. (2005). Nappe stacking resulting from subduction of oceanic and continental lithosphere below Greece. Geology, 33 (4), 325–328. https://doi.org/10.1130/G20878.1

van Hinsbergen, D.J.J., Kaymakçi, N., Spakman, W., & Torsvik, T.H. (2010). Reconciling the geological history of western Turkey with plate circuits and mantle tomography, Earth and Planetary Science Letters, 297(3–4), 674-686.

Ventouzi, C., Papazachos, C., Hatzidimitriou, P., Papaioannou, C., & EGELADOS Working Group, (2018). Anelastic P- and S- upper mantle attenuation tomography of the southern

Aegean Sea subduction area (Hellenic Arc) using intermediate-depth earthquake data. Geophysical Journal International, 215(1), 635–658. https://doi.org/10.1093/gji/ggy292

von Blanckenburg, F., & Davies, J.H. (1995). Slab breakoff: A model for syncollisional magmatism and tectonics in the Alps, Tectonics, 14(1), 120– 131. https://doi.org/10.1029/94TC02051

von Raumer, J.F., Stampfli, G.M., Arenas, R., & Martínez, S.S. (2015). Ediacaran to Cambrian oceanic rocks of the Gondwana margin and their tectonic interpretation. Geologische Rundschau = International Journal of Earth Sciences, 104, 1107–1121 (2015). https://doi.org/10.1007/s00531-015-1142-x

Walcott, C.R.Ł, & White, S.H. (1998). Constraints on the kinematics of post-orogenic extension imposed by stretching lineations in the Aegean region. Tectonophysics, 298, 155e175.

Wallace, L.M., Ellis, S., & Mann, P. (2008). Tectonic block rotation, arc curvature, and back-arc rifting: insights into these processes in the Mediterranean and the western Pacific. IOP Conference Series: Earth and Environmental Sciences, 2, 012010. https://doi.org/10.1088/1755-1307/2/1/012010

Wallace, L.M., McCaffrey, R., Beavan, J., & Ellis, S. (2005). Rapid microplate rotations and backarc rifting at the transition between collision and subduction. Geology, 33, 857–860. https://doi.org/10.1130/G21834.1

Wei, W., Zhao, D., Wei, F., Bai, X., & Xu, J. (2019). Mantle dynamics of the Eastern Mediterranean and Middle East: Constraints from P-wave anisotropic tomography. Geochemistry, Geophysics, Geosystems, 20,4505–4530. https://doi.org/10.1029/2019GC008512

Westaway, R. (1994). Present-day kinematics of the Middle East and eastern Mediterranean, Journal of Geophysical Research, 99(B6), 12071–12090. https://doi.org/10.1029/94JB00335

Westbrook, G.K., & Reston, T.J. (2002). The accretionary complex of the Mediterranean Ridge: tectonics, fluid flow and the formation of brine lakes -an introduction to the special issue of Marine Geology. Marine Geology, 186, 1-8.

Westerweel, J., Uzel, B., Langereis, C.G., Kaymakci, N., & Sözbilir, H. (2020). Paleomagnetism of the Miocene Soma basin and its structural implications on the central sector of a crustal-scale transfer zone in western Anatolia (Turkey). Journal of Asian Earth Sciences, 193, https://doi.org/10.1016/j.jseaes.2020.104305

White, R.W., Powell, R., Holland, T.J.B., Johnson, T.E., & Green, E.C.R. (2014). New mineral activity-composition relations for thermodynamic calculations in metapelitic systems. Journal of Metamorphic Geology, 32, 261– 286.

Whitney, D.L., & Bozkurt, E. (2002). Metamorphic history of the southern Menderes Massif, western Turkey. Geological Society of America Bulletin, 114(7), 829-838.

Whitney, D.L., Teyssier, C., Rey, P., & Buck, W.R. (2013). Continental and oceanic core complexes. Geological Society of America Bulletin, 125(3-4), 273–298. https://doi.org/10.1130/B30754.1

Whitney, D.L., Teyssier, C., Toraman, E., Seaton, N.C.A., & Fayon, A.K. (2011). Metamorphic and tectonic evolution of a structurally continuous blueschist-to-Barrovian terrane, Sivrihisar Massif, Turkey. Journal of Metamorphic Geology, 29, 193–212.

Woodside, J.M., Mascle, J., Huguen, C., & Volkonskaia, A. (2000). The Rhodes Basin, a post-Miocene tectonic trough. Marine Geology, 165, 1–12.

Woodside, J.M., Mascle, J., Zitter, T.A.C., Limonov, A.F., Ergün, M., & Volkonskaia, A. (2002). The Florence Rise, the Western Bend of the Cyprus Arc. Marine Geology, 185(3–4), 177-194. https://doi.org/10.1016/S0025-3227(02)00194-9

Wortel, M.J.R., & Spakman, W. (1992). Structure and dynamics of subducted lithosphere in the Mediterranean region. Proceedings of the Koninklijke Nederlandse Akademie van Wetenschappen, 95(3), 325-347.

Wortel, M.J.R., & Spakman, W. (2000). Subduction and slab detachment in the Mediterranean-Carpathian region. Science, 290, 1910-1917. https://doi.org/10.1126/science.290.5498.1910

Xypolias, P., & Alsop, G.I. (2014). Regional flow perturbation folding within an exhumation channel: A case study from the Cycladic Blueschists. Journal of Structural Geology, 62, 141-155, https://doi.org/10.1016/j.jsg.2014.02.001.

Xypolias, P., Iliopoulos, I., Chatzaras, V., & Kokkalas, S. (2012). Subduction- and exhumation-related structures in the Cycladic Blueschists: Insights from south Evia Island (Aegean region, Greece), Tectonics, 31, TC2001, doi:10.1029/2011TC002946.

Yiğitbaş, E., Kerrich, R., Yılmaz, Y., Elmas, A., & Xie, Q. (2004). Characteristics and geochemistry of Precambrian ophiolites and related volcanics from the Istanbul–Zonguldak Unit, Northwestern Anatolia, Turkey: following the missing chain of the Precambrian South European suture zone to the east, Precambrian Research, 132(1-2), 179-206. https://doi.org/10.1016/j.precamres.2004.03.003

Yilmaz, Y., Genc, C., Karacik, Z., & Altunkaynak, S. (2001). Two contrasting magmatic associations of NW Anatolia and their tectonic significance. Journal of Geodynamics, 31(3), 243-271.

Yilmaz, Y., Tüysüz, O., Yigitbas, E., Genç, C., & Şengör, A.M.C. (1997). Geology and tectonic evolution of the Pontides. In A.G. Robinson (Ed.), Regional and petroleum geology of the Black Sea and surrounding region. American Association of Petroleum Geology Memiors (Vol. 68, pp. 183-226), Tulsa, Oklahoma.

Yolsal-Çevikbilen, S., Taymaz, T., & Helvacı, C. (2014). Earthquake mechanisms in the Gulfs of Gökova, Sığacık, Kuşadası, and the Simav Region (western Turkey): Neotectonics, seismotectonics and geodynamic implications. Tectonophysics, 635, 100-124. https://doi.org/10.1016/j.tecto.2014.05.001

Yoshioka, T. (1996). Evolution of fault geometry and development of strike-slip basins: Comparative studies on the transform zones in Turkey and Japan. Island Arc, 5, 407-419. https://doi.org/10.1111/j.1440-1738.1996.tb00162.x

Zhu, L., Mitchell, B. J., Akyol, N., Çemen, I., & Kekovali, K. (2006). Crustal thickness variations in the Aegean region and implications for the extension of continental crust, Journal of Geophysical Research, 111, B01301. https//doi.org/10.1029/2005JB003770

Zitter, T.A.C., Woodside, J.M., & Mascle, J. (2003). The Anaximander Mountains: a clue to the tectonics of southwest Anatolia. Geological Journal, 38, 375-394. https://doi.org/10.1002/gj.961

Zlatkin, O., Avigad, D., & Gerdes, A. (2013). Evolution and provenance of Neoproterozoic basement and Lower Paleozoic siliciclastic cover of the Menderes Massif (western Taurides): Coupled U–Pb–Hf zircon isotope geochemistry, Gondwana Research, 23(2), 682-700. https://doi.org/10.1016/j.gr.2012.05.006

2702 **Tables**

2703 **Table 1.** Brief summary of some available ages from granitic assemblages that intrude the
2704 Istanbul-Zonguldak Zone**.**

Granite	Location[a]	Approach	Age	Reference
Late Pan-African Granitoids or Cadomian Granitoids				
Karadere (Karabuk metagranite)	1	U-Pb zrn	924±4 620±2	Chen et al. (2002)
Karadere (Karabuk metatonalite)	1	U-Pb zrn	668±7 589±4	Chen et al. (2002)
Bolu (Tüllükiris)	2	U-Pb zrn	576±6	Ustaömer et al. (2005)
Bolu (Kapıkaya)	2	U-Pb zrn	565.3±1.9	Ustaömer et al. (2005)
Karadere (Karabuk)	1	Sm-Nd grt + wr	559±8	Chen et al. (2002)
Devonian				
Bolu	2		389, 200 273-255 229.6±4.2/2.3	Ustaömer et al. (2012)
Bolu	2	$^{40}Ar/^{39}Ar$ or + hbl	381.1±7.1 93.3±2.0	Delaloye and Bingöl (2000)
Permo-Triassic				
Bolu (Sünnice Group)	2	$^{207}Pb/^{206}Pb$ zrn	262±19	Ustaömer et al. (2005)
Sancaktepe	3	U-Pb zrn	257.3±1.5 253.7±1.8	Aysal et al. (2018)
Akyazi	4	$^{40}Ar/^{39}Ar$ or + chl	240.4±4.9 86.1±2.0	Delaloye and Bingöl (2000)

2705 **[a]** See Figure 4 for locations of these granite bodies.
2706 **[b]** Abbreviations after Whitney and Evans (2010), wr= whole rock.
2707
2708
2709
2710
2711
2712
2713
2714
2715
2716
2717

2718 **Table 2.** Brief summary of some available ages from granitic assemblages that intrude the
2719 Tavşanlı Zone**.**

Granite	Location	Approach	Age	Reference
Western Tavsanli Zone: Suture Zone Granitoids				
Topuk	5	$^{40}Ar/^{39}Ar$ bt+kfs	63.5±2.8 43.0±2.7	Delaloye and Bingöl (2000)
Orhaneli	6	$^{40}Ar/^{39}Ar$ bt+hbl	57.9±1.2 31.4±0.6	Delaloye and Bingöl (2000)
Orhaneli	6	$^{40}Ar/^{39}Ar$ bt+hbl	52.6±0.4 52.4±1.4	Harris et al. (1994)
Topuk	5	$^{40}Ar/^{39}Ar$ bt+hbl	47.8±0.4	Harris et al. (1994)
Tepeldag (Gürgenyayla)	7	U-Pb zrn	44.9±0.2	Okay and Satir (2006)
Tepeldag (Gürgenyayla)	7	Rb-Sr bt	44.7±0.4	Okay and Satir (2006)
Eastern Tavsanli Granitoids				
Kaymaz	9	U-Pb zrn	84.98±6.27	Gautier (1984)
Sivrihisar	10	U-Pb zrn	79.9±8.6 42.4±2.4	Shin et al. (2013)
Sarıkavak (Topkaya)	11	U-Pb zrn	65.9±3.8	Gautier (1984)
Sivrihisar	10	$^{40}Ar/^{39}Ar$ bt+hbl	62.9±1.3 56.8±0.2	Delaloye and Bingöl (2000)
Karacaören (Günyüzü)	10	$^{40}Ar/^{39}Ar$ hbl+bt	59.3±3.0 46.7±2.3	Demirbilek et al. (2018)
Tekoren granodiorite (Günyüzü)	10	$^{40}Ar/^{39}Ar$ hbl+bt	57.8±2.3 23.4±1.1	Demirbilek et al. (2018)
Dinek granodiorite (Günyüzü)	10	$^{40}Ar/^{39}Ar$ hbl+kfs	55.9±2.7 45.3±1.8	Demirbilek et al. (2018)
Kaymaz	9	$^{40}Ar/^{39}Ar$ kfs	54.0±2.1 52.1±2.0	Demirbilek et al. (2018)
Sivrihisar	10	$^{40}Ar/^{39}Ar$ hbl	53.2±2.1 44.7±1.7	Demirbilek et al. (2018)
Kadinicik (Günyüzü)	10	$^{40}Ar/^{39}Ar$ hbl+wr	52.8±2.4 45.7±1.7	Demirbilek et al. (2018)
Kaymaz	9	U-Pb zrn	44.3±4.9 19.4±4.5	Shin et al. (2013)
Sivrihisar (Kadnıcık/Günyüzü)	10	Rb-Sr kfs+bt	47.0±1.6	Bağcı et al. (2012)
Sivrihisar	10	$^{40}Ar/^{39}Ar$ kfs	46.02±0.21	This study
Sivrihisar (Karacaören /Günyüzü)	10	Rb-Sr kfs+bt	40.8±3.0	Bağcı et al. (2012)

2720 **[a]** See Figure 4 for locations of these granite bodies.

[b] Abbreviations after Whitney and Evans (2010), wr= whole rock.

Table 3. Brief summary of some available ages from granitic assemblages associated with rocks between the Sakarya and Istanbul Zones**.**

Granite	Location	Approach	Age	Reference
Middle Eocene Magmatic Rocks (South Marmara Granitoids)				
Şevketiye	12	$^{40}Ar/^{39}Ar$ ms	71.9±1.8	Delaloye and Bingöl (2000)
İlyasdağ tonalite (Marmara Island)	13	U-Pb zrn	56.7±0.8 46.1±0.7	Ustaömer et al. (2009)
Karabiga (Lapeski)	14	U-Pb xtm	52.7±1.9	Beccaletto et al. (2007)
Fistikli (Armutlu–Yalova)	15	$^{40}Ar/^{39}Ar$ bt+ms	48.2±1.0 34.3±0.9	Delaloye and Bingöl (2000)
Karabiga (Lapeski)	14	$^{40}Ar/^{39}Ar$ bt	45.3±0.9	Delaloye and Bingöl (2000)
Kapidağ	16	$^{40}Ar/^{39}Ar$ hbl+bt	42.2±1.0 38.2±0.8	Delaloye and Bingöl (2000)
Avsa Island	17	K-Ar bt	40.9±1.1	Karacık et al. (2008)

[a] See Figure 4 for locations of these granite bodies.

[b] Abbreviations after Whitney and Evans (2010), wr= whole rock.

2752 **Table 4.** Brief summary of some available ages from granitic assemblages that intrude the
2753 Central Sakarya Zone**.**

Granite	Location	Approach	Age	Reference
Late Pan-African Grantoids or Cadomian Granitoids				
Pamukova	18	U-Pb zrn	582.0±9.1 446.0±3.8	Okay et al. (2008)
Gemlik	15	U-Pb zrn	575.5±3.6 438.9±4.5	Okay et al. (2008)
Silurian-Devonian				
Saricakaya	19	U-Pb zrn	419±6 434±7 319±5 Ma	Topuz et al. (2020)
Carboniferous				
Inhisar	18	$^{40}Ar/^{39}Ar$ ms+chl	348.5±6.6 213.5±4.4	Delaloye and Bingöl (2000)
Gevyke	20	U-Pb zrn	327±12	Ustaömer et al. (2016)
Söğüt granite (Saricakaya, Çaltı)	19	U-Pb zrn	327.2±1.9	Ustaömer et al. (2012)
Söğüt granite (Saricakaya, Küplü)	19	U-Pb zrn	324.3±1.3	Ustaömer et al. (2012)
Söğüt granite (Saricakaya, Borçak)	19	U-Pb zrn	319.5±1.1	Ustaömer et al. (2012)
Bilecik	21	$^{40}Ar/^{39}Ar$ bt+or	312.1±6.0 233.5±4.8	Delaloye and Bingöl (2000)
Permian				
Söğüt granite	19	$^{40}Ar/^{39}Ar$ bt	290±4.8	Okay et al. (2002)
Jurassic to Late Cretaceous				
Pamukova	18	$^{40}Ar/^{39}Ar$ or +chl	168.2±3.5 123.0±2.8	Delaloye and Bingöl (2000)
Beypazari	22	U-Pb zrn	95.4±4.2 70.5±3.4	Speciale et al. (2012)
Beypazari	22	$^{40}Ar/^{39}Ar$ bt	80.1±1.4 79.2±0.9	Okay et al. (2020)
Beypazari	22	U-Pb zrn	74.8±0.4 73.2±1.4	Okay et al. (2020)
Beypazari	22	$^{40}Ar/^{39}Ar$ hbl	82.9±1.8 77.7±4.5	Delaloye and Bingöl (2000)

2754 **[a]** See Figure 4 for locations of these granite bodies.
2755 **[b]** Abbreviations after Whitney and Evans (2010), wr= whole rock.
2756
2757
2758
2759

2760 **Table 5.** Brief summary of some available ages from granitic assemblages that intrude the
2761 Western Pontides Zone**.**

Granite	Location	Approach	Age	Reference
Proterozoic				
Karacabey (Tamsali)	23	U-Pb zrn (inherited cores)	1961.9±16.4 804±10.5	Aysal et al. (2012)
Evciler (Kazdağ)	24	U-Pb zrn	805, 286	Ustaomer et al. (2012)
Karaburun	25	U-Pb zrn	1800, 960, 380, 297	Ustaomer et al. (2012)
Devonian				
Güveylerobası (Çamlik-related)	26	U-Pb zrn	401.5±4.8	Aysal et al. (2012)
Karacabey (Tamsali)	23	U-Pb zrn	400.3±1.4	Aysal et al. (2012)
Eybek (Çamlik)	27	U-Pb zrn	397.5±1.4	Okay et al. (2006)
Karacabey (Tamsali)	23	Pb-Pb zrn	395.9±4.1 393.8±2.7	Sunal (2012)
Güveylerobası	26	U-Pb zrn	371.2 ± 2.3	Ustaömer et al. (2016)
Permo-Triassic				
Karacabey (Tamsali)	23	$^{40}Ar/^{39}Ar$ bt	298.3±5.8 199.4±4.0	Delaloye and Bingöl (2000)
Karacabey (Tamsali)	23	$^{40}Ar/^{39}Ar$ bt	304.5±3.7 223.0±7.5	Sunal (2012)
Kozak	28	U-Pb zrn	280.2±18.2 259.1±13.8	Black et al. (2013)
Karaburun	25	U-Pb zrn	244.4±1.5	Ustaomer et al. (2012)
Evciler	24	U-Pb zrn	229.6±0.60	Ustaomer et al. (2012)
Karacabey (Tamsali)	23	(U/Th)-He zrn	93.0±6.9	Sunal (2012)
Late Eocene-Oligocene-Miocene				
Kozak	28	$^{40}Ar/^{39}Ar$ or +bt	37.6±3.3 19.5±0.4	Delaloye and Bingöl (2000)
Kozak	28	U-Pb zrn	36.5±6.6 17.1±0.7	Black et al. (2013)
Evciler (Kazdağ)	24	$^{40}Ar/^{39}Ar$ chl+bt	36.0±1.4 26.4±0.6	Delaloye and Bingöl (2000)
Evciler (Kazdağ)	24	U-Pb zrn	24.8±4.6	Erdoğan et al. (2013)
Evciler (Kazdağ)	24	^{207}Pb-^{206}Pb zrn	28.2±4.1 26.0±5.6	Erdoğan et al. (2013)
Uludağ	29	U-Pb zrn	34.71±0.34 28.24±0.39	Topuz and Okay (2017)
Eybek	27	U-Pb zrn	32.5±3.0 21.0±1.2	Black et al. (2013)
Katrandag	30	$^{40}Ar/^{39}Ar$ hbl+chl	27.6±0.6 24.7±0.6	Delaloye and Bingöl (2000)

Uludağ	29	$^{40}Ar/^{39}Ar$ bt	26.8±0.8 24.7±0.7	Delaloye and Bingöl (2000)
Eybek	27	$^{40}Ar/^{39}Ar$ bt	26.6±0.8 21.1±0.4	Delaloye and Bingöl (2000)
Cataldag (Bozenkoy)	31	K-Ar bt+hbl	25.9±0.5 21.27±0.44	Boztuğ et al. (2009)
Evciler (Kazdağ)	24	Rb-Sr	25.0± 0.3	Birkle (1992) Genc (1998)
Kozak	28	K-Ar bt+hbl	23.0±3.8 14.6±1.0	Boztuğ et al. (2009)
Cataldag (Cataltepe)	31	K-Ar bt	22.0±0.3 21.7±0.1	Boztuğ et al. (2009)
Cataldag (Turfaldag)	31	K-Ar bt	21.9±0.6 21.2±0.6	Boztuğ et al. (2009)
Cataldag (Balicikhisar)	31	$^{40}Ar/^{39}Ar$ bt	20.8±0.4	Delaloye and Bingöl (2000)
Evciler (Kazdağ)	24	Rb-Sr	20.7±0.2 20.5±0.2	Okay and Satir (2000)
Younger South Marmara Granitoid Bodies				
Yenice	32	$^{40}Ar/^{39}Ar$ hbl	47.6±1.4 20.1±1.1	Delaloye and Bingöl (2000)
Ilica	33	K-Ar hbl	37.9±0.1 25.6±1.9	Boztuğ et al. (2009)
Kizildam	34	K-Ar wr+bt	23.9±0.6 20.7±0.8	Karacık et al. (2008)
Danisment	35	K-Ar wr+bt	23.2±1.1 22.1±0.6	Karacık et al. (2008)
Ilica	33	K-Ar wr+bt	22.8±0.5 18.4±2.2	Karacık et al. (2008)
Sarioluk	36	K-Ar hbl	22.6±0.8	Karacık et al. (2008)
Yenice	32	K-Ar wr+bt	21.9±1.1 18.8±1.3	Karacık et al. (2008)
Davutlar	37	K-Ar wr+bt	21.6±0.6 18.4±1.1	Karacık et al. (2008)
Yeniköy	36	K-Ar wr	20.1±1.0	Karacık et al. (2008)

[a] See Figure 4 for locations of these granite bodies.
[b] Abbreviations after Whitney and Evans (2010), wr= whole rock.

Table 6. Brief summary of some available ages from granitic assemblages that intrude the Rhodope-Strandja Zone (Biga Peninsula only)**.**

Granite	Location	Approach	Age	Reference
Kuscayir	38	$^{40}Ar/^{39}Ar$ hbl	39.4±0.8 35.7±0.8	Delaloye and Bingöl (2000)
Kestanbol (Ezine)	39	U-Pb zrn	26.2±2.0 18.8±1.0	Black et al. (2013)
Kestanbol (Ezine)	39	$^{40}Ar/^{39}Ar$	22.21±0.07 21.22±0.09	Akal (2013)
Kestanbol (Ezine)	39	$^{40}Ar/^{39}Ar$ hbl	20.5±0.6	Delaloye and Bingöl (2000)

[a] See Figure 4 for locations of these granite bodies.

[b] Abbreviations after Whitney and Evans (2010), wr= whole rock.

Table 7. Brief summary of some available ages from granitic assemblages that intrude the Afyon Zone**.**

Granite	Location	Approach	Age	Reference
Paleozoic Granitoids				
Sandıklı	39	U-Pb zrn	541±9	Gürsu et al. (2004)
Alaçam (basement)	41	U-Pb zrn	331.3±1.7 314.3±4.8	Candan et al. (2016)
Alaçam (basement)	41	U-Pb zrn	314.9±2.7	Hasözbek et al. (2010)
Late Eocene-Oligocene-Miocene				
Balkan (Muratdag)	40	$^{40}Ar/^{39}Ar$ or	35.5±3.0	Delaloye and Bingöl (2000)
Koyunoba	42	U-Pb zrn	30.0±3.9 14.7±2.6	Catlos et al. (2012)
Alaçam	41	$^{40}Ar/^{39}Ar$ or	27.1±1.0 18.5±1.8	Delaloye and Bingöl (2000)
Alaçam	41	U-Pb zrn	25.3±1.5 17.5±0.9	Catlos et al. (2012)
Egrigöz	43	$^{40}Ar/^{39}Ar$ bt+or	24.6±1.4 20.0±0.7	Delaloye and Bingöl (2000)
Egrigöz	43	U-Pb zrn	24.1±1.3 5.7±0.6	Catlos et al. (2012)
Egrigöz	43	U-Pb zrn	20.7±0.6	Ring and Collins (2005)
Koyunoba	42	$^{40}Ar/^{39}Ar$ kfs	20.37±0.03	Etzel et al. (2020)
Alaçam	41	Rb-Sr bt	20.17±0.20 20.01±0.20	Hasözbek et al. (2010)
Egrigöz	43	$^{40}Ar/^{39}Ar$ ms	20.2±0.3	Işık et al. (2004)
Egrigöz	43	$^{40}Ar/^{39}Ar$ kfs	20.02±0.03	Etzel et al. (2020)
Alaçam	41	U-Pb zrn	20.0±1.4 20.3±3.3	Hasözbek et al. (2010)
Baklan	40	$^{40}Ar/^{39}Ar$ wr	19.3±0.9 17.8±0.7	Aydoğan et al. (2008)

[a] See Figure 4 for locations of these granite bodies.
[b] Abbreviations after Whitney and Evans (2010), wr= whole rock.

Table 8. Brief summary of some available ages from granitic assemblages that intrude the Menderes Massif**.**

Granite	Location	Approach	Age	Reference
Late Pan-African Granitoids or Cadomian Granitoids				
Çine Massif metagranites	north of Milas	U-Pb zrn	662±3 517±6	Loos and Reichmann (1999)
Demirci–Gördes		$^{207}Pb/^{206}Pb$ zrn	537.2 ±2.4 544.1 ± 4.3	Dannat (1997)
Ödemiş–Kiraz		$^{207}Pb/^{206}Pb$ zrn	528.0 ±4.3 570 ± 5	Dannat (1997)
		$^{207}Pb/^{206}Pb$ zrn	546.0±1.6 546.4± 0.8	Hetzel and Reischmann (1996)
Çine Massif		$^{207}Pb/^{206}Pb$ zrn	521±5 572±7	Loos and Reischmann (1999)
Bafa Lake-Çine Massif		U-Pb zrn	541±14 566±9	Gessner et al. (2004)
Yatağan		$^{207}Pb/^{206}Pb$ zrn	555.5±6.2	Dora et al. (2005)
North of Yatağan		U/Pb zrn	549±26	Dora et al. (2005)
Triassic				
Alasehir	44	U-Pb zrn	222.9±1.1	Ustaömer et al. (2016)
Late Eocene-Oligocene-Miocene				
Alasehir	44	$^{40}Ar/^{39}Ar$ bt	36.4±2.2 16.6±0.3	Delaloye and Bingöl (2000)
Gordes	45	$^{40}Ar/^{39}Ar$ ms	28.8±0.6 19.4±0.7	Delaloye and Bingöl (2000)
Salihli	46	Th-Pb mnz	21.7±4.5 9.6±1.6	Catlos et al. (2010)
Turgutlu	47	Th-Pb mnz	19.2±5.1 11.5±0.8	Catlos et al. (2010)
Salihli	46	U-Pb ttn	17.07±0.2 14.36±0.3	Rossetti et al. (2017)
Turgutlu	47	U-Pb mnz	16.1±0.2	Glony and Hetzel (2007)
Salihli	46	U-Pb aln	15.0±0.3	Glony and Hetzel (2007)
Turgutlu	47	$^{40}Ar/^{39}Ar$ kfs	14.06±0.03	Etzel et al. (2020)
Salihli	46	$^{40}Ar/^{39}Ar$ kfs	5.05±0.02	Etzel et al. (2020)

[a] See Figure 4 for locations of these granite bodies.

[b] Abbreviations after Whitney and Evans (2010), wr= whole rock.

Table 9. List of selected earthquake events along the Simav Fault and associated fault systems.

No.[a]	Event-ID[b]	Time (UTC)	Latitude	Longitude	Depth (km)	Rms[c]	Mag[d]
1	465625	2/18/2020 16:09	39.1015	27.8453	14.68	0.45	5.2
2	150860	12/10/2011 5:15	38.8625	30.1883	13.44	0.96	4.2
3	319040	12/2/2015 15:52	39.1495	28.154	10.85	0.4	4.0
4	132605	6/10/2011 22:47	39.0975	28.3405	34.38	0.85	4.7
5	160143	3/29/2012 10:13	38.6035	30.004	12.77	0.73	4.2
6	367059	3/29/2017 18:10	38.2003	31.0575	14.87	0.36	4.0
7	495401	2/9/2021 15:51	38.5965	31.6318	7.01	0.49	4.7
8	495403	2/9/2021 15:53	38.59	31.6495	4.61	0.41	4.1
9	367501	4/3/2017 9:05	38.4801	31.7975	13.84	0.25	4.0
10	136512	7/27/2011 9:58	38.3278	31.8802	17.79	0.33	4.8
11	128573	5/19/2011 20:15	39.1328	29.082	24.46	0.49	5.7
12	128577	5/19/2011 20:25	39.1442	29.1078	7.00	0.44	4.6
13	128603	5/19/2011 21:12	39.113	29.0377	7.74	0.57	4.8
14	128672	5/20/2011 0:13	39.1413	29.1065	16.92	0.62	4.1
15	128701	5/20/2011 0:58	39.1147	29.0837	17.38	0.78	4.3
16	129252	5/21/2011 21:43	39.1037	29.0513	7.00	0.11	4.0
17	129791	5/24/2011 2:55	39.1013	29.0217	16.80	0.45	4.2
18	131192	5/30/2011 22:03	39.1567	29.0112	15.29	0.85	4.0
19	132022	6/5/2011 21:29	39.143	29.095	6.98	0.55	4.0
20	134386	6/29/2011 11:40	39.1232	29.0032	9.28	0.75	4.0
21	135896	7/19/2011 21:16	39.1048	29.093	17.66	0.67	4.1
22	138300	8/25/2011 4:19	39.139	29.0957	22.54	0.77	4.3
23	161414	4/16/2012 10:10	39.1227	29.1222	6.90	0.5	4.7
24	161595	4/17/2012 20:45	39.1468	29.1142	6.99	0.58	4.5
25	161902	4/20/2012 16:39	39.1525	29.0975	20.59	0.81	4.4
26	177315	10/30/2012 0:12	39.1385	29.1787	21.35	0.76	4.1
27	188611	3/12/2013 20:47	39.1203	29.0583	12.81	0.52	4.1
28	197002	6/9/2013 14:18	39.1392	29.022	15.61	0.68	4.1
29	234353	7/15/2014 12:25	39.13	29.0041	9.92	0.32	4.1
30	309933	9/3/2015 8:23	39.1226	29.1225	10.24	0.49	4.1

a. See Figure 7A for events 1-10 and Figure 7B for events 11-30.

b. Parameters were extracted from https://deprem.afad.gov.tr/depremkatalogu 1900-20XX Earthquake Catalog (M>=4.0), Turkish Ministry of the Interior, Disaster and Emergency Management Presidency, Earthquake Department (AFAD).

c. Rms= root-mean-square (RMS) travel time residual in seconds.

d. All magnitudes are ML (original magnitude relationship defined for local earthquakes), except events 1, 3, 6, 7, 9, 29, and 30, which are moment magnitudes (Mw).

Table 10. List of selected earthquake events along the Aegean-Anatolian plate boundary.

No.[a]	Event-ID[b]	Time (UTC)	Latitude	Longitude	Depth (km)	Rms[c]	Mag[d]
1	199626	7/12/2013 0:36	40.3738	25.946	27.85	0.45	4.3
2	201060	7/30/2013 5:33	40.3028	25.7902	20.01	0.52	5.3
3	184151	1/19/2013 19:26	39.6382	25.6795	20.91	0.5	4.2
4	360268	2/6/2017 10:58	39.5275	26.1373	9.83	0.21	5.3
5	183497	1/12/2013 13:47	39.6447	25.6733	6.89	0.8	4.0
6	155511	1/29/2012 21:03	38.7387	26.0447	32.39	0.68	4.2
7	101387	3/26/2010 18:35	38.1457	26.177	24.26	0.2	4.7
8	426091	11/27/2018 23:16	36.7565	25.877	16.15	0.62	4.4
9	426096	11/27/2018 23:46	36.6493	25.4535	5.95	0.75	4.1
10	418888	8/19/2018 5:46	35.8861	26.0695	28.49	0.77	4.9
11	309516	8/27/2015 0:25	34.7751	25.8068	7.06	0.52	4.5
12	472843	5/2/2020 16:44	34.5521	25.8181	6.76	0.56	5.1
13	472824	5/2/2020 13:45	34.2973	25.7371	9.63	0.98	5.2
14	472819	5/2/2020 12:51	34.2226	25.8253	6.65	0.98	6.4
15	472825	5/2/2020 13:33	33.9548	26.0141	6.5	0.96	4.6
16	472827	5/2/2020 14:21	34.2123	26.232	5.86	0.93	4.8
17	294406	4/16/2015 18:07	34.8643	26.7275	12.34	0.62	5.9
18	169403	7/4/2012 23:46	35.1613	26.9993	34.09	0.35	5.0
19	293183	3/27/2015 23:34	35.7295	26.576	56.13	0.47	5.0
20	507881	8/1/2021 4:31	36.3843	27.0805	10.86	0.17	5.5
21	187555	2/27/2013 22:05	36.7298	26.5115	140.27	0.43	4.1
22	417483	7/26/2018 8:17	37.6546	26.6698	4.5	0.52	4.5
23	483762	10/30/2020 11:51	37.879	26.703	14.9	1	6.6
24	375576	6/12/2017 12:28	38.8486	26.313	15.96	0.28	6.2
25	431610	2/20/2019 18:23	39.6011	26.4261	5.8	0.37	5.0
26	411695	5/3/2018 2:04	39.967	26.8993	10.39	0.35	4.3
27	284923	12/16/2014 9:02	40.1298	27.0845	17.35	0.29	4.3
28	115792	11/3/2010 2:51	40.3997	26.3147	28.9	0.59	5.1
29	199626	7/12/2013 0:36	40.3738	25.946	27.85	0.45	4.3

a. See Figure 11 for events.

b. Parameters were extracted from https://deprem.afad.gov.tr/depremkatalogu 1900-20XX Earthquake Catalog (M>=4.0), Turkish Ministry of the Interior, Disaster and Emergency Management Presidency, Earthquake Department (AFAD).

c. Rms= root-mean-square (RMS) travel time residual in seconds.

d. All magnitudes are ML (original magnitude relationship defined for local earthquakes), except events 4, 8-14, 16, 17, 19, 20, 23-28, which are moment magnitudes (Mw).

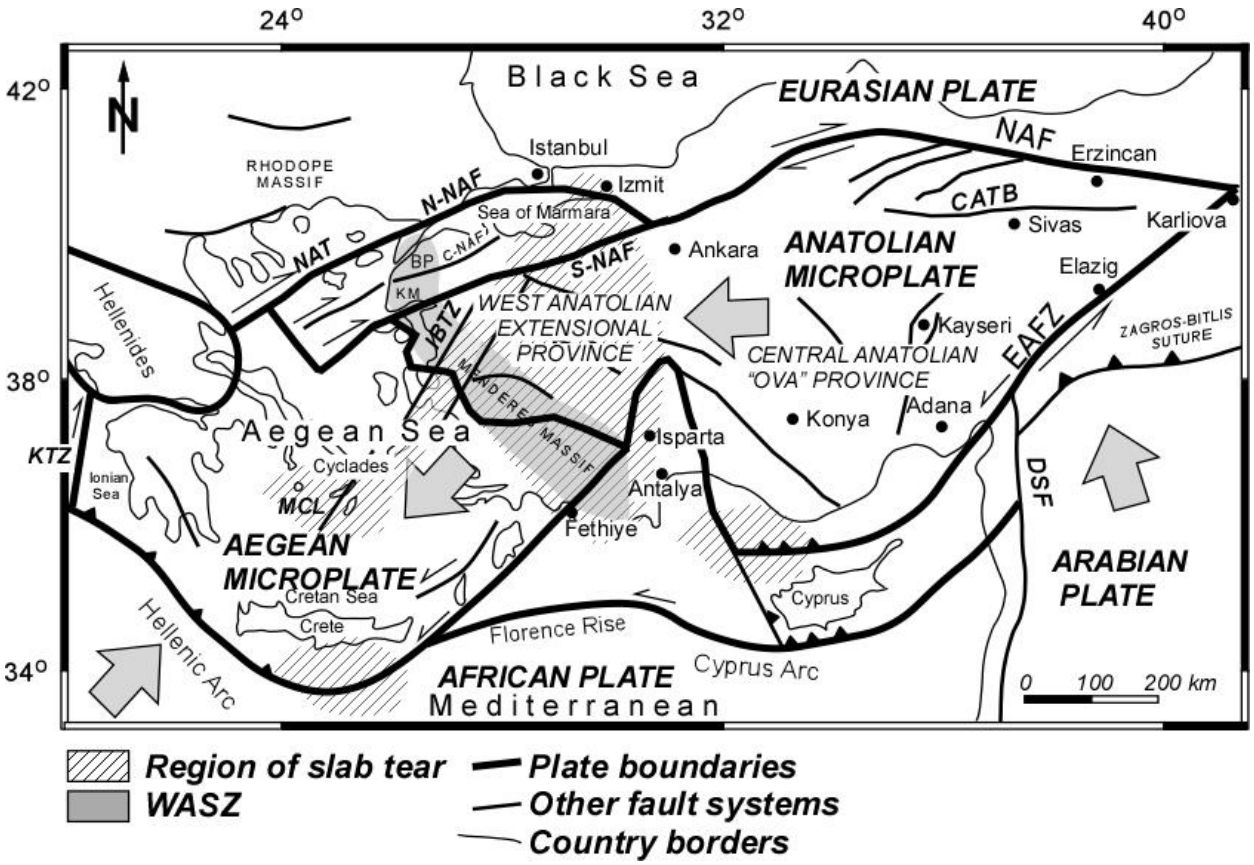

Figure 1. Tectonic map of the Aegean and Anatolian microplates. Plate boundaries after McClusky et al. (2000), Nyst & Thatcher (2004), Piper et al. (2010), Harrison et al. (2012), and Tan (2013). Only some major fault systems are labeled. NAF= North Anatolian Fault, EAFZ= East Anatolian Fault Zone, CATB = Central Anatolian Thrust Belt, DSF = Dead Sea Fault; KTZ = Kephalonia Transform Zone; MCL= Mid-Cycladic lineament; İBTZ= Izmir–Balıkesir transfer zone; NAT= North Aegean Trough; NAF = North Anatolian Fault (N-, northern, C- central, and S- southern segments); KM= Kazdağ Massif. Region of slab tear in western Turkey and the Aegean after Jolivet et al. (2015), near Crete (Özbakır et al., 2013), Cyprus (Woodside et al., 2002), and between the Aegean domain and the Menderes Massif (Roche et al., 2019). Boundaries between Central and Western Anatolia after Şengör et al. (1985).

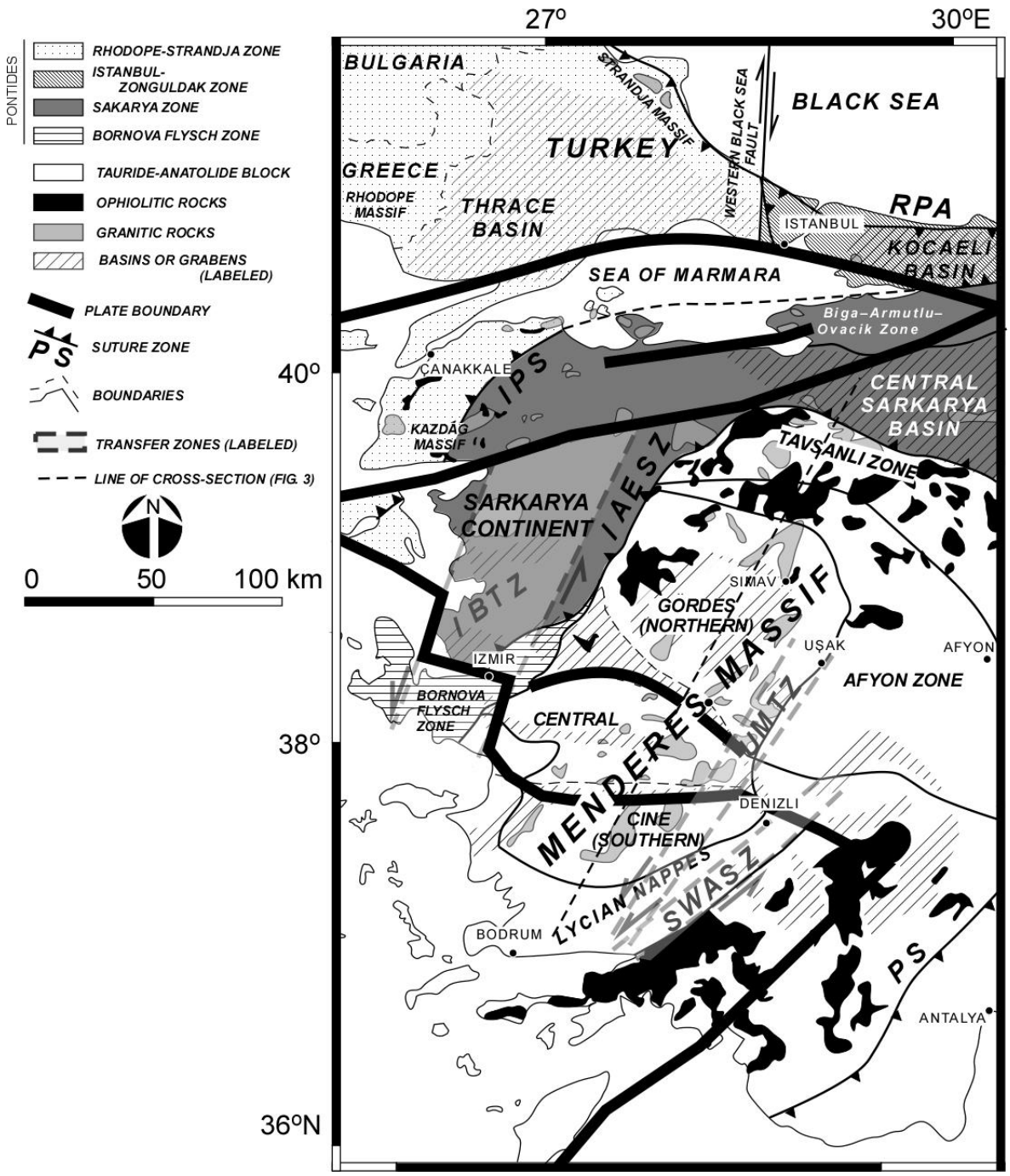

Figure 2. Geological map of Western Anatolia focusing on the ophiolite and granite assemblages along the boundary between the Aegean and Anatolia microplates. Plate boundary after Nyst & Thatcher (2004). Terrane boundaries, major fault systems, and transfer zones after Okay (2008), Akbayram et al. (2016), Oner et al. (2010), and Karaoğlu & Helvacı (2014). Abbreviations: RPA= Rhodope-Pontide Arc; İBTZ = Izmir–Balıkesir Transfer Zone (also sometimes referred to as the Western Anatolia Transfer Zone, Gessner et al., 2013; 2017); SWASZ= South West Anatolian Shear Zone; IPS= Intra-Pontide suture zone; IAESZ = Izmir-Ankara-Erzincan suture zone; PS = Pamphylian suture zone; UMTZ= Uşak-Mugla Transfer Zone.

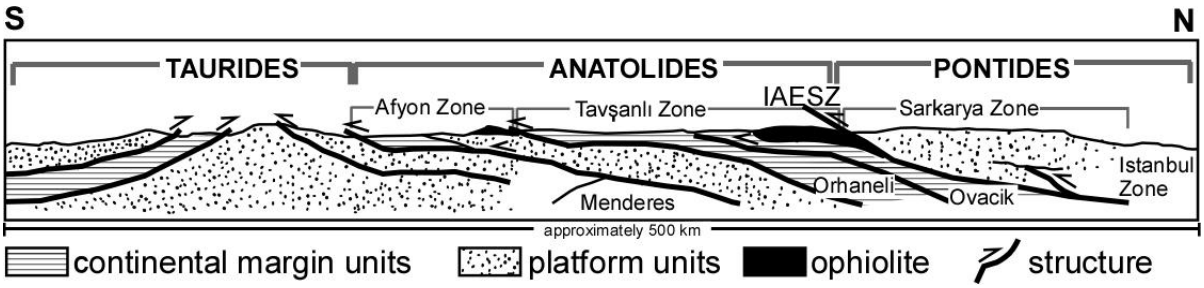

Figure 3. North–south generalized cross-section across western Turkey after Okay (1986) and Shin et al. (2013). IAESZ=İzmir-Ankara-Erzincan Suture Zone. See Figure 2 for the approximate line of section on the geological map.

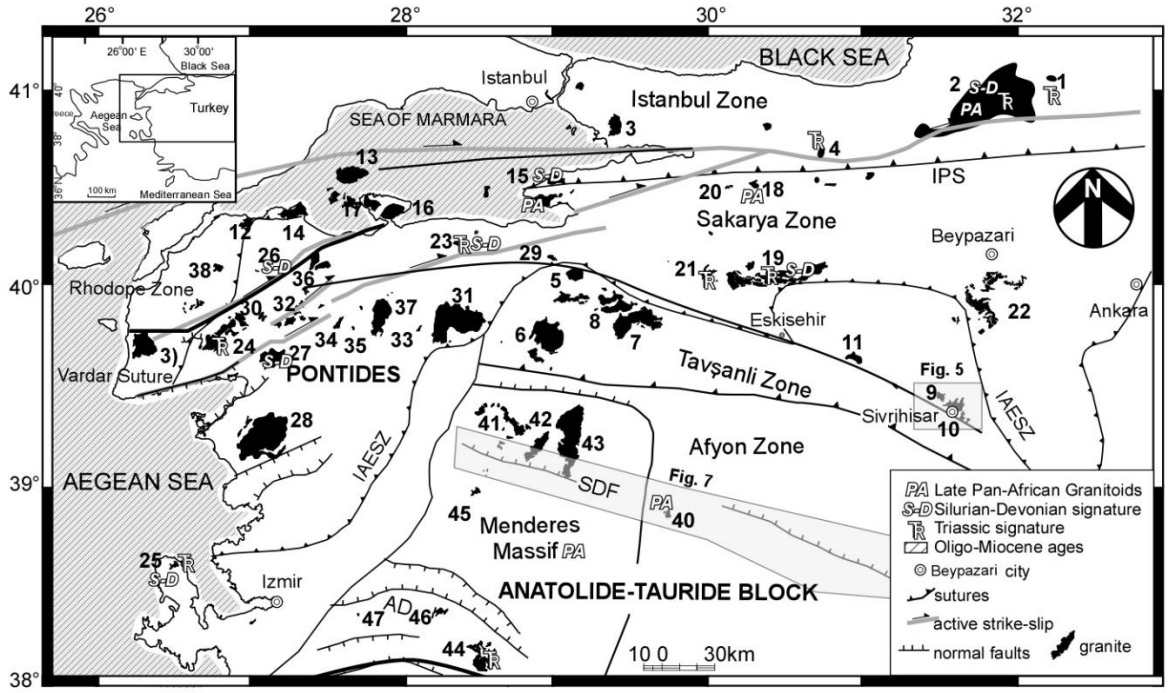

Figure 4. Geological map showing structures and locations of Western Anatolia granite bodies. Base map after Delaloye & Bingöl (2000), Senel & Aydal (2002), and Okay (2008). See Tables 1-7 for the granite names that correspond to the numbers in this figure. Abbreviations: IPS = Intrapontide Suture Zone, IAESZ = Izmir-Ankara-Erzincan Suture Zone, SDF= Simav Detachment Fault, AD= Alasehir Detachment. Locations of Figures 5 and 7 are indicated.

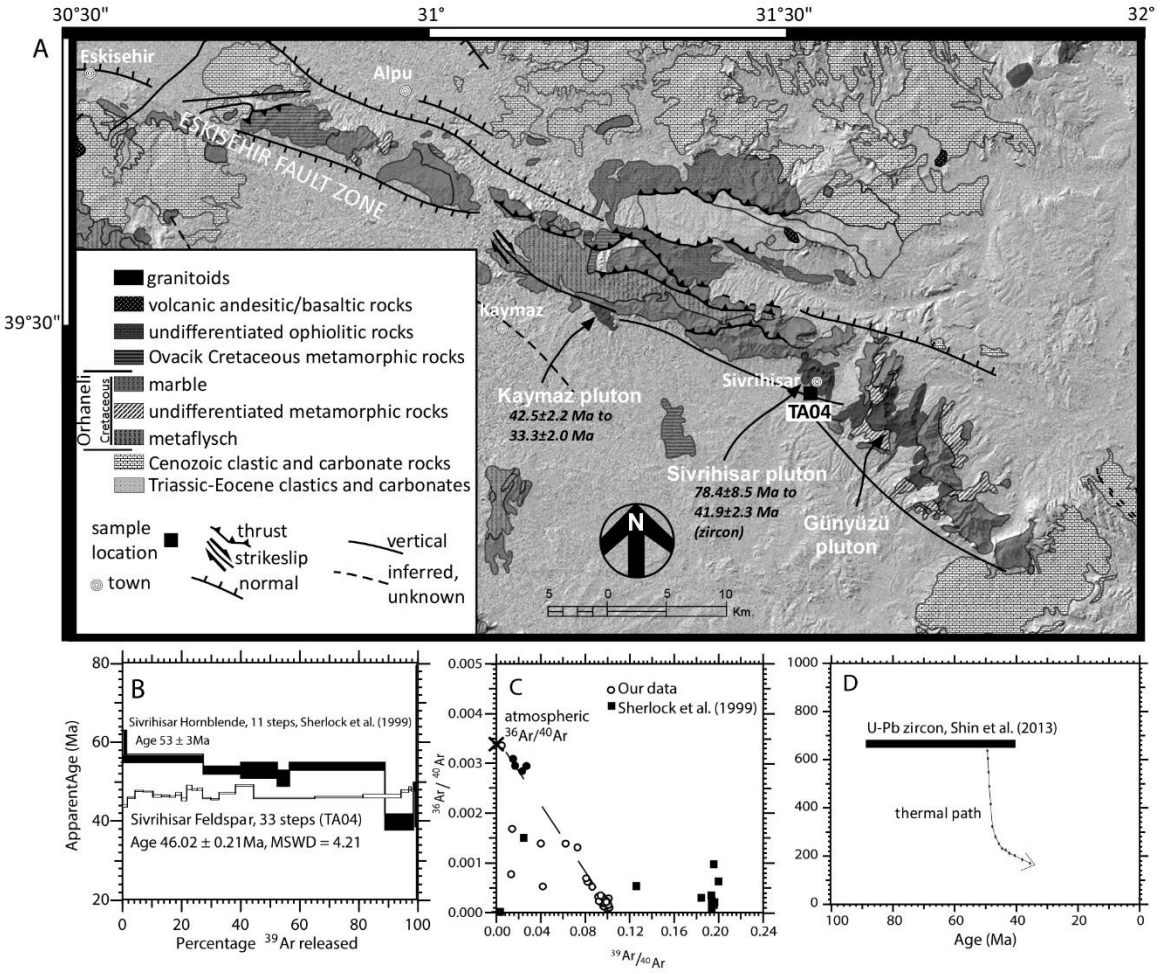

Figure 5. (A) Simplified geologic map of the Sivrihisar Massif (eastern Tavşanlı Zone) overlain on a hillshade raster. Map after Senel & Aydal (2002), Özsayin & Dirik (2007), and Shin et al. (2013). See the data repository for the color figure. (B) Sivrihisar granite K-feldspar age spectra for sample TA04. The upper profile by Sherlock et al. (1999) and the lower are our results. (C)$^{36}Ar/^{40}Ar$ vs. $^{39}Ar/^{40}Ar$ plot comparing our data to Sherlock et al. (1999). Our results show mixing between a radiogenic and atmospheric component of argon with four lower points from initial isothermal steps. Sherlock et al. (1999) data is affected by excess argon (ArE). (D) One possible thermal history path for the Sivrihisar granite based on the rapidly cooled K-feldspar ages, zircon ages, and zircon saturation temperature from Shin et al (2013).

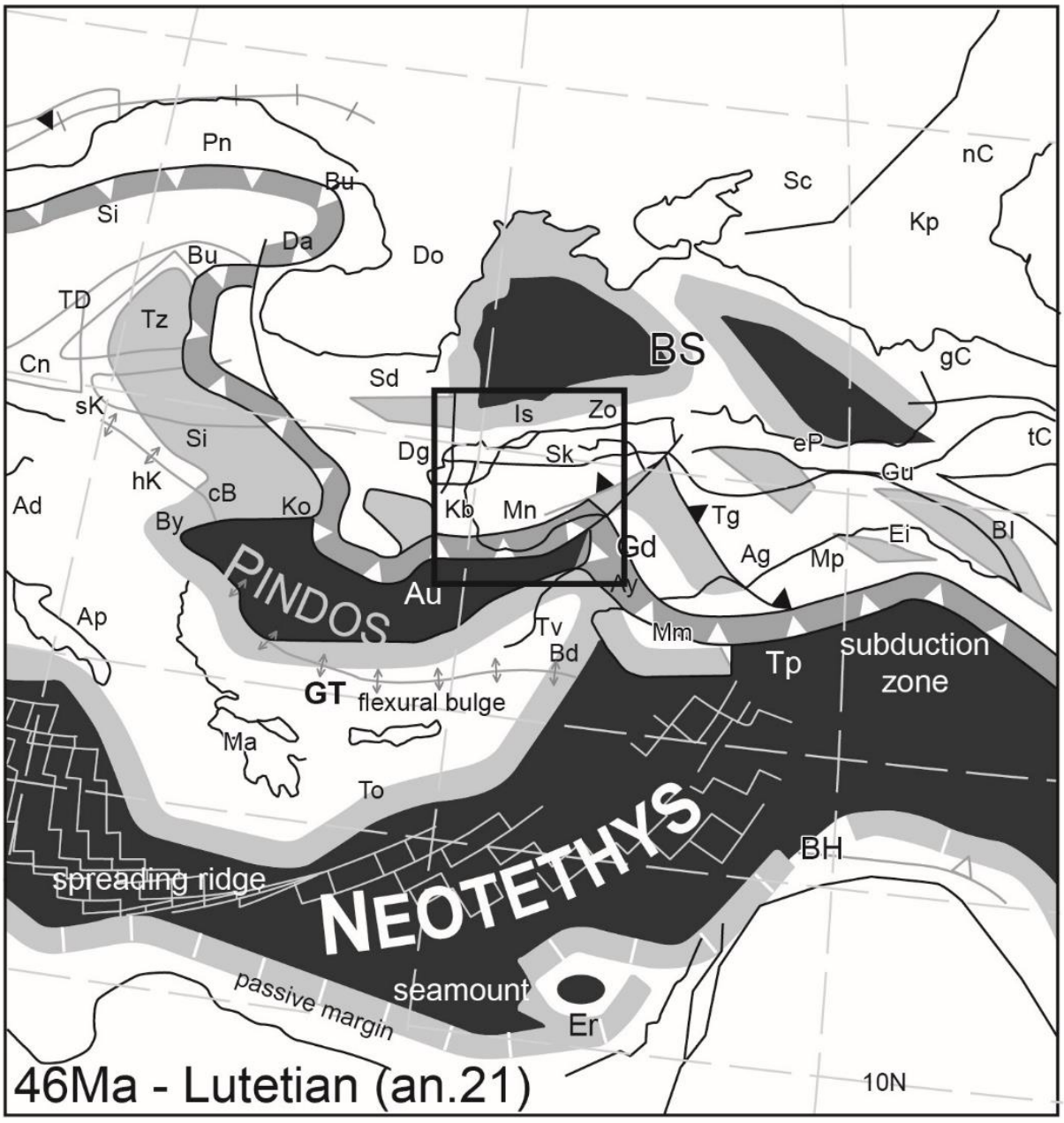

Figure 6. Paleogeographic reconstruction of Western Anatolia (center box) and the surrounding region at 46 Ma prior to the onset of extension (after Stampfli & Kozur, 2006). Abbreviations relevant to Western Anatolia are Mn=Menderes Massif, Kb=Karaburun, Dg=Denizgören ophiolite, Sk=Sakarya Is=Istanbul, Zo=Zonguldak, BS= Black Sea, Er= Eratosthenes seamount. For other abbreviations, please see Stampfli & Kozur (2006).

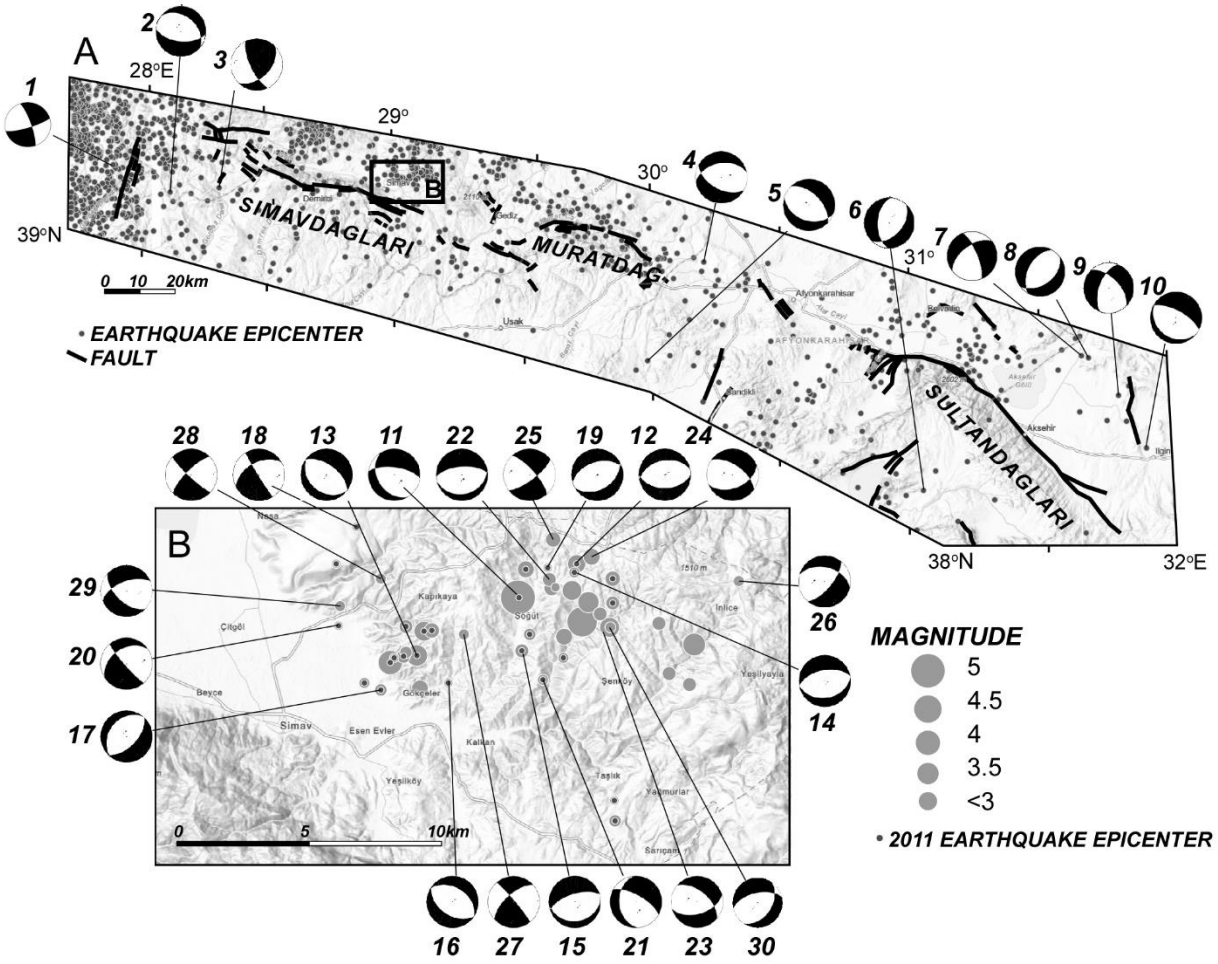

Figure 7. (A) Map of the Simav Fault and associated structures. Small dots are extracted from the USGS Earthquake Catalog magnitude 2.5+ (http://earthquake.usgs.gov/earthquakes/search) of events from 1952-2021. Location of fault strands after Konak (2002). Inset shows the location near the town on Simav in panel (B). (B) Map of the surrounding area of Simav with earthquakes plotted. In this map, events were extracted from the Turkish Ministry of the Interior, Disaster and Emergency Management Presidency, Earthquake Department Earthquake Catalog (M>=4.0), 1900-20XX (https://deprem.afad.gov.tr/depremkatalogu). The size of the circle represents magnitude. The figure highlights 2011 earthquakes by additional solid dots. Base maps in both panels are from ESRI. Focal mechanism solutions in both panels were extracted from the Turkish catalog. See Table 9 for details of the events. For locations of faults in panel (B), see Mutlu (2020).

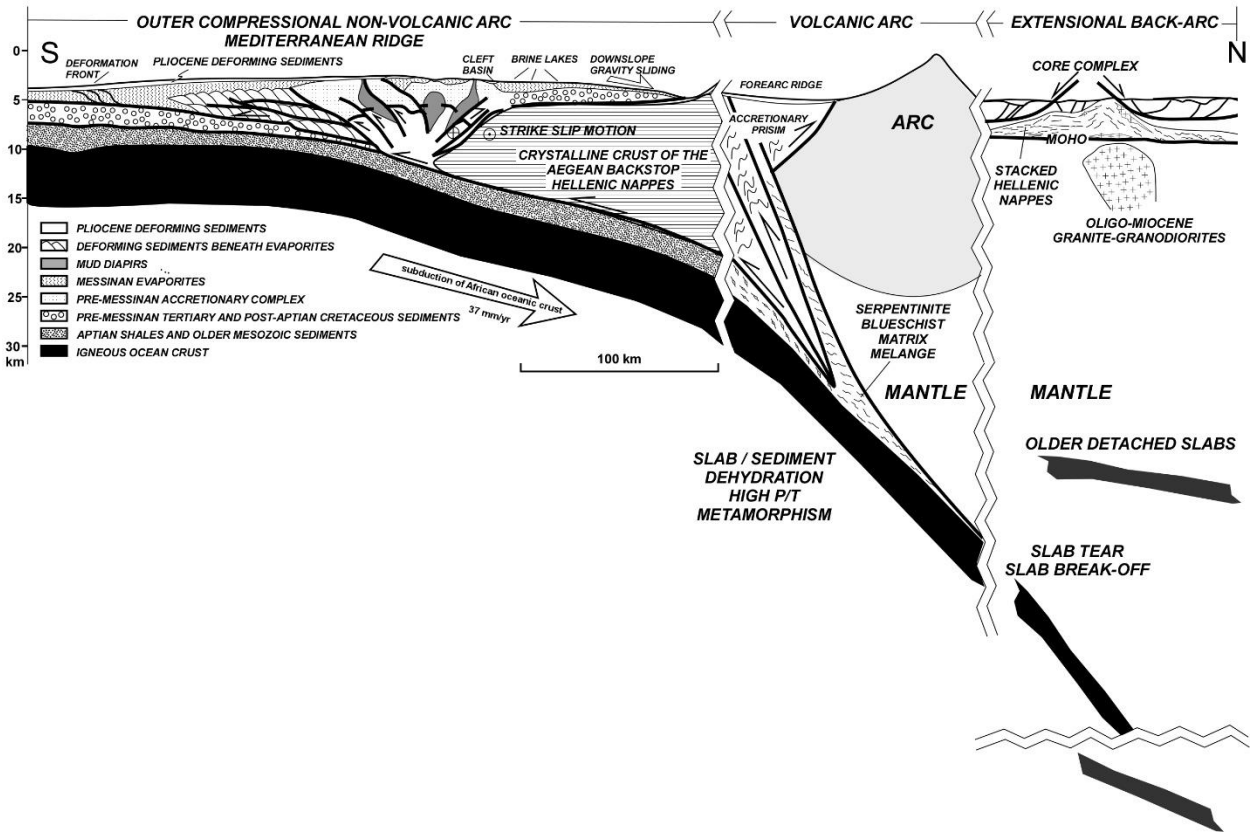

Figure 8. North-south generalized cross-section through the Hellenic arc system showing the key structural elements. Map of the Mediterranean Ridge after Westbrook & Reston (2002).

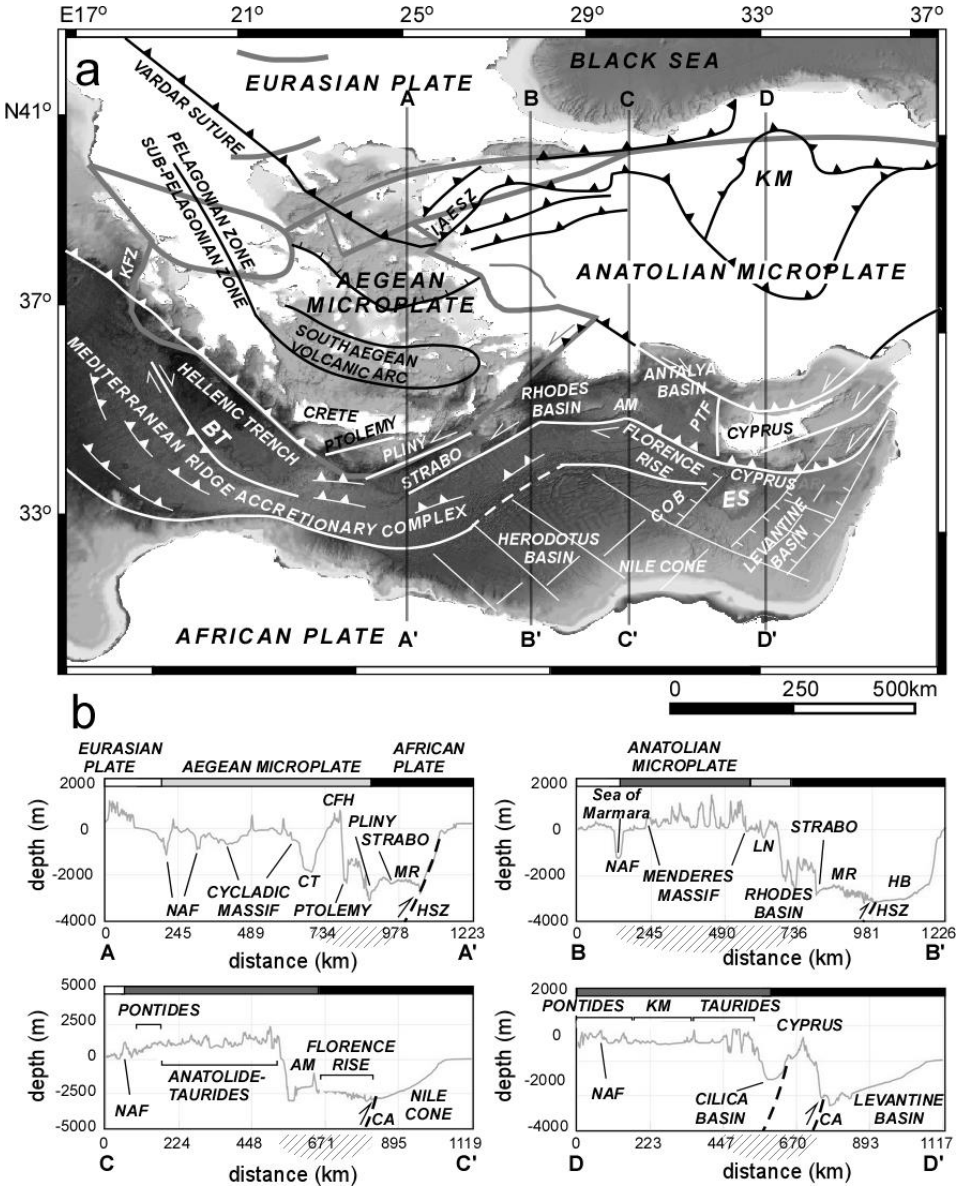

Figure 9. (A) EMODnet Digital Bathymetry map with some structures overlain. The Aegean and Anatolian microplate boundaries are shown in grey after Nyst and Thatcher (2004). Other structures after Hall et al. (1984) and (2009), Woodside et al. (2002), Peterek & Schwarze (2004), Meier et al. (2007); Kinnaird & Robertson (2012), and Symeou et al. (2018). Abbreviations: BT= Backthrust; KFZ = Kephalonia Fault Zone; IAESZ = Izmir-Ankara-Erzincan Suture Zone; KM= Kirşehir Massif, AM= Anaximander Mountains; PTF = Paphos Transform Fault, ES = Eratosthenes Seamount. (B) Profiles along the lines of section shown in panel (A). Abbreviations: CT= CFH = LN= Lycian Nappes, MR= Mediterranean Ridge Accretionary Complex, HB = Herodotus Basin, HSZ= Hellenic Shear Zone, NAF= North Anatolian Fault; AM = Anaximander Mountains; CA= Cyprus Arc. Hashed regions in panel (B) indicate area speculated to be affected by slab tear (e.g., Woodside et al., 2002; Özbakır et al., 2013; Jolivet et al., 2015). See supplementary files for the color figure.

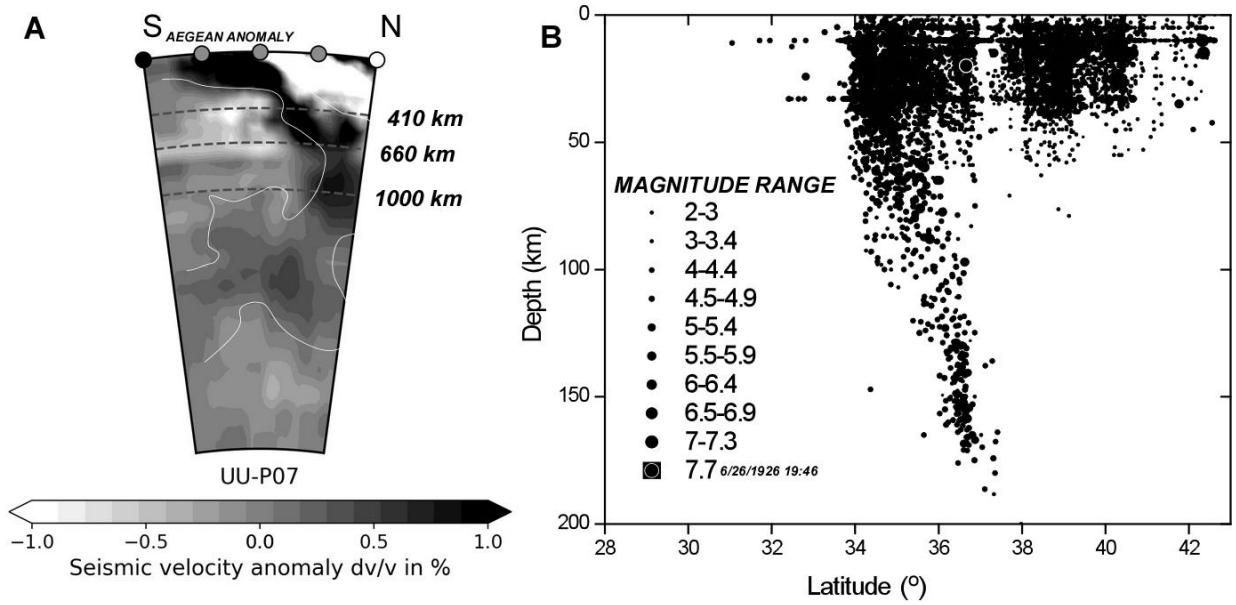

Figure 10. (A) Cross-section of the Aegean anomaly interpreted as the African slab using the UUP07 P-wave model (Amaru, 2007). The line of section used latitude of 28°-43° and longitude of 24°-28°. For more detailed views of the anomaly, see van der Meer et al. (2018), Wei et al. (2019), Blom et al. (2020), and El-Sharkawy et al. (2021). The depths of the dashed lines are 410, 660, 1000 km from the surface. Interpretations of the geology below 1000 are debated and discussed in the text. Image created using Hosseini et al. (2018). (B) Depth vs. estimated earthquake depth for the same latitude and longitude as seen in panel (A). In this map, events were extracted from the Turkish Ministry of the Interior, Disaster and Emergency Management Presidency, Earthquake Department Earthquake Catalog (M>=4.0), 1900-20XX (https://deprem.afad.gov.tr/depremkatalogu). Events are from 01/24/1900 to 6/17/2021. We indicate the largest event (6/26/1926, 19:46).

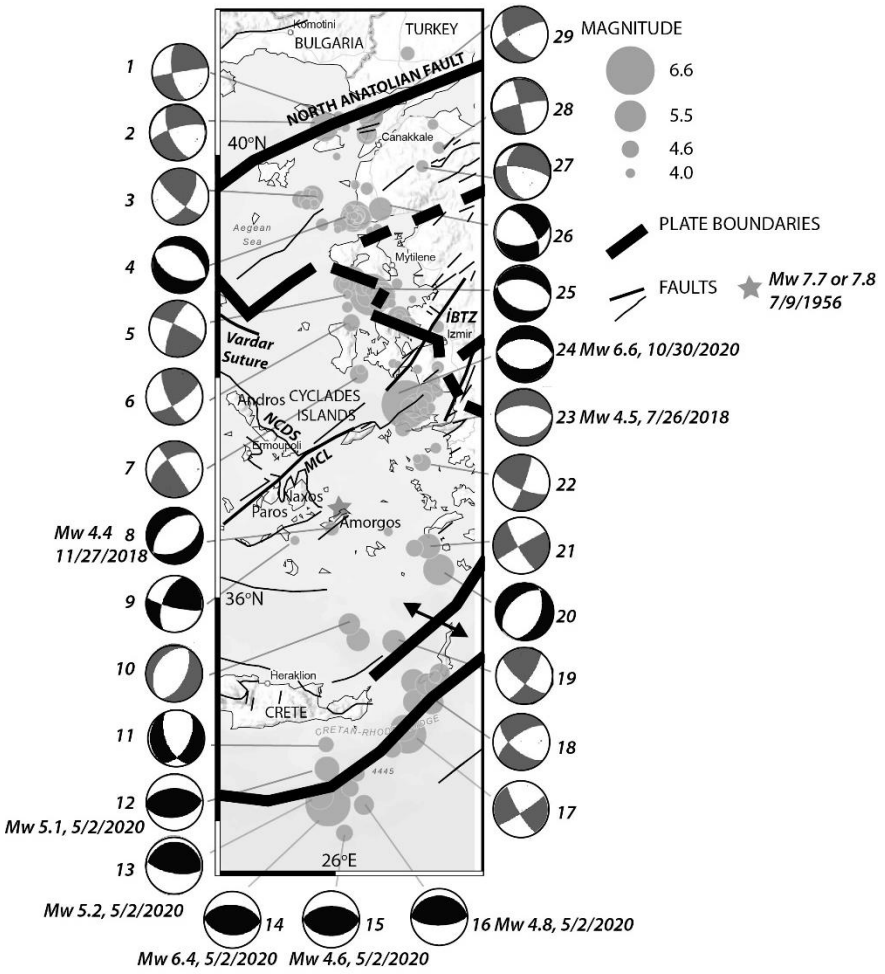

Figure 11. Map of plate boundaries between the Aegean and Anatolian microplates with some faults indicated (after Nyst & Thatcher, 2004; Uzel et al., 2013; Pe-Piper et al., 2002; Menant et al., 2016). Focal mechanisms are from the Turkish Ministry of the Interior, Disaster and Emergency Management Presidency, Earthquake Department Earthquake Catalog (M>=4.0), 1900-20XX (https://deprem.afad.gov.tr/depremkatalogu). Events are only from 2010-2020 and details are presented in Table 10. The size of the circle represents magnitude. The 9 July 1956 Amorgos earthquake epicenter is also indicated after Alatza et al. (2020). See Okal et al. (2009) for discussions regarding the focal mechanism of this event. The base map is from ESRI. The abbreviations İBTZ = Izmir–Balıkesir transfer zone; NCSD= North Cyclades Detachment System; MCL= Mid-Cycladic Lineament.

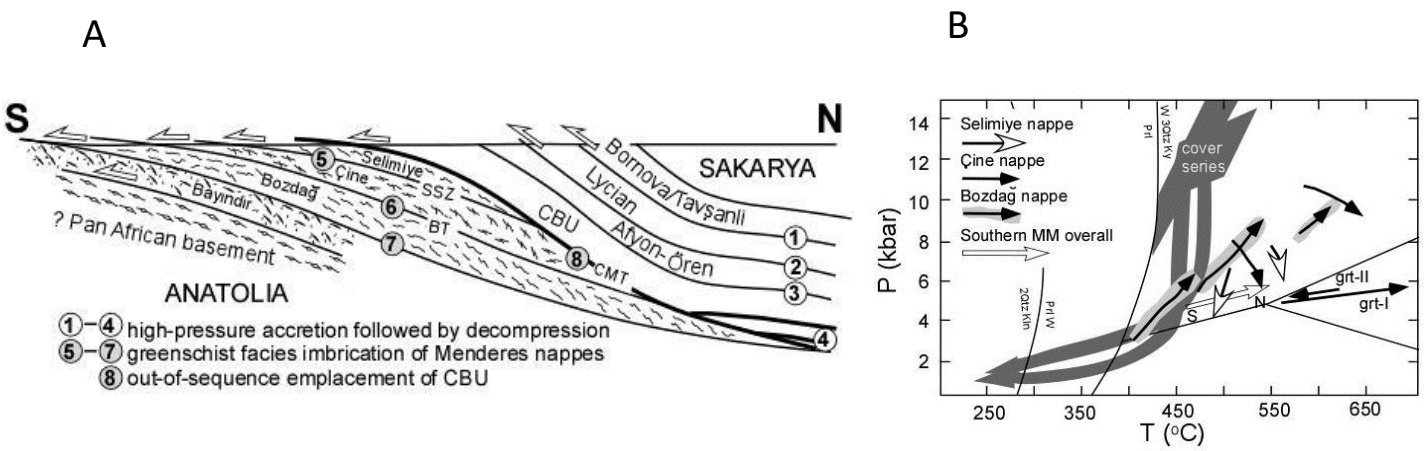

Figure 12. (A) Interpretative thrust sequence during the formation of Anatolide belt after Gessner et al. (2013). CBU= Cyclades Blueschist Unit; CMT= Cyclades Menderes Thrust; SSZ= Selimiye Shear Zone, BT= Bozdag Thrust. (B) P-T paths from Menderes Massif nappes (Ring et al., 2001; Whitney & Bozkurt, 2002; Rimmelé et al., 2005; Régnier et al., 2007).

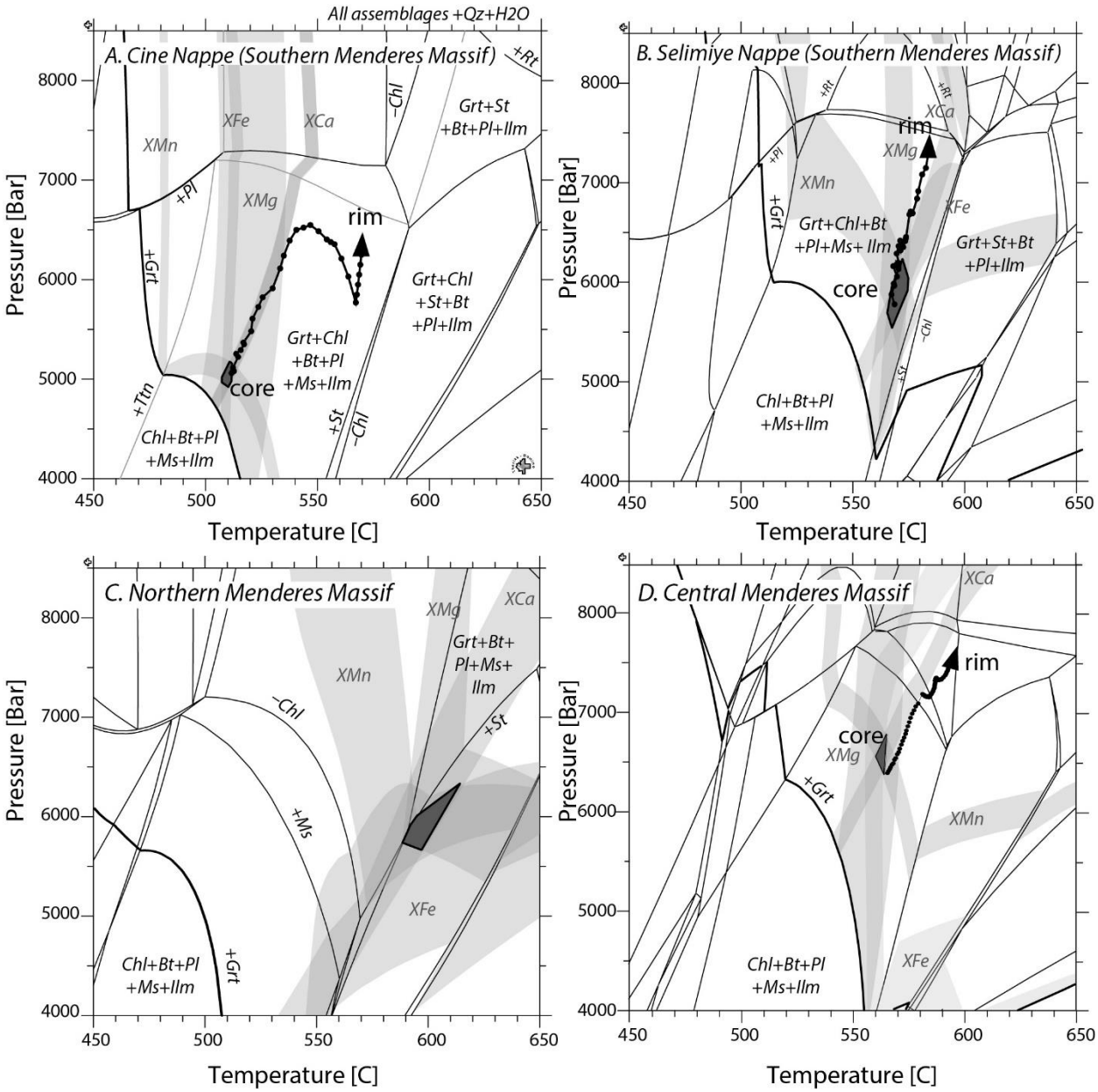

Figure 13. Isochemical phase diagrams with overlapping garnet core compositional isopleths for garnet-bearing samples from the **(A)** Çine nappe, **(B)** Selimiye nappe after Etzel et al. (2019), **(C)** Northern Menderes Massif using data from Cenki-Tok et al. (2016), and **(D)** the Central Menderes Massif (Etzel et al., 2020). Mineral abbreviations after de Capitani and Brown (1987) and de Capitani and Petrakakis (2010). Labeled stripes are compositional isopleths of ±0.1 mole fraction for endmember garnet core compositional contents, except for panel **(D)**, which overlies ±0.2 mole fraction and is for the reported representative composition for that garnet by Cenki-Tok et al. (2016). The grey polygon in each diagram represents the conditions estimated for garnet growth in the samples. High-resolution P-T paths for the samples are shown in panels **(A), (B),** and **(D).** See supplementary figures for this figure in color.

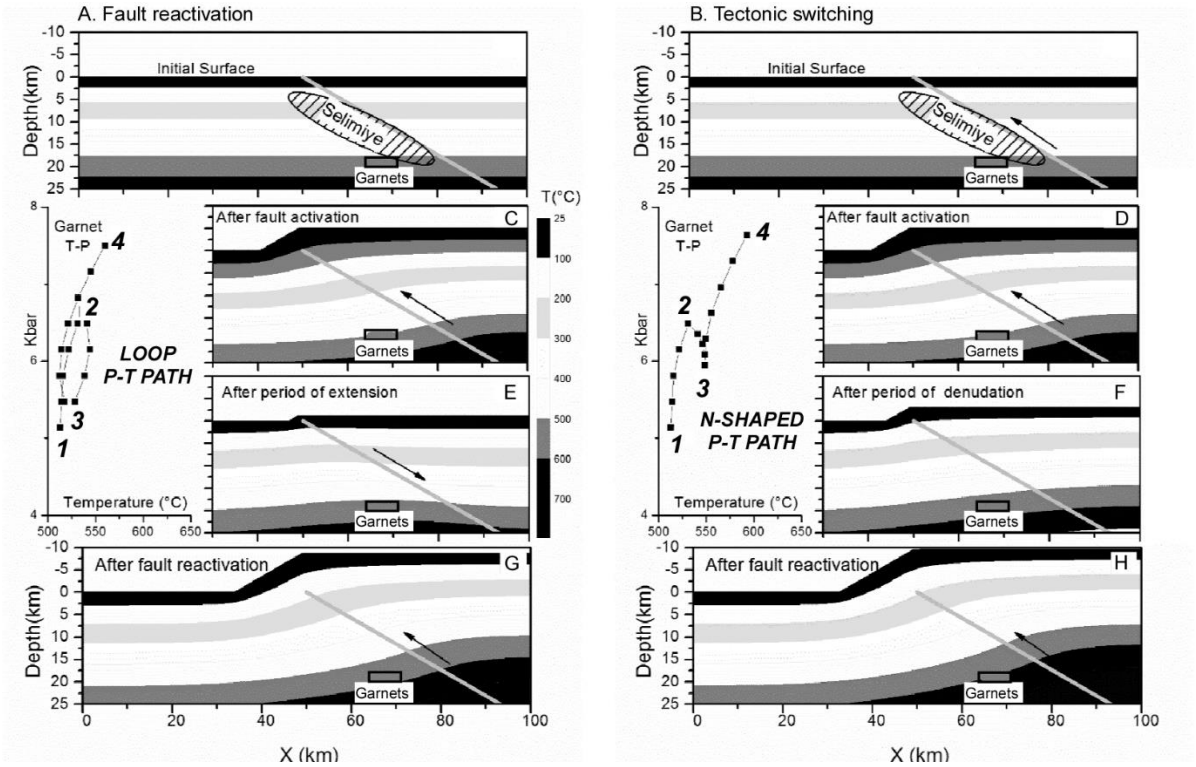

Figure 14. Snapshots of thermal models of the Çine nappe for the (left) fault reactivation and (right) tectonic switching model after Etzel et al. (2019). (A) and (B) are the upper equilibrium thermal grid (depth vs. horizontal distance) before faulting with the position of fault (grey line) arbitrarily selected at 30°. Fault displacement varies linearly. The grid includes reflecting side boundaries and top and bottom maintained at 25°C and 700°C and an initial geothermal gradient at 25°C/km indicated by shaded bars. The position of the Selimiye samples is inferred by a hatch area, and the grey bar represents the approximate initial location of the Çine nappe garnet with the N-shaped P-T path. This is also represented by point 1 in P-T path insets. In panels (C) and (D), the fault is activated and a finite-difference solution to the diffusion-advection equation is used to examine the P-T variations in the hanging wall and footwall as a result of motion. The rock sample experiences the path from 1 to 2 on the P-T path insets. In panels (E) and (F), motion stops. In panel (E), extension occurs, whereas denudation occurs in panel (F). This is modeled based on the mid-rim lower pressure portion of the garnet P-T path and is represented by points 2 to 3 on the P-T path insets. In panels (G) and (H), the fault is reactivated, represented by points 3 to 4 on the P-T path insets.